`

# Bleomycin, From Start to Finish; Total Synthesis of Novel Analogues to *in vitro* Fluorescence Microscopy Imaging

by

Trevor C. Bozeman

A Dissertation Presented in Partial Fulfillment
of the Requirements for the Degree
Doctor of Philosophy

Approved November 2013 by the
Graduate Supervisory Committee:

Sidney M. Hecht, Chair
John Chaput
Ian Gould

ARIZONA STATE UNIVERSITY

December 2013

ABSTRACT

The bleomycins are a family of glycopeptide-derived antibiotics isolated from various Streptomyces species and have been the subject of much attention from the scientific community as a consequence of their antitumor activity. Bleomycin clinically and is an integral part of a number of combination chemotherapy regimens. It has previously been shown that bleomycin has the ability to selectively target tumor cells over their non-malignant counterparts.

Pyrimidoblamic acid, the N-terminal metal ion binding domain of bleomycin is known to be the moiety that is responsible for $O_2$ activation and the subsequent chemistry leading to DNA strand scission and overall antitumor activity. Chapter 1 describes bleomycin and related DNA targeting antitumor agents as well as the specific structural domains of bleomycin. Various structural analogues of pyrimidoblamic acid were synthesized and subsequently incorporated into their corresponding full deglycoBLM $A_6$ derivatives by utilizing a solid support. Their activity was measured using a pSP64 DNA plasmid relaxation assay and is summarized in Chapter 2.

The specifics of bleomycin–DNA interaction and kinetics were studied via surface plasmon resonance and are presented in Chapter 3. By utilizing carefully selected 64-nucleotide DNA hairpins with variable 16-mer regions whose sequences showed strong binding in past selection studies, a kinetic profile was obtained for several BLMs for the first time since bleomycin was discovered in 1966.

The disaccharide moiety of bleomycin has been previously shown to be a specific tumor cell targeting element comprised of L-gulose-D-mannose, especially between MCF-7 (breast cancer cells) and MCF-10A (“normal” breast cells). This phenomenon

was further investigated via fluorescence microscopy using multiple cancerous cell lines with matched “normal” counterparts and is fully described in Chapter 4.

ACKNOWLEDGEMENTS

My gratitude first and foremost is extended to my research advisor, Professor Sidney M. Hecht. He has without a doubt challenged me to the greatest extent possible and assisted in developing my own independent and innovative problem solving abilities. I would also like to thank supporting faculty members John Chaput, Ian Gould and Petra Fromme for assisting and seeing me through my comprehensive oral examination and/or technical review and dissertation defense.

In addition to an outstanding faculty research advisor and great supporting faculty I would not have succeeded without the support of numerous mentors and colleagues throughout the Hecht laboratory and Arizona State University. A sincere and most heartfelt thank you goes out to Drs. Ryan Schmaltz (and Sarah Schmaltz) who provided a great foundation as a mentor and who both were there for me during the most difficult times; chemistry synthesis and otherwise. Another special thanks goes out to Dr. Damien "Big D" Duveau who always offered his help and was a true team player who wanted only the absolute best out of everyone and every experiment. Big D, always had an answer for any question, thus his title. Thank you also, Dr. David Fash for your assistance and hands-on training during my first few semesters in a research laboratory, you were always around at the right (or otherwise wrong) times.

Additional gratitude is extended to many colleagues who have helped me with various things over the last 5 years and facilitated my graduation; Drs. Ryan and Jeannette Nangreave, Basab Roy, Rumit Maini, Meg Schmierer, Rakesh Paul, Cameron Cripe, Manikandadas Mathilakathu Madathil ("Das"), Omar Kdour, Larisa Dedkova, Nour Eddine Fahmi and Parvez Alam.

I would also like to thank my supporting friends outside the realm of chemistry and the lab. Bailey Kirth, Kendra Smith and D.A. who helped keep me motivated during lunch throughout the week and many Thursday afternoons. Thank you C. C. for showing me true happiness does exist in the real world, and showing me what really matters in life and supporting me unconditionally through the hardest part of my degree, I could/would not have finished this all without you. Also, to my roommate and future PhD Kris Fecteau, thanks for the companionship and comradery during the last 4+ years of graduate school and many, many things outside the scope of these particular acknowledgements.

Finally to my sister and my parents, thank you all so much for an immeasurable level of support which continues to last indefinitely even after my PhD is finished, you believed in me even when I didn't believe in myself. My sister Molly especially, the only woman in my life who has never left nor betrayed me, this is ultimately dedicated to you girl, cheers.

TABLE OF CONTENTS

Page

# LIST OF ABBREVIATIONS

| | |
|---|---|
| aq | aqueous |
| atm | atmosphere |
| BLM | bleomycin |
| Boc | t-butoxycarbonyl |
| $(Boc)_2O$ | t-butoxycarbonyl anhydride |
| BOP | (benzotriazol-1-yloxy)tris(dimethylamino)phosphonium hexafluorophosphate |
| Bn | benzyl |
| Br | broad |
| $^{o}C$ | degrees celsius |
| $^{13}C$ | carbon nuclear magnetic resonance |
| CBz | benzyloxycarbonyl |
| CD | circular dichroism |
| $CDCl_3$ | deuterated chloroform |
| $CH_2Cl_2$ | methylene chloride |
| $(CH_3)_2S$ | dimethyl sulfide |
| $CH_3CN$ | acetonitrile |
| Cy5 | potassium 2-((1*E*,3*E*,5*E*)-5-(1-(5-carboxypentyl)-3,3-dimethyl-5-sulfonatoindolin-2-ylidene)penta-1,3-dien-1-yl)-1-ethyl-3,3-dimethyl-3H-indol-1-ium-5-sulfonate |

| | |
|---|---|
| Cy5** | potassium 2-((1E,3E,5E)-5-(1-(5-carboxypentyl)-3,3-dimethyl-5-sulfonatoindolin-2-ylidene)penta-1,3-dien-1-yl)-3-methyl-1,3-bis(4-sulfobutyl)-3H-indol-1-ium-5-sulfonate |
| d | doublet |
| DAPI | 2-(4-amidinophenyl)-6-indolecarbamidine dihydrochloride |
| DCC | dicyclohexylcarbodiimide |
| DEAD | diethyl azodicarboxylate |
| DMF | *N,N*-dimethylformamide |
| DMSO | dimethyl sulfoxide |
| EtOH | ethanol |
| EtOAc | ethyl acetate |
| $Et_2O$ | diethyl ether |
| $Et_3N$ | triethylamine |
| Fmoc | fluorenylmethyloxycarbonyl |
| g | gram(s) |
| $^1H$ NMR | proton nuclear magnetic resonance |
| h | hours |
| $H_2$ | hydrogen gas |
| $H_2O$ | water |
| HATU | (1-[bis(dimethylamino)methylene]-1H-1,2,3-triazolo[4,5-b]pyridinium 3-oxid hexafluorophosphate) |
| HBTU | *N,N,N′,N′*-tetramethyl-*O*-(1*H*-benzotriazol-1-yl)uronium hexafluorophosphate |

| | |
|---|---|
| HCl | hydrogen chloride gas |
| HOAt | 1-hydroxy-7-azabenzotriazole |
| HOBt | hydroxybenzotriazole |
| Hunig's base | *N*,*N*-diisopropylethylamine |
| $K_2CO_3$ | potassium carbonate |
| m | multiplet |
| M | molarity |
| MeOH | methanol |
| mg | milligram |
| $MgSO_4$ | magnesium sulfate (anhydrous) |
| min | minute(s) |
| mL | milliliter(s) |
| mmol | millimole(s) |
| N | normal |
| $N_2$ | nitrogen gas |
| $NaBH_4$ | sodium borohydride |
| NaCl | sodium chloride |
| $NaHCO_3$ | sodium bicarbonate |
| $NaOCH_3$ | sodium methoxide |
| $NH_3$ | ammonia gas |
| NHS | *N*-hydroxysuccinimide |
| $NH_4O_2CCH_3$ | ammonium acetate |
| NMR | nuclear magnetic resonance |

| | |
|---|---|
| nt | nucleotide (i.e. 16-nt; 16-nucleotide) |
| PBA | pyrimidoblamic acid |
| PBS | phosphate buffered saline |
| $PCl_5$ | phosphorus pentachloride |
| Pd | palladium |
| rt | room temperature |
| s | singlet |
| satd | saturated |
| $SOCl_2$ | thionyl chloride |
| SPR | surface plasmon resonance |
| t | triplet |
| Ts-Cl | 4-toluenesulfonyl chloride |
| TFA | trifluoroacetic acid |
| THF | tetrahydrofuran |
| TLC | thin layer chromatography |

List of Figures, Equations and Tables

List of Schemes

# Chapter 1

## 1.01 Introduction

Cancer is a family of diseases for which there is currently no certain cure and one that has a global and devastating effect on its victims and their families; cancer claims millions of lives worldwide every single year.[1] The need for selective chemotherapeutic agents for use in diagnostics, imaging and treatment of cancers has never been more critical and remains the subject of intense ongoing research efforts. Chemotherapeutic agents are compounds whose mechanisms involve inhibiting or perturbing normal cellular functions by targeting, for example, protein synthesis,[2] cell division,[3] and deoxyribonucleic acid (DNA) replication and transcription.[4] DNA has shown to be an especially effective target for many classes of chemotherapeutic agents. This includes both intercalators, which work directly on DNA itself and groove binders (Figure 1.01), which allow for the disruption of critical DNA–protein interactions during cell division.

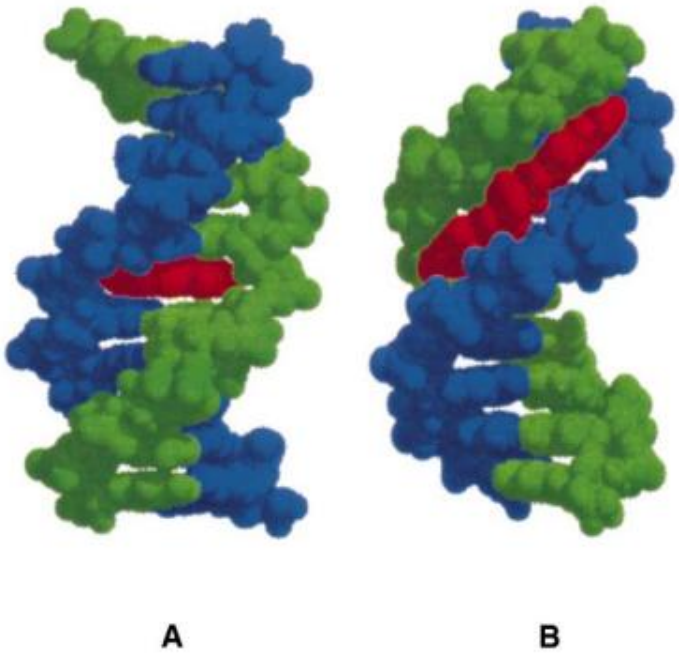


**Figure 1.01** Schematic representation of DNA-chemotherapeutic interaction, A) intercalation; B) minor groove-binding[5]

Bleomycin is a minor groove-binding agent and belongs to a unique class of chemotherapeutics.

The bleomycins (BLMs) are a family of glycopeptide-derived antibiotics originally isolated from a culture broth of *Streptomyces verticillus* species as its natural copper chelate.[6] Bleomycin was first isolated in 1966 by Umezawa and co-workers and has been studied extensively due to its antitumor activity.[7] Bleomycin is currently employed clinically, in The United States under the trade name Blenoxane and used in conjunction with other antitumor agents as part of standard combination chemotherapy regiments (ABVD, BEACOPP, etc). Blenoxane is a mixture of several congeners, consisting predominantly of bleomycins $A_2$ (~60%) and $B_2$ (~30%), that differ in structure solely at the C-terminus (Figure 1.02). In other parts of the world, including China, bleomycin is administered primarily as the single BLM $A_5$ congener.

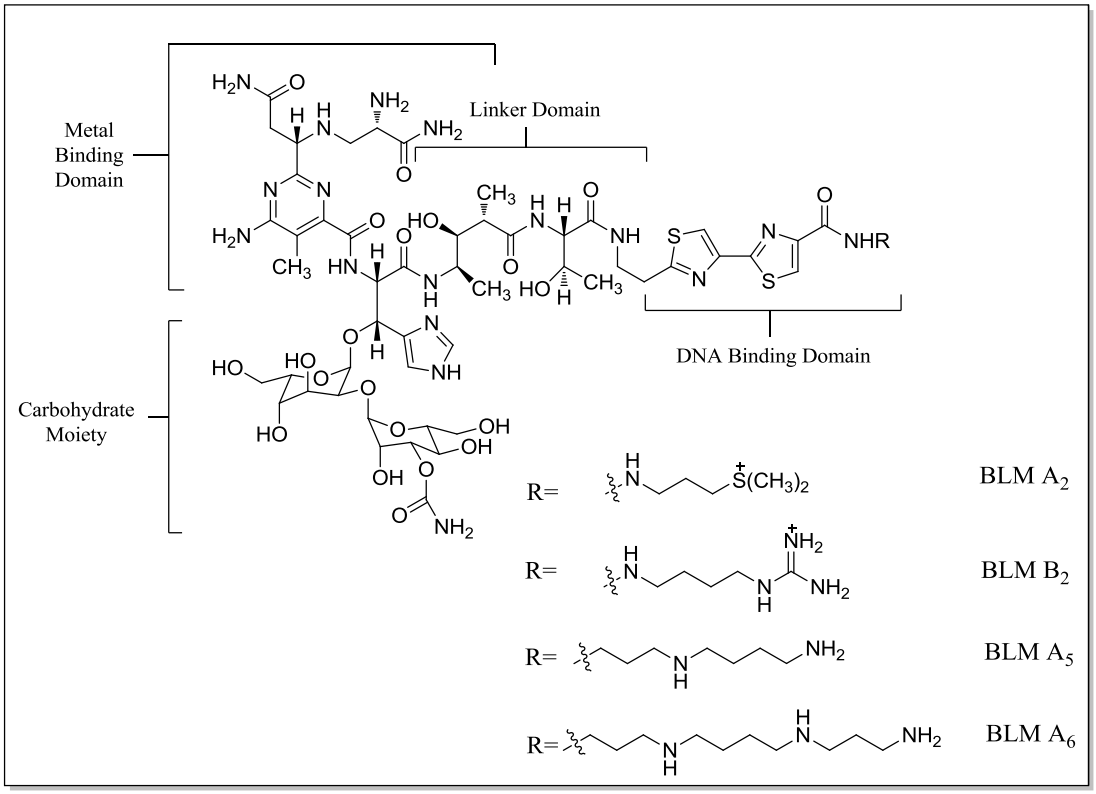


**Figure 1.02** BLMs $A_2$, $B_2$, $A_5$ and $A_6$

Bleomycin is used to treat a variety of malignancies, including squamous cell carcinomas, testicular cancers and Hodgkin's lymphomas. One of the primary drawbacks of bleomycin therapy is the risk to patients for developing pulmonary fibrosis. The most logical explanation of this phenomenon is DNA cleavage by bleomycin that is oxygen dependent and thus much more likely to occur in pulmonary tissue where oxygen availability is significantly higher than other tissues. Another possibility is that the polyamine side chain found primarily in BLMs $A_5$ and $A_6$ contribute to its pulmonary toxicity, as much simpler polyamines are well known to be toxic to lung tissue.[8] Other structurally related glycopeptide antibiotics, such as the phleomycins (PLMs), zorbamycin (ZBM) or the tallysomycins (TLMs) (Figure 1.03) are known to exhibit antitumor activity in a similar way.[9,10]

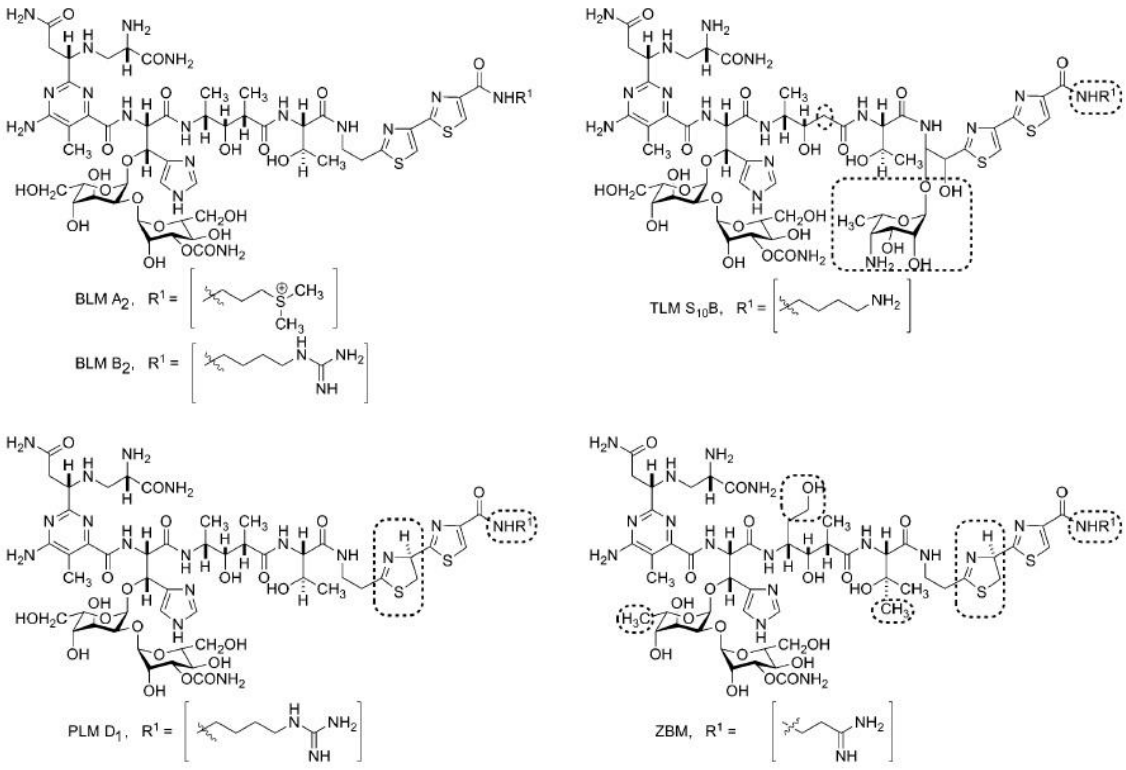


**Figure 1.03** Structural comparisons of antitumor antibiotics: BLM $A_2$ and $B_2$, tallysomycin (TLM) $S_{10}B$, phleomycin (PLM) $D_1$, and zorbamycin (ZBM). Structural differences from the BLMs have been highlighted.[9]

In an effort to verify the exact structure of the BLMs and to study the specific mechanism of action of these antibiotics, the total synthesis of BLM $A_2$ was completed by both the Hecht[11] and Umezawa[12] laboratories in 1982 and by the Boger laboratory in 1994.[13] However, it was not until 2000 when the Hecht group synthesized BLM using a solid-phase approach that an extensive BLM library could be realized. Following this discovery, a combinatorial library of 108 deglycoBLM analogues was created in 2003 to further explore the mechanism of action and the structure-activity relationships (SAR) of BLM.[14]

The structure of bleomycin can be divided into four distinct regions; the N-terminal metal ion binding domain (also known as pyrimidoblamic acid), the C-terminal bithiazole DNA binding domain, the methylvalerate-threonine linker region and the disaccharide region (Figure 1.02). In terms of function the metal ion binding domain pyrimidoblamic acid (PBA), is responsible for metal ion binding (and has demonstrated the ability to bind many first row transition metals including Fe, Cu, Co, Mn, Ni, Ru, V and Zn) as well as being responsible for oxygen activation.[15,16] While in a clinical setting bleomycin is administered in its apo-form (metal free) but is believed to quickly coordinate with metals *in vivo.* Iron may be the most abundant cofactor available; accordingly Fe•BLM has been the most extensively studied metallobleomycin.[12] Given the attention afforded to this metallobleomycin within the scientific community and literature, the arrangement of the ligands was a subject of much debate. Recently, Buda and coworkers published a computational model taking into consideration past experimental and multinuclear NMR evidence (Figure 1.04).[15]

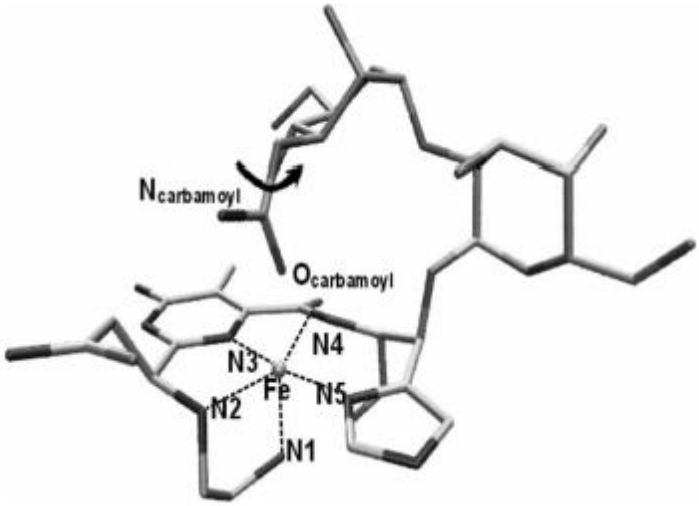


**Figure 1.04** Model of the metal coordination domain of Fe(II)•BLM[15]

Pyrimidoblamic acid has been well described as the primary metal chelating domain of bleomycin.[12,13,15,17-19] The equatorial ligands consist of the secondary amine of the β-aminoalanineamide moiety, the pyrimidine (N3), the imidazole ring (N5) and the amide nitrogen of the β-hydroxyhistidine. The axial ligands include the primary amine of the β-aminoalanineamide moiety and the oxygen atom of the carbamoyl group at the C3 position of the mannose in the sugar moiety.

At the C-terminus of bleomycin, there is a bithiazole moiety linked to a variety of functionalized side chains shown in Figure 1.02. Each of these side chains contains an inherent positive charge (BLM $A_2$, BLM $B_2$) or a polyamine chain that is positively charged in physiological environments (BLM $A_5$, BLM $A_6$). This structural property allows for strong interaction between BLM and the negatively charged phosphate backbone of nucleic acids thereby facilitating the binding of the bithiazole moiety into the minor groove of DNA and subsequent cleavage.

To further understand the interaction between the C-terminus of bleomycin and DNA binding, bithiazole analogues have been synthesized, incorporated into

deglycobleomycin and studied.[20] Several monothiazole analogues were prepared in which one of the two thiazole heterocycles was substituted with *S*-methyl-L-cysteine (Figure 2.05).

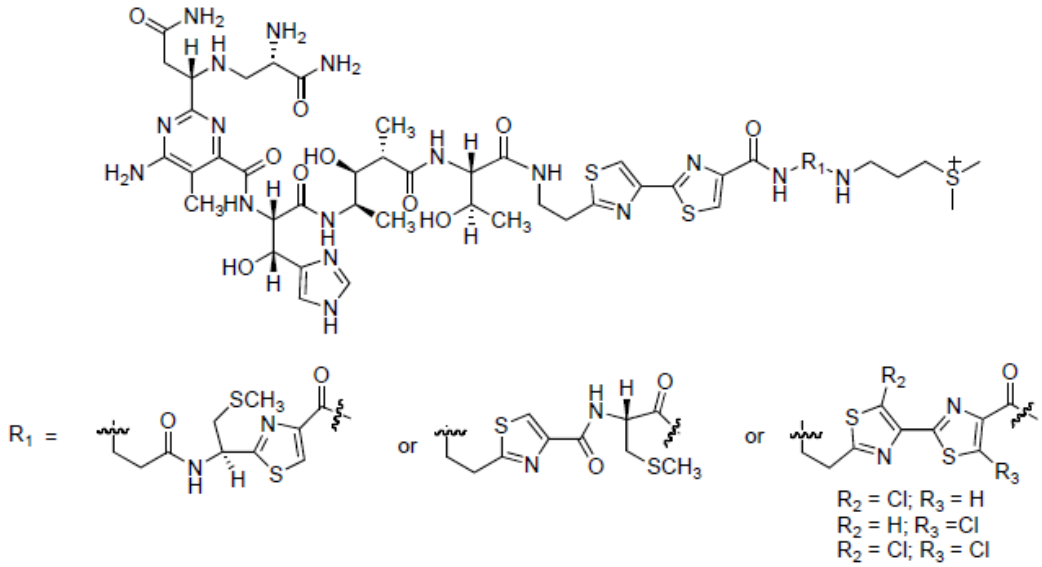


**Figure 1.05** DeglycoBLM congeners containing monothiazole analogues[20,21]

In this study it was found that the deglycobleomycin $A_2$ analogues altered in the bithiazole moiety had a substantial decrease in their ability to cleave DNA. Additionally the analogues showed a lack of sequence selective selectivity. It was concluded that this dramatic decline in activity was due to inefficient DNA binding and suggested the bithiazole moiety was necessary for sequence-selective DNA cleavage. Further evidence of this was shown by Hecht and coworkers, where a trithiazole moiety (Figure 1.05) exhibited altered sequence selectivity from the primary 5′-GC-3′ patterns to less commonly observed 5′-GT-3′.[22]

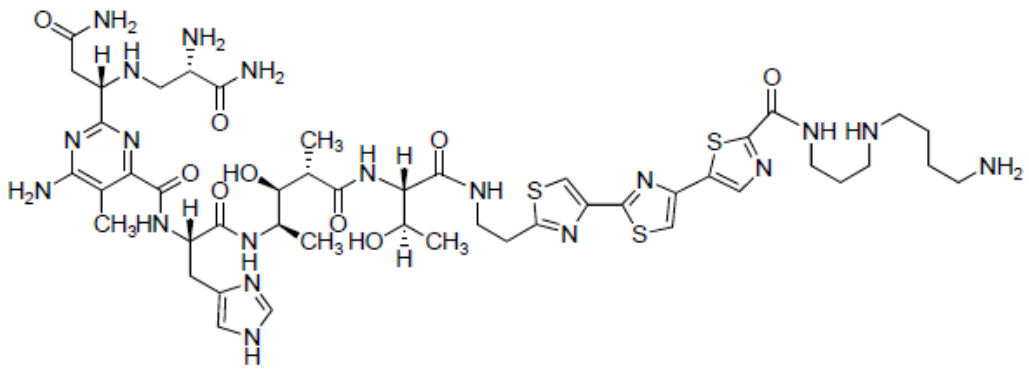

**Figure 1.06**. DeglycoBLM congener containing a trithiazole moiety[22]

Between the N-terminal metal ion binding domain (PBA) and the C-terminal DNA binding domain is a linker region composed of L-threonine and methylvalerate moieties. Other than simply acting as a tether between the N- and C-termini of BLM, the complete functionality of the linker region was not fully understood until nearly a decade after bleomycin was isolated.[23.24] In a previous by Boger and coworkers, the linker region was studied by substituting a peptide chain that lacked the peripheral substituents (Figure 2.06).[25]

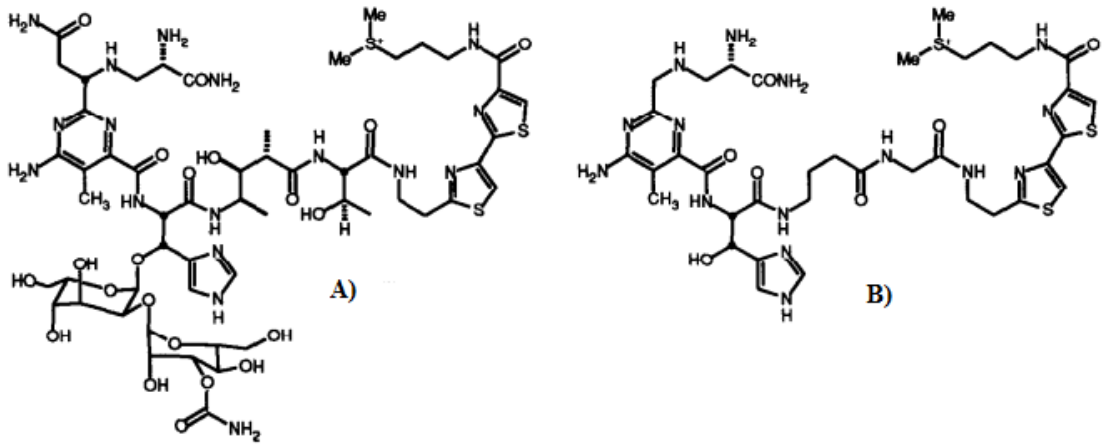


**Figure 2.07** A) BLM $A_2$ B) (deglyco)BLM $A_2$ altered in the linker region[26]

It was found that the BLM $A_2$ congener with the altered linker region

displayed significantly lower cleavage activity when compared with deglycoBLM $A_2$. In a study in the Hecht laboratory, a similar result was also seen when threonine was replaced with an (oligo)glycine spacer (one, two or four residues).[26] The observed cleavage efficiency decreased dramatically and the sequence selectivity was also affected. Lastly, as a comprehensive study involving derivatization of the methylvalerate region was reported by Hecht and coworkers[27] and concluded that not only the stereochemistry of the methylvalerate but also the length of the moiety served to alter the DNA cleavage efficiency of the fully incorporated deglycoBLM $A_6$ analogues. These studies suggest that the linker region and its precise structure serve to facilitate DNA interaction or cleavage and not just simply connect the two functional domains of bleomycin.

The last, non-extensively discussed domain of bleomycin is the disaccharide moiety, composed of L-gulose and D-mannose, it continues to be a subject of ongoing study as a consequence of its purported ability to contribute to cellular recognition and uptake.[28] Especially important within the disaccharide is a C-3 carbamoyl group thought to be necessary in cellular recognition as well. In an ongoing study in the Hecht laboratory it was found that when changing the position of the carbamoyl group (Figure 2.08), altered cellular uptake was observed in fluorescence microscopy studies (unpublished results).

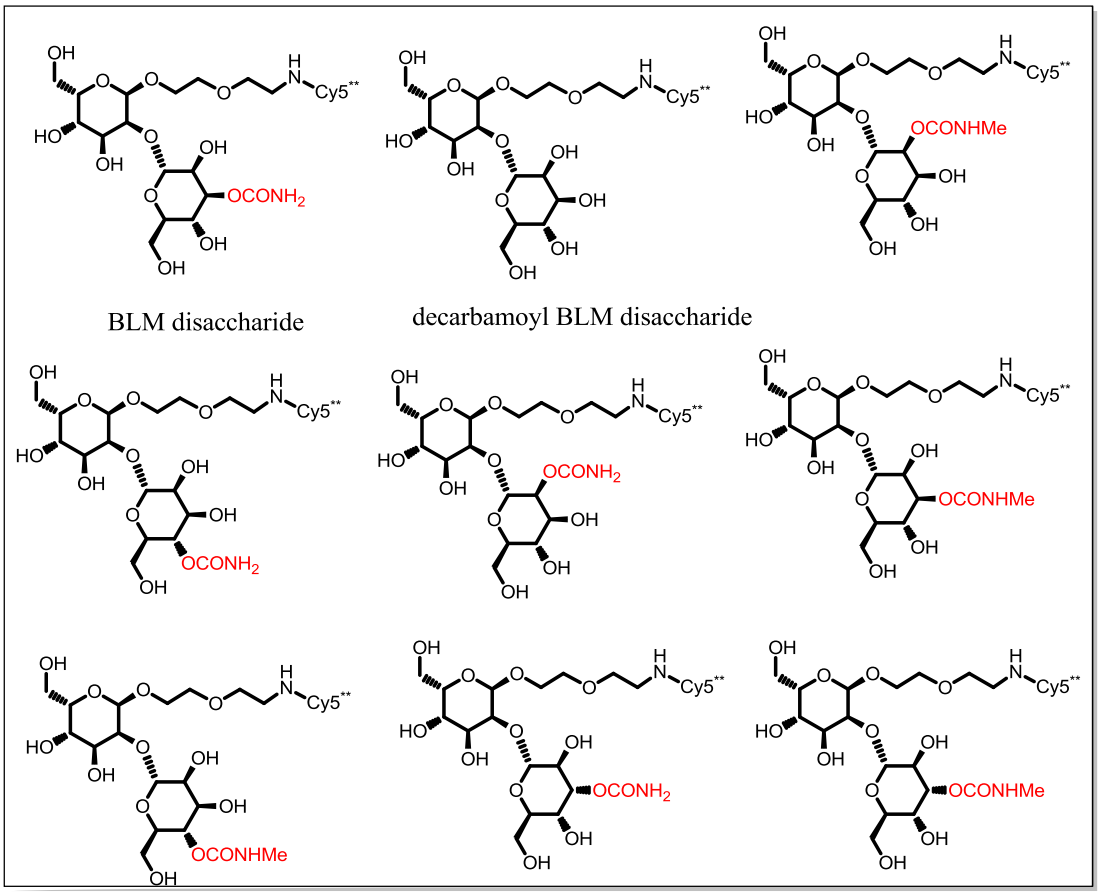


**Figure 1.08** Bleomycin disaccharide with an altered carbamoyl position

Displacement of the native C-3 carbamoyl group by molecular oxygen is believed to be the first step in the formation of an "activated bleomycin"[15,29] that is responsible for mediating the chemistry of DNA strand scission.

There are two primary pathways associated with bleomycin-mediated DNA cleavage. One is frank strand scission, which produces base propenals and results directly in DNA cleavage. The second is via modified nucleotides that result in akali labile lesions and subsequent cleavage sites in the presence of a base such as alkali or *n*-butylamine (Figure 1.09).

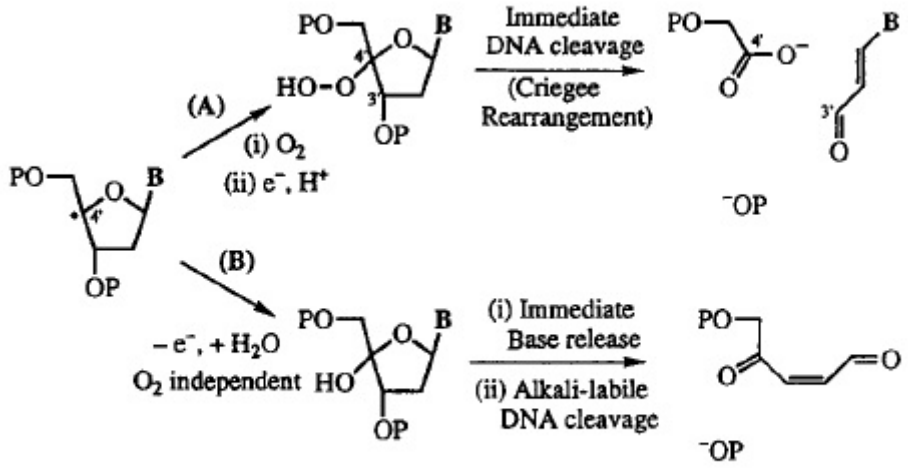


**Figure 1.09** DNA degradation products; (A) frank strand cleavage and (B) oxidative base release.[17]

The two sets of DNA products include oligomers terminating with 5′-phosphate and 3′-phosphoroglycolate moieties,[30] and compounds characterized as base propenals. The second set of DNA products includes free nucleic bases and an alkali-labile deoxyribose product. Bleomycin was once thought to exert its cytotoxicity exclusively through DNA degradation;[31-33] however, there exists evidence of collateral damage of other cellular components associated with bleomycin activation as well. Bleomycin has also been shown to attack RNA[34,35] and even cell walls.[36] In addition to biochemical entities, bleomycin (especially in high concentrations) has demonstrated the ability to mediate chemical transformations of small organic molecules.[16,37,38] An early study carried out by Hecht et al.[16] investigated the chemistry of activated BLM with small substrates known to be cytochrome P-450 substrates, as the mechanism of action is reminiscent of that of cytochrome P-450.[39] Using Fe(III)•BLM $A_2$ conjugates and iodosobenzene as an oxygen surrogate, transformations were observed on a variety of olefins summarized below (Table 1.01).[16]

**Table 1.01** Summary of chemical transformations on small molecules by bleomycin $A_2$[16]

| oxidant | substrate | products, yields[a] | | | | method of det yield[b] |
|---|---|---|---|---|---|---|
| Fe(III)·BLM $A_2$ + $C_6H_5IO$ | 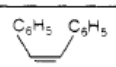 | 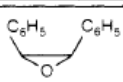 (25, 22) | 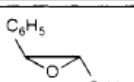 (1) | 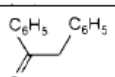 (7) | 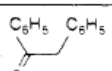 (5-7) | B, C, D |
| Fe(III)·BLM $A_2$ + $C_6H_5IO$ | 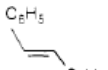 | 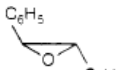 (3) | 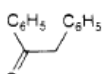 (2) | 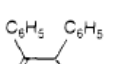 (2) | | B, C, D |
| Fe(III)·BLM $A_2$ + $C_6H_5IO$ |  |  (9) | 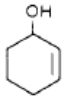 (12) | 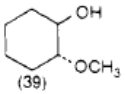 (39) |  (trace) | A |
| Fe(III)·BLM $A_2$ + $C_6H_5IO$ |  | 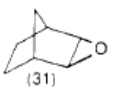 (31) | 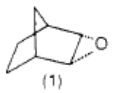 (1) | 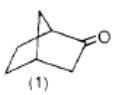 (1) | | A |
| Fe(III)·BLM $A_2$ + $C_6H_5IO$ | 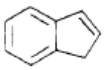 | 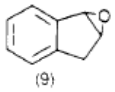 (9) | | | | C |

[a] Yields based on amount of added iodosobenzene; quantitative conversion was assumed. [b] (A) Gas chromatography–mass spectrometry, (B) HPLC analysis, (C) isolation, (D) 360-MHz $^1H$ NMR analysis.

The degradation of DNA occurs in a multistep fashion, whose mechanism is not entirely understood. It is quite complex and has been the subject of ongoing research efforts. The first steps towards the activation of BLM have been previously studied using stopped-flow spectroscopy.[40,41] Researchers postulate that the first step in the process is likely to be the addition of $O_2$ to Fe(II)•BLM, followed by displacement of the carbamoyl group as a metal binding ligand as shown in Figure 1.04. This transient complex (*in vitro)* has been suggested to yield the bleomycin superoxide species $^{\cdot}O_2^{-}$•Fe(III)•BLM. This species is then hypothesized to subsequently undergo disproportionation where a peroxide-Fe(III)•BLM becomes the active species or "activated BLM" (Figure 1.10). This activated species or even the superoxide species intermediate have been suggested to have the ability to interact with and degrade DNA when in close proximity (as would be facilitated by the bithiazole moiety of BLM).

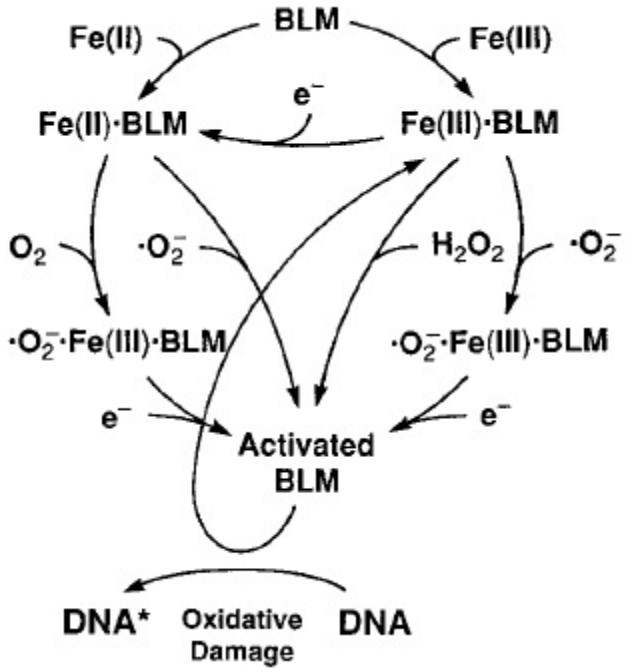


**Figure 1.10** Activated bleomycin formation pathways; reactions with oxygen species and reductants form transient ferric peroxide "activated bleomycin".[17]

Fe(III)•BLM can also give rise to steady-state levels of activated bleomycin by reactions with peroxides to form base propenals as DNA cleavage products.

Additionally, superoxide can contribute to activated bleomycin formation and subsequent DNA degradation (Figure 1.11).

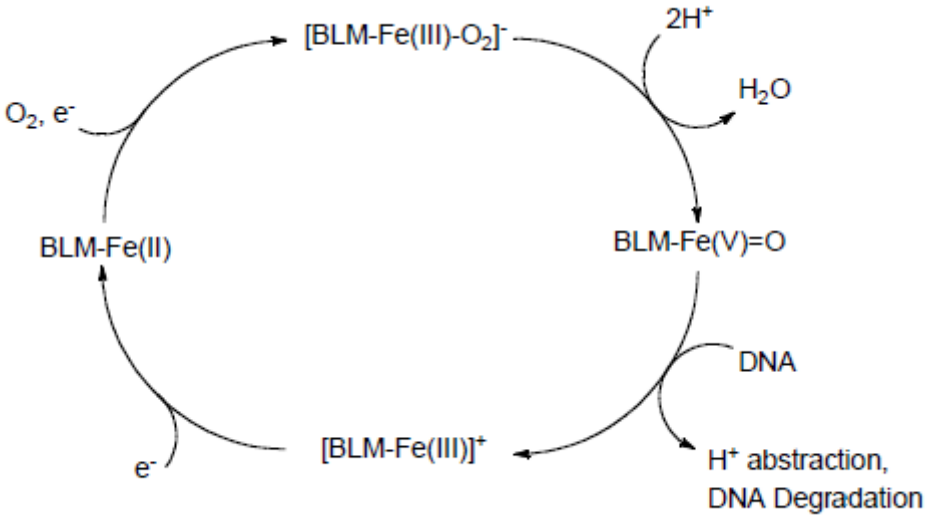


**Figure 1.11** Proposed catalytic cycle of DNA degradation by BLM[42,43]

As previously described BLM exerts its antitumor effects through the creation of high reactive metal-oxo-bleomycin complexes. Specifically, $Fe^{2+}$, a redox-active first row transition element found physiologically, is believed to be the metal ion initially bound to these complexes. Reaction of the Fe•BLM complex with molecular oxygen results in the generation of a metal bound peroxide species which subsequently induces DNA strand scission through abstraction of the C4′ hydrogen atom of ribose.

It was the intention of my research to contribute to the construction of a bleomycin library from which a structure-activity relationship (SAR) could be derived, and also could afford more efficacious BLM analogues, possibly for clinical use.

# Chapter 2

## 2.01 Introduction

Although bleomycin is employed clinically in its metal free forms, Blenoxane (BLM $A_2$, $B_2$) in the United States and BLM $A_5$ in various parts of Asia, the need for novel and even more efficacious analogues remains a research priority. Previously in the Hecht laboratory, a 108-member deglycoBLM combinatorial library was synthesized on a solid support[14,44] in a parallel fashion (Figure 2.01). This included three bithiazole (C-terminal DNA binding domain) derivatives, three threonine and three methylvalerate (linker region) derivatives and four histidine derivatives. The natural pyrimidoblamic acid was used for all 108 deglycoBLM analogues (Figure 2.04).

While each member of the library was found to be active to some extent in a concentration-dependent plasmid DNA relaxation assay, two of the analogues exhibited increased efficiency relative to the parent molecule deglycobleomycin $A_6$. Identification of novel analogues whose potency surpasses that of the parent natural product continues to be a research goal. Using a methodology similar to attachment of a solid-support in the parallel library, it is possible to create a large number of deglycoBLM $A_6$ analogues using a "split-and-mix" library approach (Figure 2.03).

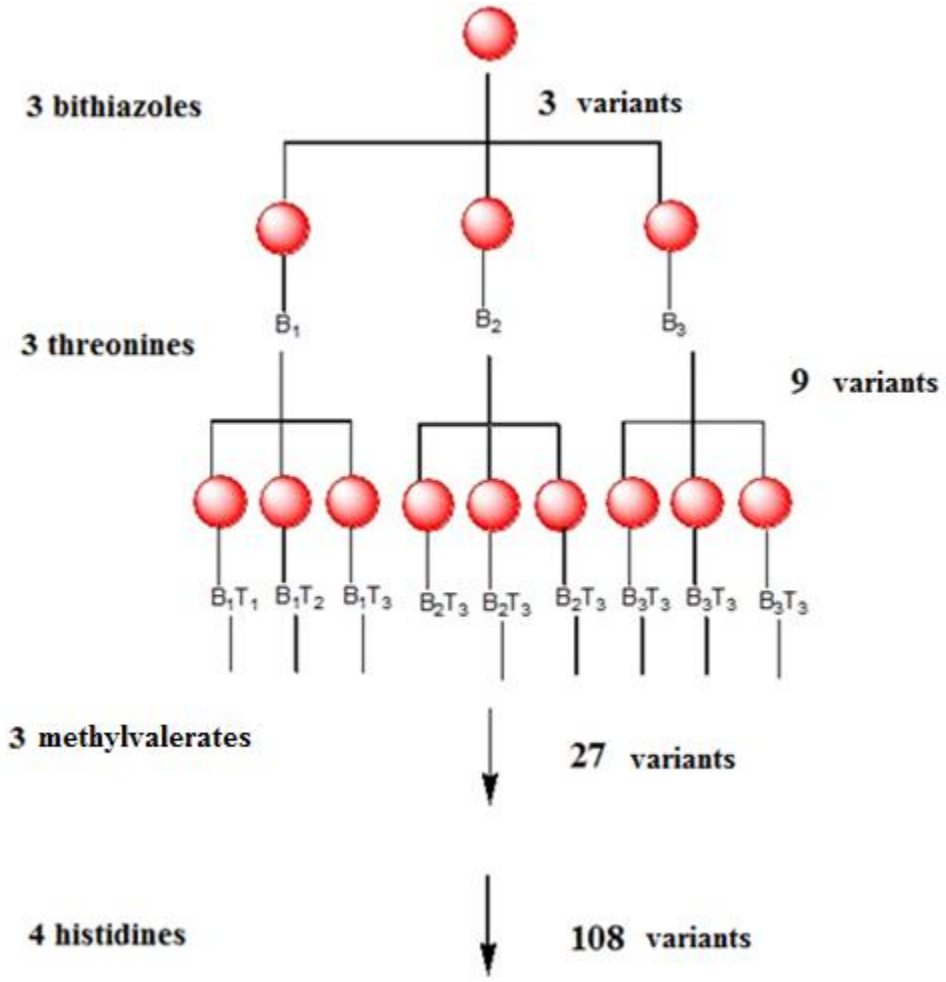


**Figure 2.01** Parallel library synthesis of 108 deglycoBLM analogues

While each member of the library was found to be active to some extent in a concentration-dependent plasmid DNA relaxation assay, two of the analogues exhibited increased efficiency relative to the parent molecule deglycobleomycin $A_6$. Identification of novel analogues whose potency surpasses that of the parent natural product continues to be a research goal. Using a methodology similar to attachment of a solid-support in the parallel library, it is possible to create a vast number of deglycoBLM $A_6$ analogues using a "split-and-mix" library approach (Figure 2.03). This technique allows the synthesis of many different analogues simultaneously; however, the need for a visual/fluorescence assay to identify the active members of such a library continues to be an obstacle for

RNA. Previous studies have led to the development of a 16-nt hairpin DNA substrate that fluoresces in the presence of Fe(II)•BLM (Figure 2.02).

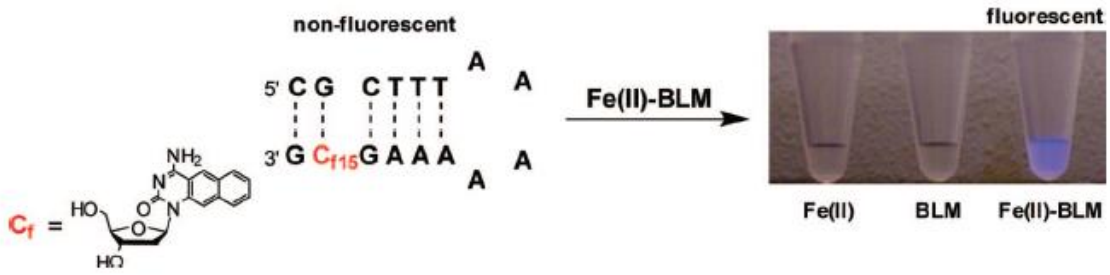


**Figure 2.02** A 16-nucleotide DNA hairpin containing 4-aminobenzo[*g*]quinazoline-2-one 2′-deoxyribose at position 15 was prepared and found to lack significant fluorescence. When treated with Fe(II)·BLM, the hairpin was found to undergo oxidative transformation selectively at position 15. The pro-fluorescent DNA hairpin was used as a substrate for 15 bleomycin congeners.[45]

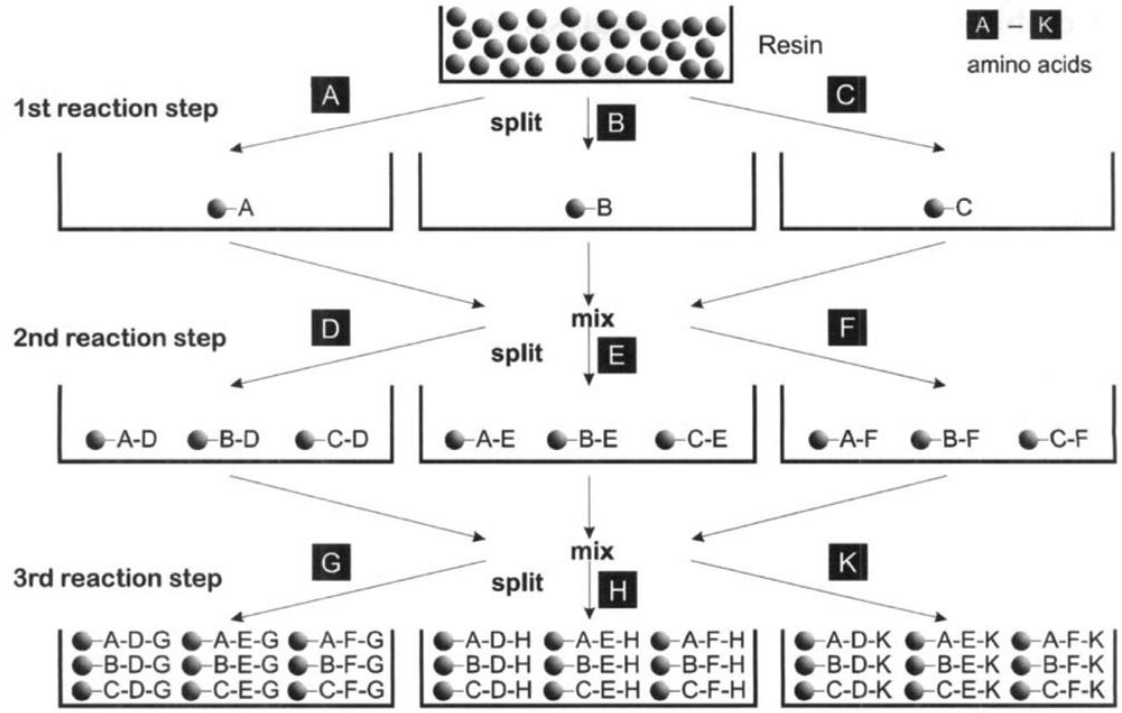


**Figure 2.03** Split-and-mix library methodology scheme

Whereas the previous parallel library technique provided single analogues to assay, the "split-and-mix" library technique affords a mixture of many beads, each of

which contains numerous molecules of a single analogue. This necessitates a strategy for identifying individual compounds with the desired properties. Previous strategies include mass spectrometry techniques.

There are several synthetic routes available for each of the six amino acids that comprise (deglyco)BLM, with pyrimidoblamic acid being the most difficult to prepare. Previous attempts to alter and simplify and change the structure of the heterocycle in pyrimidoblamic acid have been successful and given rise to three primary types of synthetic analogues (Figure 2.04).

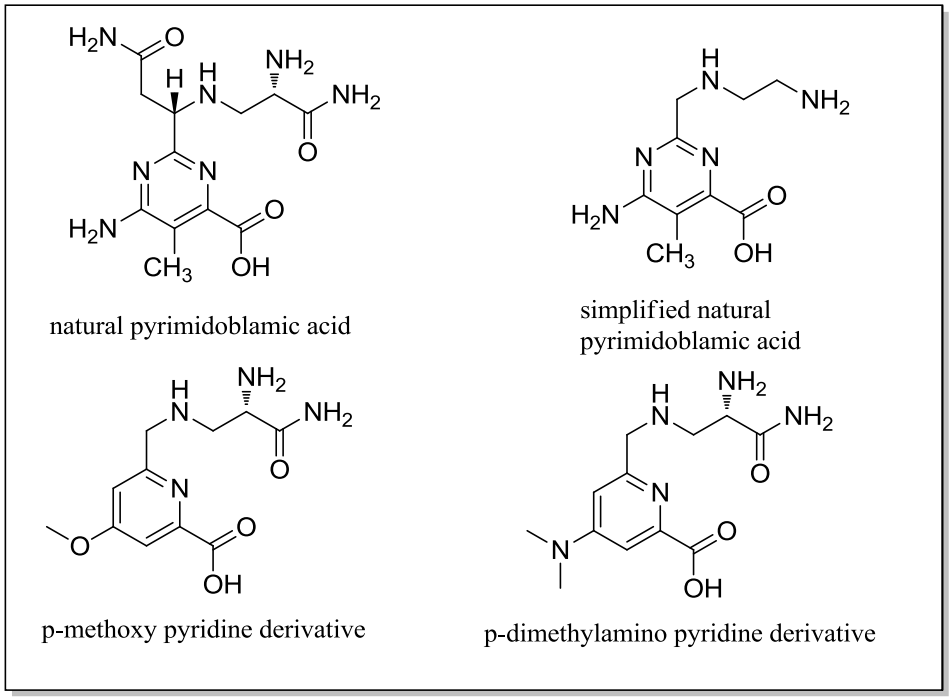


**Figure 2.04** Natural pyrimidoblamic acid and several simplified pharmacophores

The total synthesis of pyrimidoblamic acid has been described previously[12,17,18,46] and its key structurally active elements, (those which play a critical role in $O_2$ activation in the mechanism of BLM) identified. The synthesis of the complete compound containing two stereocenters involves very complicated chemical transformations

including stereoselective reactions and preparative TLC or HPLC separation of enantiomeric or diastereomeric intermediates. Due to the arduous nature of the diastereomeric selective total synthesis, and the subsequent separations involved, simplified analogues of PBA (those which retain activity when incorporated into deglycoBLM) have been identified. This included the omission of a stereocenter (which incorporation into PBA is synthetically complex) and the associated C-2 acetamido side chain to create an analogue which behaved similarly when incorporated into BLM.[47]

Further investigations and computational studies based on electron density profiles, showed certain para-substituted pyridine heterocycles could be substituted in place of the more complex pyrimidine moiety.[4,6] This knowledge enabled the creation of a small library of substituted pyridine and pyrimidine based pyrimidoblamic acid analogues which were subsequently incorporated into novel deglycoBLM $A_6$ analogues by solid phase peptide synthesis (Scheme 2.07) and whose activities were analyzed using a pSP64 supercoiled DNA plasmid relaxation assay (Figures 2.07-2.09).

## 2.02 Results

Boc-Ser-OH and *O*-benzylhydroxylamine HCl were coupled using DCC in a 1:1 THF–$H_2O$ solution at pH ~4.5 to afford **2.01** in 60% yield.[48] Alcohol **2.01** was cyclized via an intramolecular mitsunobu reaction in THF to give amide **2.02** in good yield (89%).[13,18] Amide **2.02** was treated with a saturated methanolic ammonia solution at 0 $^oC$ to give amine **2.03** in 81% yield. Amine **2.03** was deprotected using 10% Pd/C in MeOH under an $H_2$ atmosphere at room temperature over two days and subsequently converted to its corresponding HCl salt by treatment with HCl gas in a 1:5 MeOH–$Et_2O$ solution at 0 $^oC$ to give **2.05** in 74% yield over the two steps (Scheme 2.01).[18]

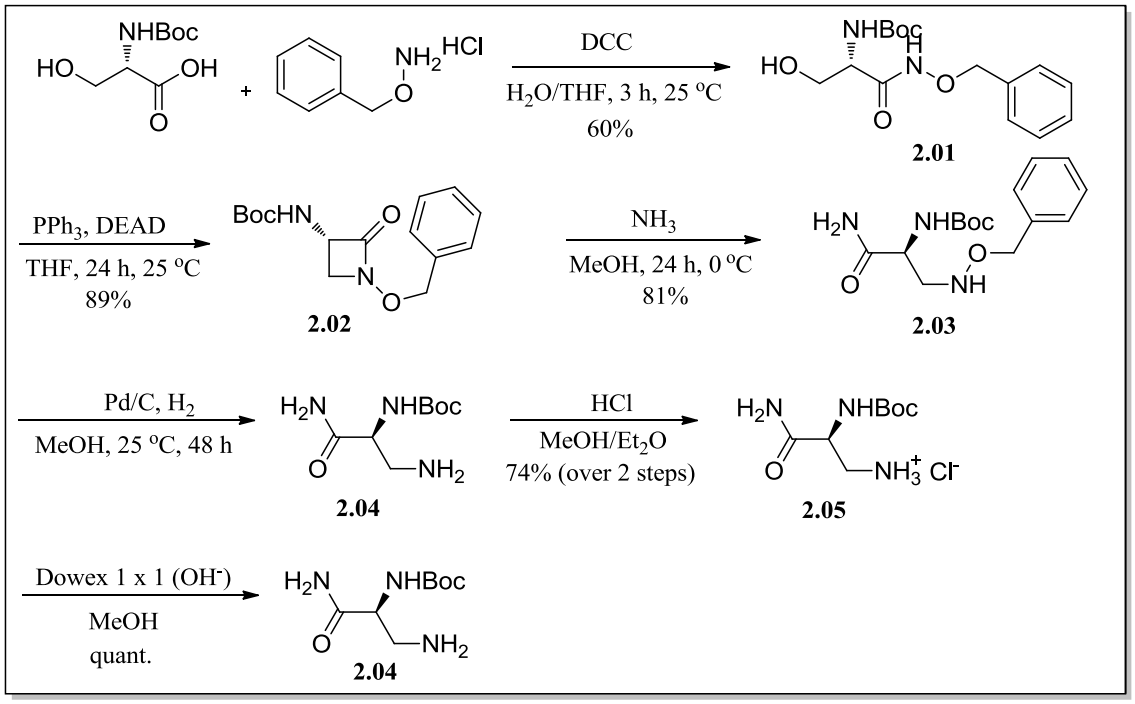


**Scheme 2.01** Synthesis of the β-aminoalanineamide moiety of PBA (2.04)

Propionamidine HCl was prepared as previously described by Rapaport and co-workers[49] by treatment of propionitrile with HCl to form the imidate hydrate intermediate, and then by treatment with $NH_3$ to give propionamidine HCl **2.06** (Scheme 2.02) in excellent 99% yield.

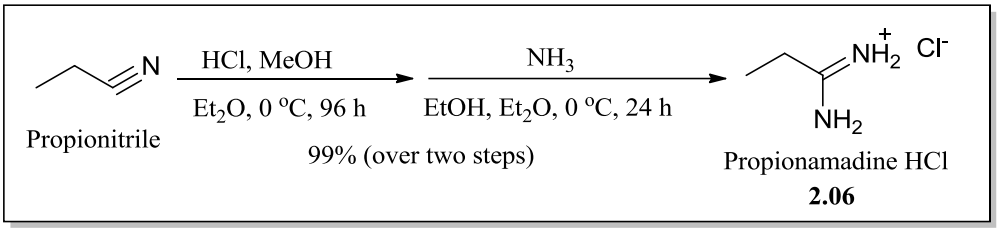


**Scheme 2.02 S**ynthesis of propionamidine HCl (2.06)[49]

Pyrimidine **2.07** was prepared by warming a 2:1 mixture of previously prepared propionamidine HCl, **2.06** and commercially available triethyl 1,3,5-triazine-2,4,6-tricarboxylate in DMF over a period of three days (Scheme 2.23). Crystallization of the crude mixture from EtOAc–hexanes provided pyrimidine **2.07** in 49% yield. Treatment of **2.07** with $NaBH_4$ (1 eq.) in EtOH at 5 $^oC$ over a period of 6 days gave the selectively reduced 2-hydroxymethylpyrimidine **(2.08)** in modest 25% yield. Alcohol **2.08** was converted to the corresponding tosylate by treatment with Ts-Cl (1.5 eq.) and $K_2CO_3$ (2 eq.) in $CH_3CN$ at room temperature for 24 h. Flash column chromatography on silica gel afforded pure tosylate **2.09** in 78% yield.[13] Compound **2.09** was coupled with commercially available *N*-Boc-ethylenediamine via an $S_N2$ displacement reaction. A mixture of the tosylate, $NaHCO_3$ (2 eq.), and *N*-Boc-diamine (4 eq.) in $CH_3CN$ was stirred overnight at 25 $^oC$. Filtration, followed by concentration of the solvent *in vacuo*, gave the crude coupling product as a colorless oil. Treatment with $(Boc)_2O$ (2 eq.) and $Et_3N$ (4 eq.) in $CH_2Cl_2$ at room temperature overnight provided the corresponding Boc protected product **2.10** in nearly quantitative yield (90%) over two steps following the purification via flash column chromatography on silica gel. Hydrolysis of ester **2.10** afforded the final pyrimidoblamic acid analogue **2.11** using 1 N aq LiOH (2 eq.) in a mixture of 3:1:1 THF–MeOH–$H_2O$. An extensive aqueous workup and subsequent purification by flash column chromatography on silica gel gave final compound **2.11** as a

colorless solid in 60% yield.[12,29]

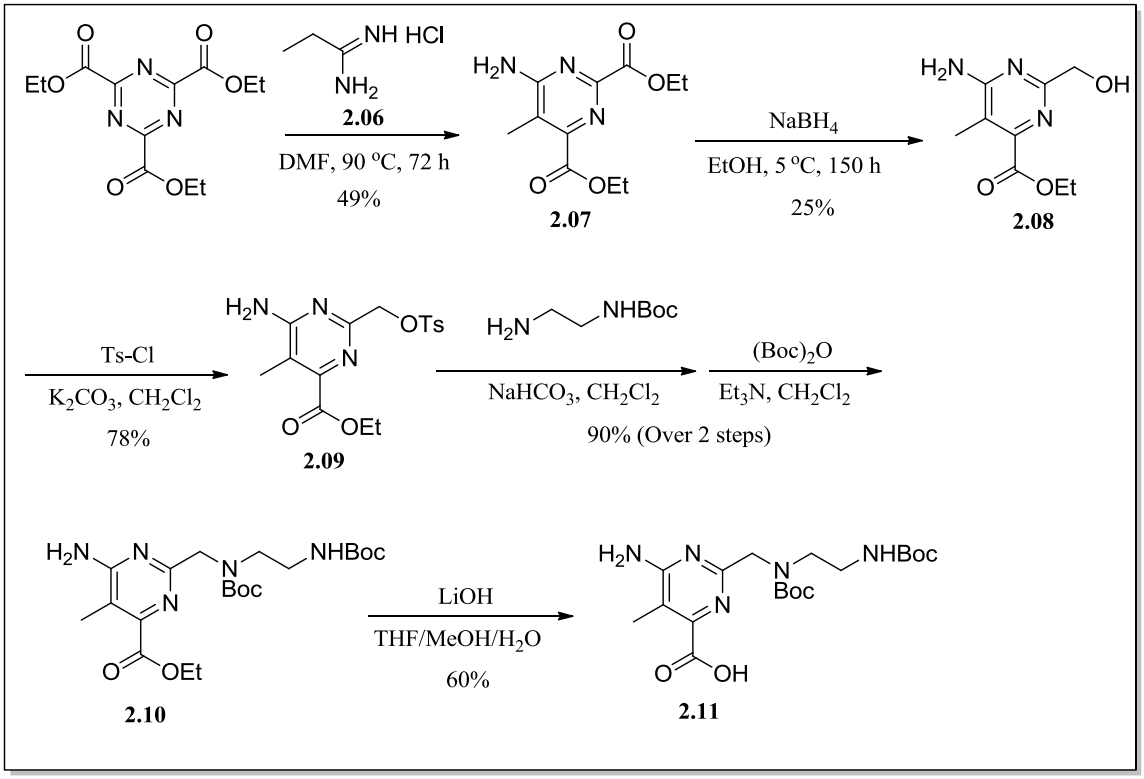


**Scheme 2.03** Synthesis of 6-amino-2-(((*tert*-butoxycarbonyl)(2-((*tert*-butoxycarbonyl)amino)ethyl)amino)methyl)-5-methylpyrimidine-4-carboxylic acid (2.11)

Tosylate **2.09** was coupled with commercially available cyclic amines **a-f** (Scheme 2.24) via an $S_N2$ displacement reaction. A mixture of the tosylate **2.09**, $NaHCO_3$ (2 eq.), and the simple *N*-Boc-protected amine (3 eq.) in $CH_3CN$ was stirred overnight at 25 °C. Filtration through Celite® followed by concentration of the solvent *in vacuo* gave the crude coupling products as a colorless oils. Subsequent treatment with $(Boc)_2O$ (2 eq.) and $Et_3N$ (4 eq.) in $CH_2Cl_2$ at room temperature overnight provided the corresponding Boc protected products **2.12a-f** in yields ranging from 65-98% (over two steps). Hydrolysis of esters **2.13a-f** using LiOH (2 eq.) in a mixture of 3:1:1 THF–MeOH–$H_2O$ gave the corresponding final carboxylic acid products **2.13a-f** in moderate to

good yields (27-83%) following silica gel flash column chromatography.

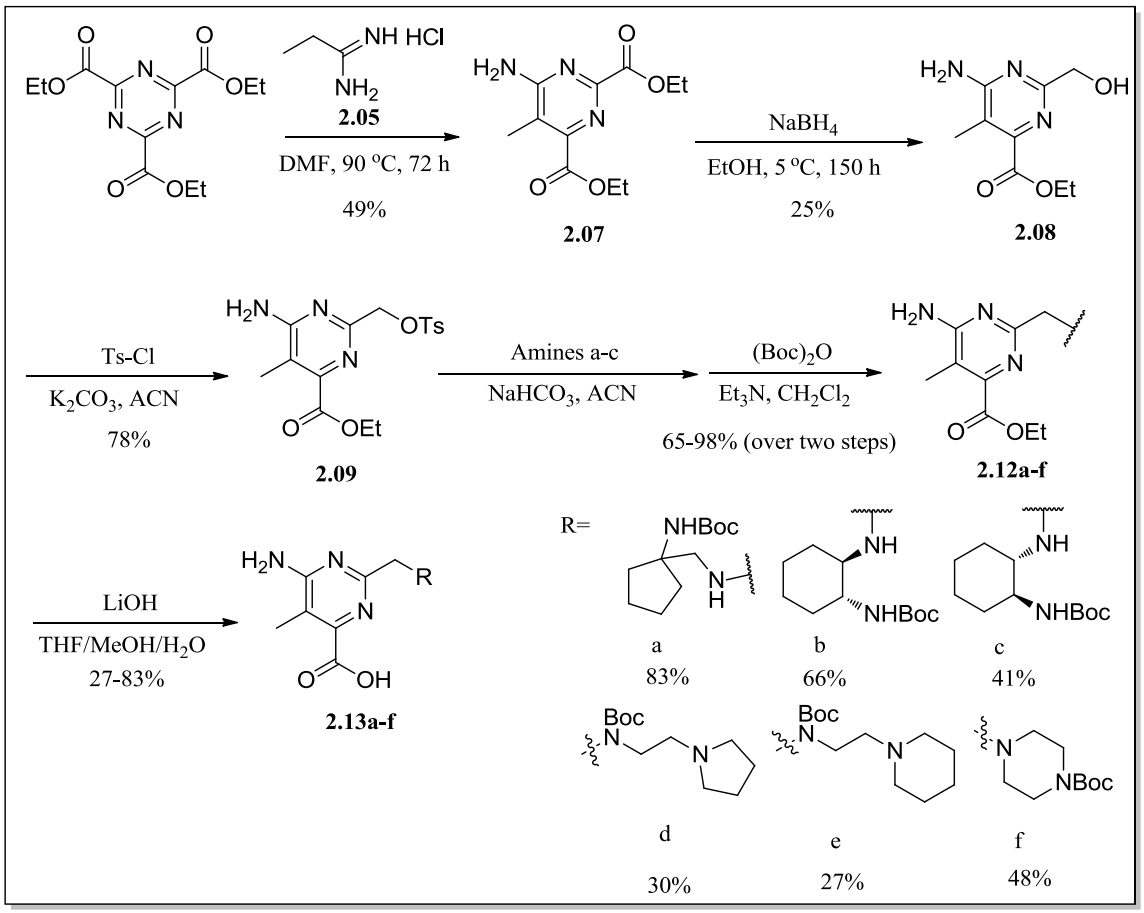


**Scheme 2.04** Synthesis of cyclic pyrimidoblamic acid analogues (2.13a-f)

The esterification of commercially available chelidamic acid monohydrate using 5.5 equivalents of $SOCl_2$ in MeOH at room temperature over a period of three days afforded diester **2.14** as a colorless solid in 71% yield (Scheme 2.05). Dimethyl chelidamate **2.14** was then treated with three equivalents of dimethyl sulfate and $K_2CO_3$ in DMF at room temperature to give pyridine **2.15** as a colorless solid in 48% yield.[50,51] Substituted pyridine **2.15** was selectively reduced using $NaBH_4$ in a 6:1 MeOH–$CH_2Cl_2$ solution to give alcohol **2.16** as a colorless solid in 84% yield.[51-53] Alcohol **2.16** was treated with ten equivalents of $MnO_2$ in $CH_2Cl_2$ at room temperature for 24 h to give aldehyde **2.17** as a colorless solid in 64% yield.

A methanolic solution of **2.05** was passed through a Dowex 1 x 2 ion exchange column ($^{-}$OH form) to regenerate free base **2.04** in quantitative yields.[18] A solution of aldehyde **2.17** in $CH_3CN$ was added to a solution of the freshly prepared free amine **2.04** in $CH_3N$ in the presence of 4Å powdered molecular sieves at room temperature. The Schiff base coupling intermediate was treated with 10% Pd/C in MeOH at room temperature under an $H_2$ atmosphere for 24 hours to generate the corresponding amine, subsequent protection by treatment with $(Boc)_2O$ and $Et_3N$ in $CH_2Cl_2$ at room temperature over 24 hours afforded the protected coupling product **2.18** in 80% yield over the three step sequence (Scheme 2.26). Hydrolysis of ester **2.18** was performed to obtain the final pyrimidoblamic acid analogue **2.19** using 1 N aq LiOH (2 eq.) in a mixture of 3:1:1 THF–MeOH–$H_2O$. An extensive aqueous workup and subsequent purification by flash column chromatography on silica gel gave final compound **2.19** as a colorless solid in 58% yield. [13,18]

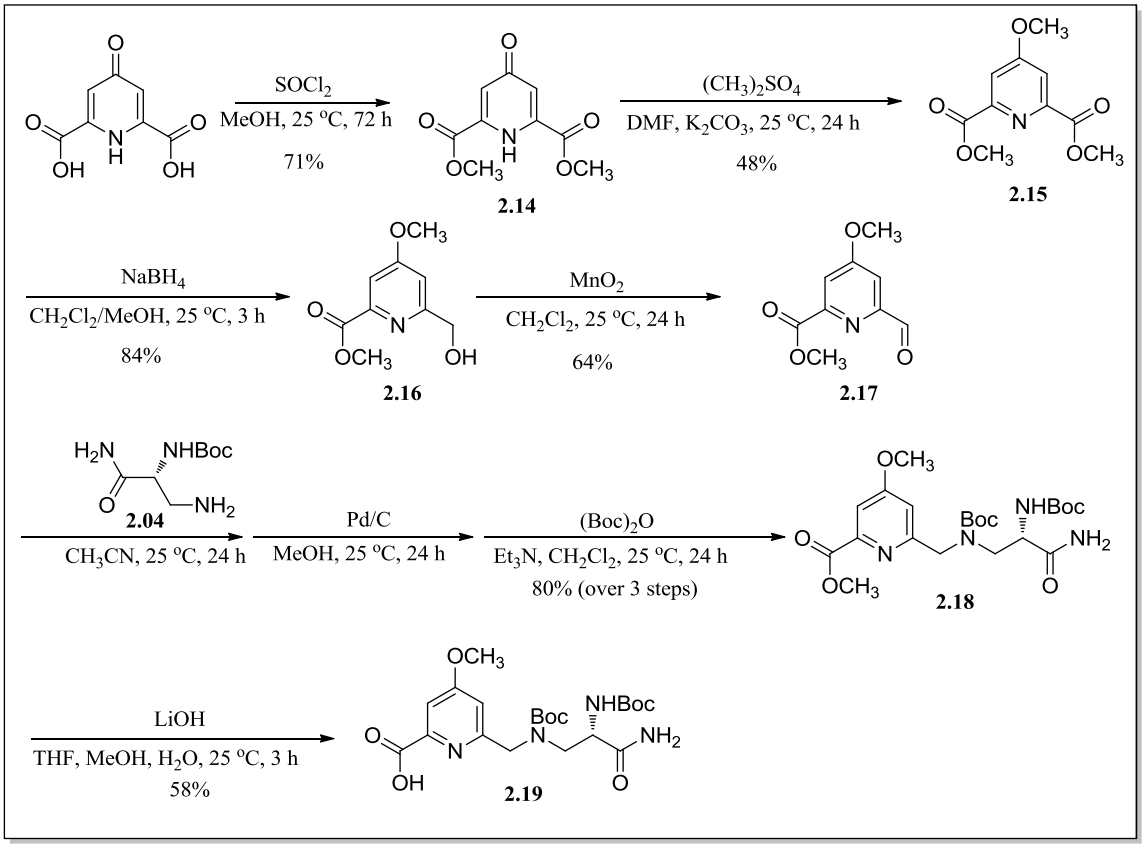


**Scheme 2.05** Synthesis of (*S*)-6-(((3-amino-2-(*tert*-butoxycarbonylamino)-3-oxopropyl)(*tert*-butoxycarbonyl)amino)methyl-4-methoxypicolinic acid (2.19).

Chlorination and esterification of commercially available chelidamic acid monohydrate using 3.2 equivalents of $PCl_5$ in $CCl_4$ and MeOH at reflux followed by crystallization from MeOH afforded diester **2.20** as colorless needles in 58% yield (Scheme 2.06).[53,54] Diester **2.20** was hydrolyzed to the corresponding diacid by treatment with 1 N aq NaOH to give crude **2.21** in quantitative yields. Crude diacid **2.21** underwent nucleophilic aromatic substitution in 40% (w/w) aq *N*,*N*-dimethylamine solution under pressure to give the crude 4-*N*,*N*-dimethylaminopyridine diacid **2.22** in 97% yield. Subsequent treatment with 10 equivalents of $SOCl_2$ in MeOH at reflux followed by crystallization from acetone provided the corresponding 4-*N*,*N*-dimethylamino diester **2.23** as colorless needles in good yield (78%).[54] Reduction with

1.7 eq. of $NaBH_4$ in a 7:1 $CH_2Cl_2$–MeOH solution afforded the alcohol **2.24** in a modest 46% yield followed by oxidation with ten eq. of $MnO_2$ in warm $CH_3CN$ to yield the corresponding aldehyde **2.25** in 80% yield.

A methanolic solution of **2.05** was passed through a Dowex 1 x 2 ion exchange column ($^-$OH form) to regenerate free base **2.04** in quantitative yields.[18] A solution of aldehyde **2.25** in $CH_3CN$ was added to a solution of the freshly prepared free amine **2.04** in $CH_3CN$ in the presence of 4Å powdered molecular sieves at room temperature. The Schiff base coupling intermediate was treated with 10% Pd/C in MeOH at room temperature under an $H_2$ atmosphere for 24 hours to generate the corresponding amine, then subsequent protection by treatment with $(Boc)_2O$ and $Et_3N$ in $CH_2Cl_2$ at room temperature over 24 hours afforded the protected coupling product **2.26** in 39% yield over the three step sequence (Scheme 2.06). Hydrolysis of ester **2.26** was performed to obtain the final pyrimidoblamic acid analogue **2.27** using 1 N aq LiOH (2 eq.) in a mixture of 3:1:1 THF–MeOH–$H_2O$. An extensive aqueous workup and subsequent purification by flash column chromatography on silica gel gave final compound **2.27** as a colorless solid in 57% yield.[13,18]

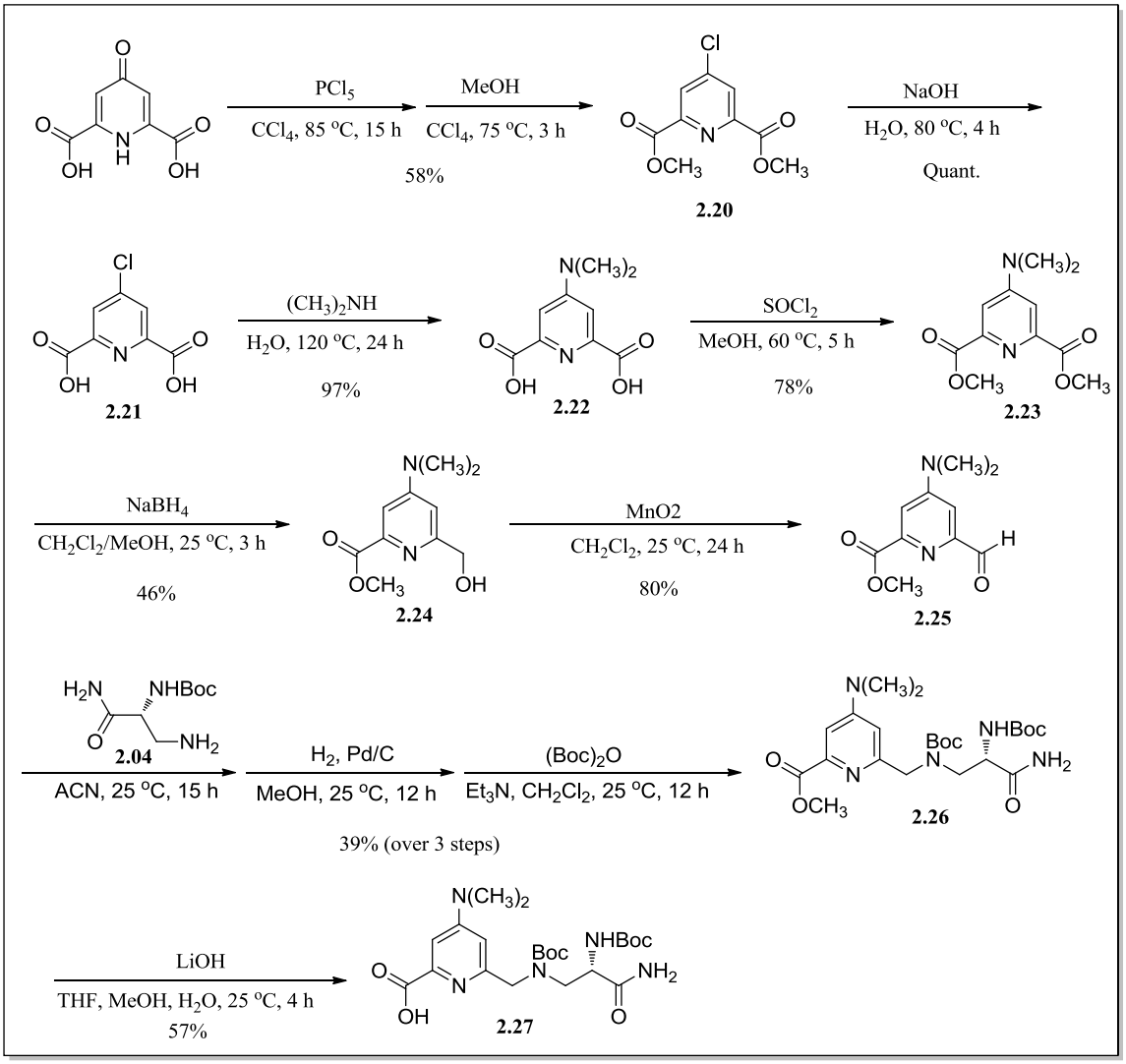


**Scheme 2.06** Synthesis of (*S*)-6-(((3-amino-2-((*tert*-butoxycarbonyl)amino)-3-oxopropyl)(*tert*-butoxycarbonyl)amino)methyl)-4-(dimethylamino)picolinic acid (2.27)

Synthesis of the novel deglycoBLM $A_6$ analogues **(2.32-2.40)** proceeded efficiently, without complications and followed established protocols in the literature for solid phase peptide synthesis (Scheme 2.07).[14,44] Functionalization of the NovaSyn resin with linker (10 eq.) was done using HBTU and Hunig's base in DMF and was measured qualitatively using the Kaiser test. Addition of the Boc-protected spermine was done similarly using 9 eq. of reagent and was also measured qualitatively using the Kaiser test. Attachment of the natural Fmoc-bithiazole was accomplished using 3 eq. each, of the

Fmoc-protected amino acids, HBTU and Hunig's base. This process was repeated for each of the first four amino acids, with the addition of each amino acid measured by quantitative Fmoc cleavage analysis using 20% piperidine in DMF, and with a yield >90% for each amino acid addition. For attachment of each of the synthetic novel pyrimidoblamic acid analogues (Figure 2.07) **(2.11, 2.13a-2.13f, 2.19, 2.27)** 1.5 eq. of each were used in addition to 1.5 eq. BOP coupling reagent and 3 eq. of Hunig's base. Complete deprotection of the fully synthesized deglycoBLM $A_6$ analogues was done using triisopropylsilane, $(CH_3)_2S$ and TFA to remove the Boc and trityl protecting groups on the resin-bound peptide. Treatment with successive aliquots of a 2% hydrazine in DMF solution afforded the crude hexapeptide in solution, cleaved from the resin. The crude deglycoBLM $A_6$ was purified via HPLC, and its mass measured spectrophotometrically. Each deglycoBLM $A_6$ analogue **(2.32-2.40)** was analyzed using a supercoiled DNA plasmid relaxation assay (Figures 2.07-2.09).

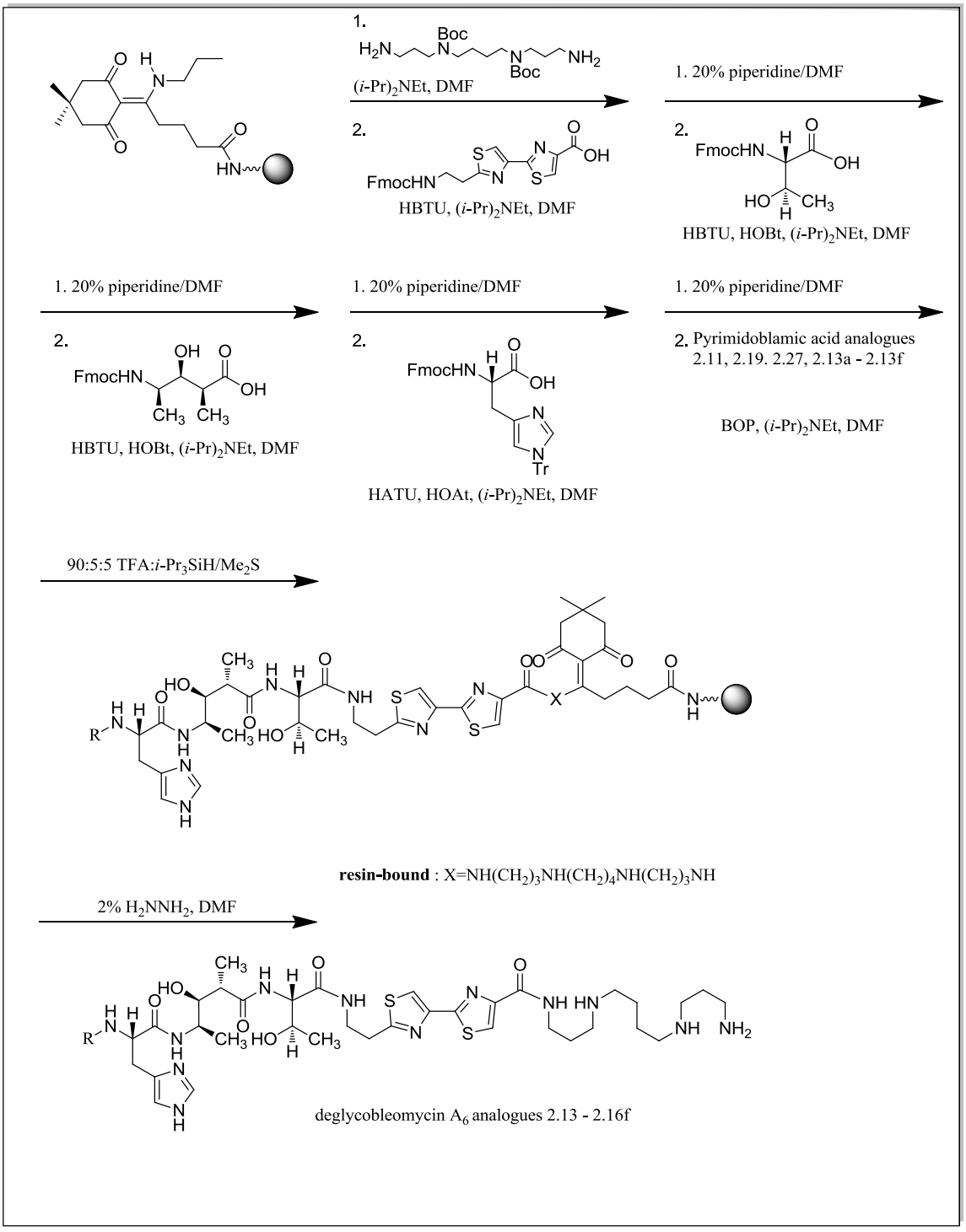


**Scheme 2.07** Representative scheme for solid phase synthesis of deglycoBLM $A_6$ analogues[14]

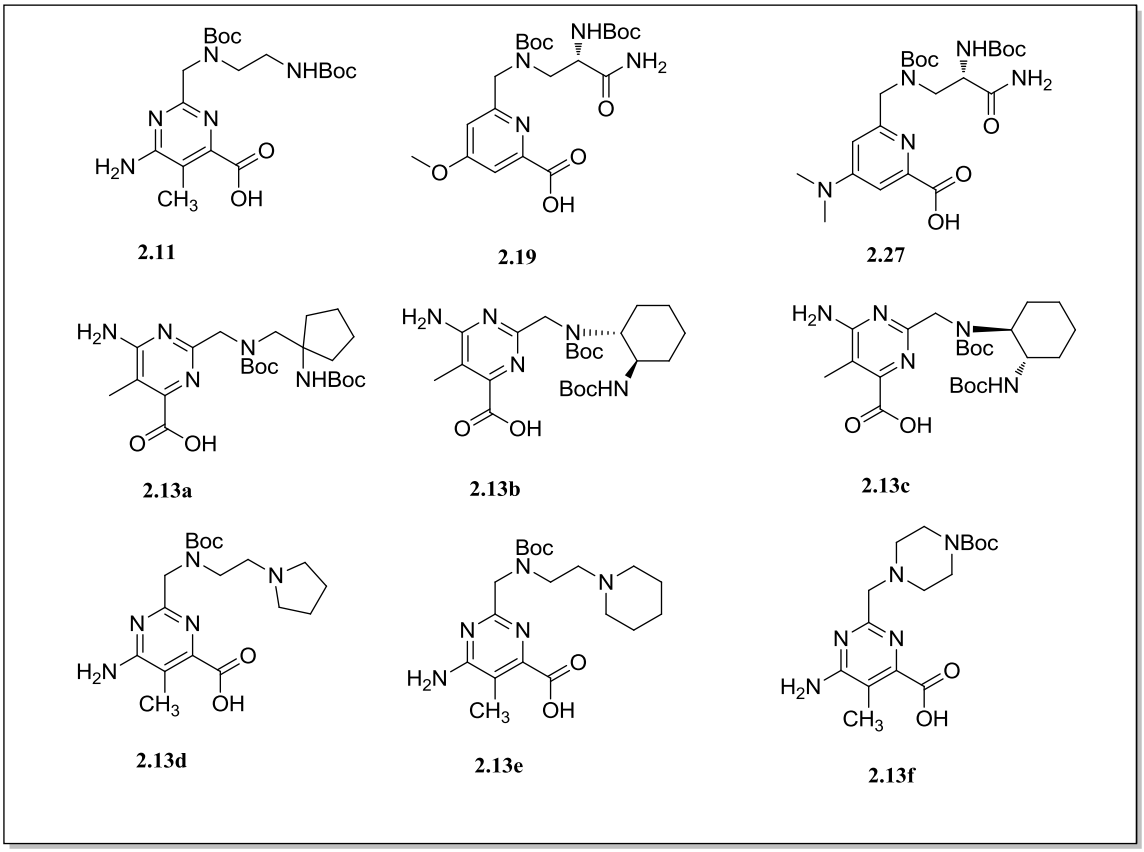


**Figure 2.05** Pyrimidoblamic acid analogues incorporated into solid phase synthesis of novel deglycoBLM $A_6$ analogues[55]

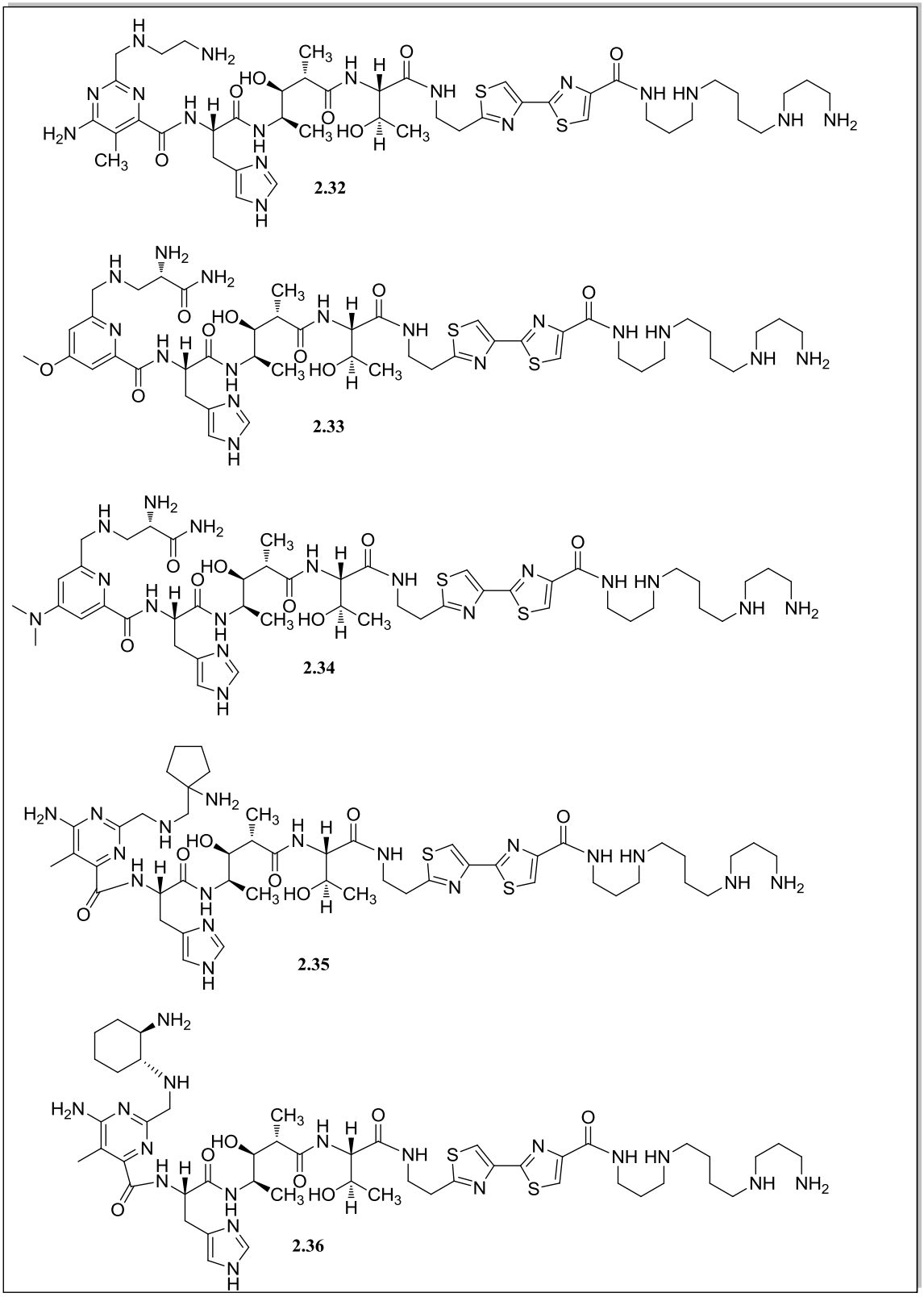


**Figure 2.06** Novel deglycoBLM $A_6$ analogues

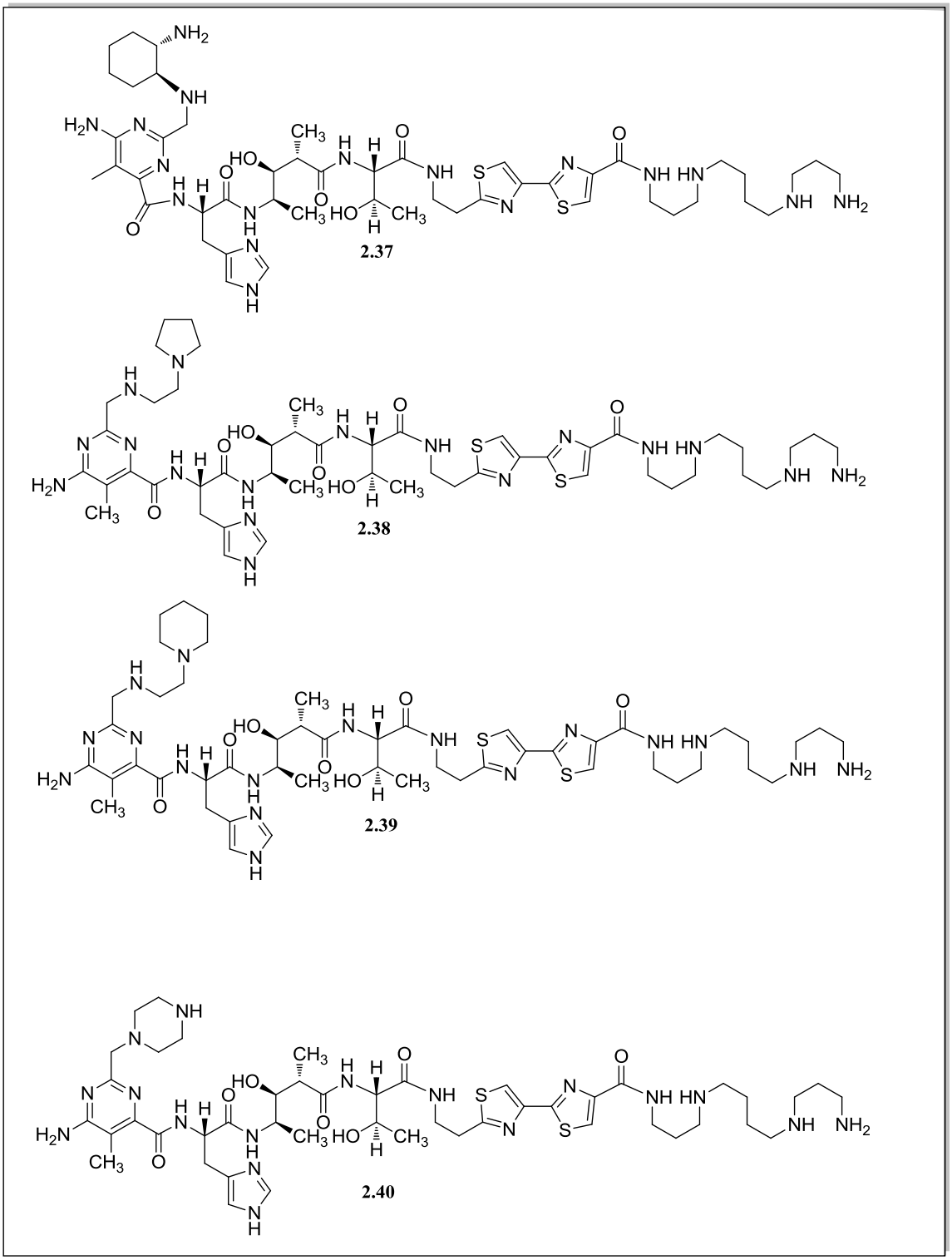


**Figure 2.06** Novel deglycoBLM $A_6$ analogues (cont'd)

**Biochemical Results – pSP64 supercoiled DNA plasmid relaxation assay**

The series of novel deglycoBLM $A_6$ analogues **(2.32-2.40)** were analyzed for their ability to cleave DNA in a simple supercoiled DNA plasmid relaxation assay on an agarose gel. Positive (deglycoBLM $A_5$, lanes 2-6) and negative (DNA alone; lane 1, DNA + Fe(II); lane 2) controls were run in addition to the three concentrations (2, 10 and 16 μM) of the analogues. Three forms of DNA are observed on the agarose gel (I,II,III); Form I, is the supercoiled plasmid DNA, Form II is a single (or minimally nicked) coiled plasmid DNA and Form III indicates linear duplex DNA (Figures 2.07-2.09).

In the first gel (Figure 2.07), analogues **2.32-2.34** all showed DNA relaxation activity only at the highest (16 μM) concentration. Compound **2.32** displayed minimal activity at 10 μM whereas compounds **2.33** and **2.34** both showed stronger activity at 10 μM concentration and yielded primarily relaxed coil DNA (Form II). All three analogues (**2.32-2.34**) showed similar activity at 10 μM but decreased activity at 16 μM compared to the control compound, deglycoBLM $A_5$ (Figure 2.07, control; lanes 1-6). As can be seen for the parent compound deglycoBLM $A_5$ at 16 μM, the entire lane (lane 6) has been nearly cleared, while none of the analogues displayed such strong activity at 16 μM.

In the second agarose gel (Figure 2.08) where deglycoBLM $A_6$ analogues **2.35-2.37** were analyzed, it was found that the three compounds had similar activity at both 10 μM and 16 μM concentrations, and all three appeared inactive at 2 μM. Compound **2.36**, produced relaxed coil DNA (Form II) almost exclusively at 10 and 16 μM concentrations. Compounds **2.36** and **2.37** showed a more balanced distribution of relaxed coil (Form II) and linear duplex (Form III) at the higher concentrations (10 μM;

lanes 13-14, 16 μM; lanes 17-18). All three compounds showed similar activity to the control at 10 μM, giving rise to complete depletion of the supercoiled DNA band and yielding primarily relaxed coil DNA (Form II). At the highest concentration of 16 μM (lanes 10, 14 and 18), the three compounds displayed decreased activity over the control (lane 6).

In the third agarose gel (Figure 2.09) where deycloBLM $A_6$ analogues **2.38**-**2.40** were analyzed, it was found that the three compounds were similarly inactive at 2 μM. Compound **2.38** and **2.39** showed strong activity at both 10 and 16 μM concentrations yielding almost exclusively relaxed coil DNA (Form II) with minimal linear duplex DNA (Form III) seen, with the exception of **2.39** at 16 μM where there appeared a more equal distribution of degraded DNA. Compound **2.40** displayed different activities at 10 and 16 μM, showing stronger activity than compounds **2.38** and **2.39** at identical concentrations but decreased activity compared to the control compound deglycoBLM $A_5$ whose lane was almost completely cleared (lane 6).

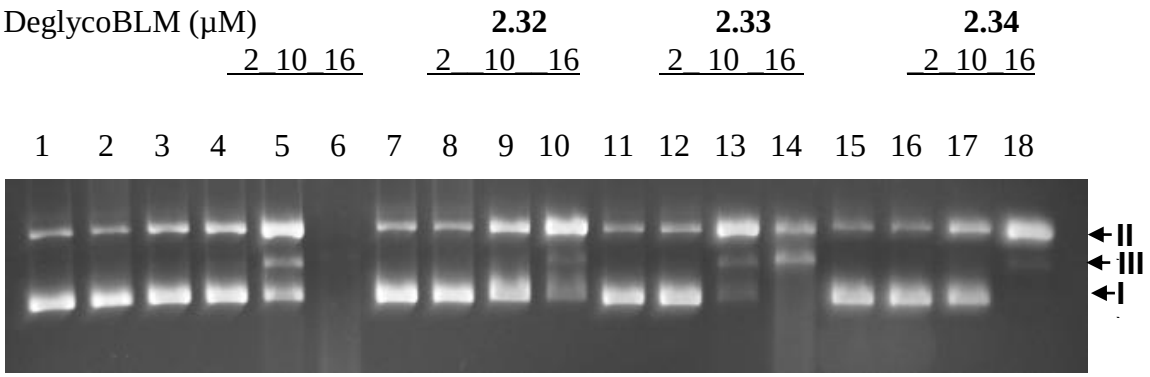


**Figure 2.07** pSP64 DNA plasmid relaxation assay on an agarose gel; deglycoBLM $A_6$; analogues 2.32-2.34 (I – supercoiled, II – relaxed coil, III – linear duplex)
Lane 1, 100 ng DNA alone; Lane 2, 16μM Fe(II); Lane 3, 16 μM deglycoBLM $A_5$; Lane 4, 2 μM Fe(II)•deglycoBLM $A_5$; Lane 5, 10 μM Fe(II)•deglycoBLM $A_5$; Lane 6, 16 μM Fe(II)•deglycoBLM $A_5$; Lane 7, 16 μM Fe(II)•deglycoBLM $A_6$ analogue **2.32**; Lane 8, 2 μM Fe(II)•deglycoBLM $A_6$ analogue **2.32**; Lane 9, 10 μM Fe(II)•deglycoBLM $A_6$ analogue **2.32**; Lane 10, 16 μM Fe(II)•deglycoBLM $A_6$ analogue **2.32**; Lane 11, 16 μM Fe(II)•deglycoBLM $A_6$ analogue **2.33**; Lane 12, 2 μM Fe(II)•deglycoBLM $A_6$ analogue **2.33**; Lane 13, 10 μM Fe(II)•deglycoBLM $A_6$ analogue **2.33**; Lane 14, 16 μM Fe(II)•deglycoBLM $A_6$ analogue **2.33**; Lane 15, 16 μM Fe(II)•deglycoBLM $A_6$ analogue **2.34**; Lane 16, 2 μM Fe(II)•deglycoBLM $A_6$ analogue **2.34**; Lane 17, 10 μM Fe(II)•deglycoBLM $A_6$ analogue **2.34**; Lane 18, 16 μM Fe(II)•deglycoBLM $A_6$ analogue **2.34**;
This experiment was performed by Chenhong Tang.

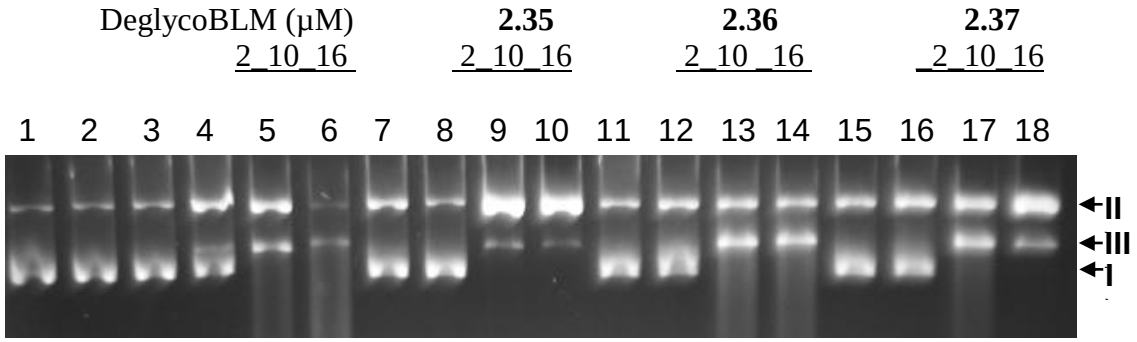


**Figure 2.08** – pSP64 DNA plasmid relaxation assay on an agarose gel; deglycoBLM $A_6$; analogues 2.35-2.37 (I – supercoiled, II – relaxed coil, III – linear duplex)
Lane 1, 100 ng DNA alone; Lane 2, 16μM Fe(II); Lane 3, 16 μM deglycoBLM $A_5$; Lane 4, 2 μM Fe(II)•deglycoBLM $A_5$; Lane 5, 10 μM Fe(II)•deglycoBLM $A_5$; Lane 6, 16 μM Fe(II)•deglycoBLM $A_5$; Lane 7, 16 μM Fe(II)•deglycoBLM $A_6$ analogue **2.35**; Lane 8, 2 μM Fe(II)•deglycoBLM $A_6$ analogue **2.35**; Lane 9, 10 μM Fe(II)•deglycoBLM $A_6$ analogue **2.35**; Lane 10, 16 μM Fe(II)•deglycoBLM $A_6$ analogue **2.35**; Lane 11, 16 μM Fe(II)•deglycoBLM $A_6$ analogue **2.36**; Lane 12, 2 μM Fe(II)•deglycoBLM $A_6$ analogue **2.36**; Lane 13, 10 μM Fe(II)•deglycoBLM $A_6$ analogue **2.36**; Lane 14, 16 μM Fe(II)•deglycoBLM $A_6$ analogue **2.36**; Lane 15, 16 μM Fe(II)•deglycoBLM $A_6$ analogue **2.37**; Lane 16, 2 μM Fe(II)•deglycoBLM $A_6$ analogue **2.37**; Lane 17, 10 μM Fe(II)•deglycoBLM $A_6$ analogue **2.37**; Lane 18, 16 μM Fe(II)•deglycoBLM $A_6$ analogue **2.37**;
This experiment was performed by Chenhong Tang.

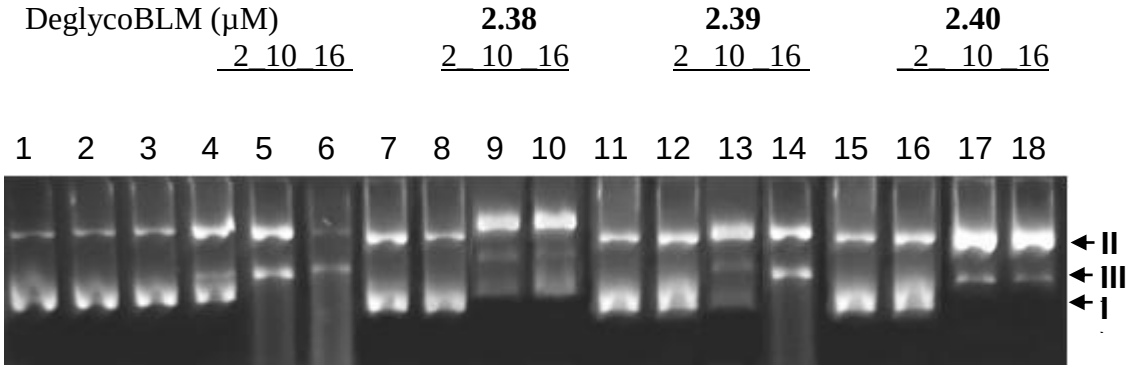


**Figure 2.09** – pSP64 DNA plasmid relaxation assay on an agarose gel; deglycoBLM $A_6$; analogues 2.38-2.40 (I – supercoiled, II – relaxed coil, III – linear duplex)
Lane 1, 100 ng DNA alone; Lane 2, 16μM Fe(II); Lane 3, 16 μM deglycoBLM $A_5$; Lane 4, 2 μM Fe(II)•deglycoBLM $A_5$; Lane 5, 10 μM Fe(II)•deglycoBLM $A_5$; Lane 6, 16 μM Fe(II)•deglycoBLM $A_5$; Lane 7, 16 μM Fe(II)•deglycoBLM $A_6$ analogue **2.38**; Lane 8, 2 μM Fe(II)•deglycoBLM $A_6$ analogue **2.38**; Lane 9, 10 μM Fe(II)•deglycoBLM $A_6$ analogue **2.38**; Lane 10, 16 μM Fe(II)•deglycoBLM $A_6$ analogue **2.38**; Lane 11, 16 μM Fe(II)•deglycoBLM $A_6$ analogue **2.39**; Lane 12, 2 μM Fe(II)•deglycoBLM $A_6$ analogue **2.39**; Lane 13, 10 μM Fe(II)•deglycoBLM $A_6$ analogue **2.39**; Lane 14, 16 μM Fe(II)•deglycoBLM $A_6$ analogue **2.39**; Lane 15, 16 μM Fe(II)•deglycoBLM $A_6$ analogue **2.40**; Lane 16, 2 μM Fe(II)•deglycoBLM $A_6$ analogue **2.40**; Lane 17, 10 μM Fe(II)•deglycoBLM $A_6$ analogue **2.40**; Lane 18, 16 μM Fe(II)•deglycoBLM $A_6$ analogue **2.40**;
This experiment was performed by Chenhong Tang.

## 2.03 Discussion

It was anticipated that structural changes within the N-terminal metal ion binding domain of BLM would afford analogues having improved biochemical properties. The pyrimidoblamic acid analogues chosen were structurally similar to the natural pyrimidoblamic acid or the truncated (but still active) structures (Figure 2.04) whose fully synthesized deglycoBLM $A_6$ counterparts displayed similar, altered or decreased activity in the pSP64 supercoiled DNA plasmid relaxation study (Figures 2.07-2.09).

The two pyridine analogues both contained the full native β-aminoalanineamide side chain while the remaining pyrimidine analogues contained the native core with various side chains that contained some variation of the simplified ethylene diamine moiety (partially) responsible for binding the metal co-factor(s).The simplified ethylene diamine itself is used as the side chain for pyrimidoblamic acid analogue **2.11** and shows retention of activity in the pSP64 supercoiled DNA plasmid relaxation study (Figure 2.07, lanes 7-10) using the PBA analogue incorporated in the fully synthesized deglycoBLM $A_6$ analogue **2.32**. Further structural changes or even minute additions to the ethylene diamine side chain **(2.13a-2.13f)** had a profound effect on the cleavage efficiency for deglycoBLM $A_6$ analogues **2.35-2.40.** The resulting cleavage activity was initially thought to occur and deviate from the parent compound deglycoBLM $A_5$ because of the possible inability to bind DNA as efficiently as a result of the structural change in the pyrimidoblamic acid side chain. However, further consideration led to the idea that the novel deglycoBLM $A_6$ analogues were unable to chelate a metal co-factors as easily and thus were less or variably active as a result. Circular dichroism (CD) studies (data not presented) were done in an attempt to assess which of these hypotheses was more

accurate. The studies did show a difference in CD profile from the native Cu(II) chelated pyrimidoblamic acid (assumed from the interpretation of the difference in spectra obtained for the analogues **2.35-2.37**). The CD studies did not provide enough evidence to conclude which hypothesis may be playing a stronger role in the difference in cleavage activities.

Additional plasmid relaxation assays using different conditions and/or varying the concentrations of deglycoBLM $A_6$ analogues or its co-factors may reveal more information about the cleavage activity. Further studies using 3′- or 5′- $^{32}P$ labeled hairpin DNA substrates (similarly done in Chapter 3, Figure 3.03) would also lead to more complete conclusions, including the specific site(s) of cleavage and the preference for sequence selective cleavage.

## 2.04 Experimental

**General Methods:** All solvents used were of analytical grade. Anhydrous solvents were of DriSolv® quality and purchased from VWR. All experiments were run under a dry nitrogen atmosphere in flame-dried glassware. All other chemicals were purchased from Aldrich and used without further purification. Flash chromatography was carried out using Silicycle 200-400 mesh silica gel. Analytical TLC was carried out using 0.25 mm EM silica gel 60 $F_{250}$ plates that were visualized by UV irradiation (254 nm). HPLC separations were performed on an Agilent 1100 series HPLC system using a diode array detector. The crude products were purified on an Alltech Alltima $C_{18}$ reversed phase semi-preparative (250 x 10 mm, 5 μm) HPLC column using aq 0.1% TFA and $CH_3CN$ mobile phases. UV-Vis spectrophotometric analysis and quantifications were done using a Beckman DU Series 500 UV/Vis spectrophotometer equipped with a single cell module. $^{1}H$ and $^{13}C$ NMR spectra were recorded on a 400 MHz Varian Liquid-State NMR in chloroform-*d*. Chemical shifts were reported in parts per million (ppm, δ) referenced to the residual $^{1}H$ resonance of the solvent ($CDCl_3$, 7.26 ppm). $^{13}C$ spectra were referenced to the residual $^{13}C$ resonance of the solvent ($CDCl_3$, 77.0 ppm). Splitting patterns were designated as follows: s, singlet; br, broad; d, doublet; dd, doublet of doublets; t, triplet; q, quartet; m, multiplet. High resolution mass spectra were obtained in the Arizona State University CLAS High Resolution Mass Spectrometry Laboratory or in the Michigan State University Mass Spectrometry Facility.

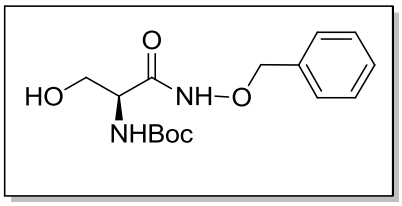


***N*-Boc-L-serine-*O*-benzylamide (2.01).**[18] To a stirred solution of 6.90 g (33.6 mmol) Boc-Ser-OH in 70 ml THF was added a solution of 10.7 g (67.3 mmol) of *O*-benzylhydroxylamine HCl in 275 mL of $H_2O$ at pH ~4.5, at 25 $^oC$. The solution was cooled to 0 $^oC$ and a solution of 13.9 g (67.3 mmol) of DCC in 205 mL of THF was added slowly. The reaction mixture was allowed warm to room temperature and was stirred at 25 $^oC$ for 3 h. The reaction mixture was concentrated under diminished pressure and filtered. The precipitate was suspended in 400 mL of hot EtOAc (~60 $^oC$) and filtered. The filtrate was concentrated under diminished pressure to give crude **2.01**. Crystallization from EtOAc gave **2.01** as a colorless solid: yield 6.31 g (60%); mp 129-130 $^oC$, lit.[18] 130-131 $^oC$; silica gel TLC $R_f$ 0.43 (1:1 EtOAc–hexanes); $^1H$ NMR ($CDCl_3$) δ 1.41 (s, 9H), 3.32 (br s, 1H), 3.59 (br s, 1H), 4.02 (m, 2H), 4.89 (s, 2H), 5.58 (m, 1H), 7.36 (m, 5H) and 9.47 (br s, 1H); $^{13}C$ NMR ($CDCl_3$) δ 28.2, 53.1, 62.5, 78.3, 97.5, 128.5, 128.8, 129.2, 134.8, 156.0 and 168.9; mass spectrum (MALDI-TOF) *m/z* 311.1670 $(M+H)^+$ ($C_{15}H_{23}N_2O_5$ requires 311.1609).

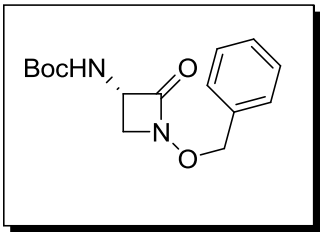


**(2*S*)-*N*-(Benzyloxy)-2-azetidinone (2.02).**[18] To a stirred solution of 2.83 g (9.12 mmol)

of **2.02** and 2.87 g (10.0 mmol) of $PPh_3$ in 60 mL of THF was added 1.57 mL (10.9 mmol) of DEAD at 0 $^oC$. The solution was allowed to warm to room temperature and was stirred at 25 $^oC$ for 24 h. The solution was concentrated under diminished pressure and the residue was purified by flash column chromatography on a silica gel column (20 x 4 cm). Elution with 1:1 EtOAc–hexanes gave **2.02** as a colorless solid: yield 2.37 g (89%); mp 90-91 $^oC$, lit.[18] 91-92 $^oC$; silica gel TLC $R_f$ 0.69 (1:1 EtOAc–hexanes); $^1H$ NMR ($CDCl_3$) δ 1.42 (s, 9H), 3.21 (m, 1H), 3.51 (br s, 1H), 4.53 (br s, 1H), 4.96 (s, 2H), 5.06 (br s, 1H) and 7.39 (m, 5H); $^{13}C$ NMR ($CDCl_3$) δ 28.5, 53.6, 54.7, 78.1, 80.8, 127.6, 128.9, 134.9, 155.2, 163.2 and 168.7; mass spectrum (MALDI-TOF) *m/z* 293.1544 $(M+H)^+$ ($C_{15}H_{21}N_2O_4$ requires 293.1503).

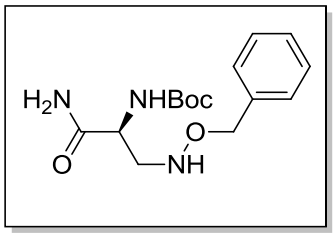


**(2*S*)-3-[(Benzyloxy)amino]-2-[(*tert*-butoxycarbonyl)amino]propanamide (2.03).** [18] Through a stirred solution of 4.57 g (15.6 mmol) of **2.02** in 70 mL of MeOH was bubbled $NH_3$ gas for 20 min at 0 $^oC$. The solution was stirred at 0 $^oC$ for 24 h and then concentrated under diminished pressure. The residue was purified by flash chromatography on a silica gel column (10 x 4 cm). Elution with 1:1:0.05 EtOAc–hexanes–MeOH gave **2.03** as a colorless oil: yield 3.89 g (81%); silica gel TLC $R_f$ 0.18 (1:1:0.05 EtOAc–hexanes–MeOH); $^1H$ NMR ($CDCl_3$) δ 1.45 (s, 9H), 3.12 (m, 1H), 3.33 (m, 1H), 4.30 (br s, 1H), 4.69 (s, 2H), 5.62 (d, 1H), 5.74 (br s, 1H), 6.56 (br s, 1H) and 7.35 (m, 5H); $^{13}C$ NMR ($CDCl_3$) δ 28.2, 52.3, 52.8, 75.9, 80.1, 127.9, 128.4, 137.3, 155.7

and 173.8; mass spectrum (MALDI-TOF) *m/z* 310.1819 $(M+H)^+$ ($C_{15}H_{24}N_3O_4$ requires 310.1769).

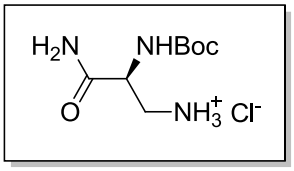


**(2*S*)-3-Amino-2-[(*tert*-butoxycarbonyl)amino]propanamide Hydrochloride (2.05).**[18] To a stirred solution of 3.89 g (12.5 mmol) of **2.02** in 60 mL MeOH was added a catalytic amount of 10% Pd/C at 25 $^oC$. The solution was stirred under a $H_2$ atmosphere at 25 $^oC$ for 48 h. The reaction mixture was filtered through a Celite® pad, the pad waswashed with MeOH. The filtrate was concentrated under diminished pressure to give a colorless oil. The oil was dissolved in 10 mL MeOH and 45 mL of $Et_2O$ and to the solution was added 15 ml of HCl saturated MeOH at 0 $^oC$. The reaction mixture was diluted with 600 mL of $Et_2O$ and the resulting suspension was stored at 0 $^oC$ for 24 h and then filtered to give **2.05** as a colorless solid: yield 2.22 g (74%); mp 178-180 $^oC$, lit.[18] mp 179-180 $^oC$; $^1H$ NMR ($D_2O$) δ 1.45 (s, 9H), 3.22 (m, 2H), 3.45 (m, 1H), 4.43 (br s, 1H), 5.13 (br s, 2H) and 6.64 (br s, 2H); $^{13}C$ NMR ($D_2O$) δ 28.3, 43.6, 55.0, 79.9, 155.8 and 174.0; mass spectrum (MALDI-TOF) *m/z* 240.1188 $(M+H)^+$ ($C_8H_{19}N_3O_3Cl$ requires 240.1117).

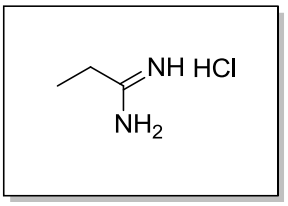


**Propionamidine HCl (2.06).**[49] To a solution of 5.5 mL (77.1 mmol) of propionitrile in 37 mL dry $Et_2O$ and 5 mL dry MeOH was bubbled HCl gas for 15 min at 0 $^oC$. The reaction mixture was stirred at 0 $^oC$ for 48 h. The solution was allowed to warm to room temperature and was then concentrated under diminished pressure to give a white residue. The residue was suspended in 50 mL dry EtOH, bubbled with ammonia gas for 20 min and stirred for at 25 $^oC$ for 24 h. The reaction mixture was treated with 90 mL of dry $Et_2O$ and stirred at 0 $^oC$ for 24 h. The resulting precipitate was collected and air dried at 25 $^oC$ to give **2.06** as a colorless solid: yield 8.37 g (99%); mp 130 $^oC$, lit.[49] mp 128-130 $^oC$; $^1H$ NMR (DMSO) δ 1.15 (t, 3H, *J* = 7.6 Hz), 2.39 (q, 2H, *J* = 7.6 Hz) and 9.11 (br s, 3H); $^{13}C$ NMR (DMSO) δ 10.1, 29.8 and 168.9; Mass spectrum (MALDI-TOF) *m/z* 109.0556 $(M+H)^+$ ($C_3H_{10}N_2Cl$ requires 109.0534).

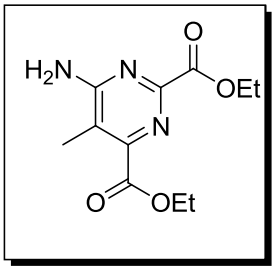


**Diethyl 6-Amino-2,4-bis(ethoxycarbonyl)-5-methylpyrimidine (2.07).**[13,17,18] A solution of 2.50 g (8.41 mmol) of triethyl-1,3,5-triazine-2,4,6-tricarboxylate and 1.83 g (16.8 mmol) of **2.06** in 43 mL of DMF was warmed to 90 $^oC$, stirred for 72 h and then

concentrated under diminished pressure. The residue was dissolved in 100 mL of warm (~70 $^{o}$C) EtOAc and filtered. The filtrate was concentrated under diminished pressure and the residue was crystallized from EtOAc–hexanes to give **2.07** as an orange solid: yield 1.04 g (49%); mp 148-151 $^{o}$C, lit.[13] mp 155-156 $^{o}$C; silica gel TLC $R_f$ 0.35 (95:5 $CH_2Cl_2$–MeOH); $^{1}$H NMR ($CDCl_3$) δ 1.42 (t, 3H, *J* = 7.0 Hz), 1.44 (t, 3H, *J* = 7.0 Hz), 2.29 (s, 3H), 4.43 (q, 2H, *J* = 7.0 Hz), 4.48 (q, 2H, *J* = 7.0 Hz) and 5.93 (br s, 2H); $^{13}$C NMR δ 12.2, 14.1, 14.1, 62.3, 62.6, 114.8, 153.7, 153.8, 163.7, 164.0 and 165.3; mass spectrum (MALDI-TOF) *m/z* 254.1188 $(M+H)^{+}$ ($C_{11}H_{16}N_3O_4$ requires 254.1143).

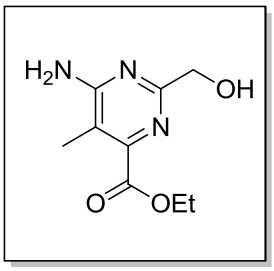


**Ethyl 6-Amino-2-(hydroxymethyl)-5-methylpyrimidine-4-carboxylate (2.08).**[13,18,52] To a stirred solution of 1.85 g (7.31 mmol) of **2.07** in 47 mL EtOH was added 276 mg (7.31 mmol) of $NaBH_4$ at 0 $^{o}$C. The solution was allowed to warm to 5 $^{o}$C and was stirred for 150 h. To the solution was added 40 mL of satd aq $NaHCO_3$ and 40 mL of 5% aq $H_2O_2$ and the solution was stirred for an additional 4 h at 5 $^{o}$C and then concentrated under diminished pressure. The resulting aqueous solution was extracted with five 40–mL portions of 4:1 $CHCl_3$–2-propanol, and the organic extract combined was concentrated under diminished pressure. The residue was purified by flash chromatography on a silica gel column (15 x 6 cm). Elution with 95:5 $CH_2Cl_2$–MeOH

gave **2.08** as a colorless solid: yield 390 mg (25%); mp 169 $^{o}$C, lit.[13] mp 169 $^{o}$C; silica gel TLC $R_f$ 0.27 (95:5 $CH_2Cl_2$–MeOH); $^{1}$H NMR ($CDCl_3$) δ 1.38 (t, 3H, $J$ = 7.0 Hz), 2.14 (s, 3H), 3.31 (br s, 1H), 4.39 (q, 2H, $J$ = 7.0 Hz), 4.48 (s, 2H) and 5.77 (br s, 2H); $^{13}$C NMR δ 12.0, 14.4, 63.1, 65.2, 111.28, 154.5, 165.7, 167.0 and 167.7; mass spectrum (MALDI-TOF) *m/z* 211.1098 $(M+H)^+$ ($C_9H_{14}N_3O_3$ requires 212.1037).

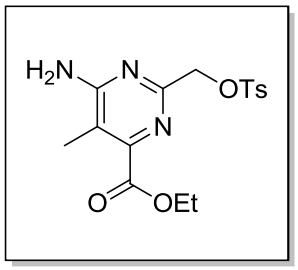


**Ethyl 6-Amino-5-methyl-2-(tosylmethyl)pyrimidine-4-carboxylate (2.09).**[13] To a stirred solution of 390 mg (1.85 mmol) of **2.08** in 25 mL $CH_3CN$ was added 528 mg (2.77 mmol) of Ts-Cl and 510 mg (3.70 mmol) of $K_2CO_3$ at 25 $^{o}$C and the solution was stirred in the dark for 24 h. The solution was filtered through a Celite® pad and the pad was washed with $CH_3CN$. The filtrate was concentrated under diminished pressure and the residue was purified by flash chromatography on a silica gel column (15 x 3 cm). Elution with 98:2 $CH_2Cl_2$–MeOH gave **2.09** as a colorless solid: yield 527 mg (78%); mp 128 $^{o}$C, lit.[13] mp 128 $^{o}$C; silica gel TLC $R_f$ 0.55 (95:5 $CH_2Cl_2$–MeOH); $^{1}$H NMR ($CDCl_3$) δ 1.37 (t, 3H, $J$ = 7.0 Hz), 2.22 (s, 3H), 2.43 (s, 3H), 4.39 (q, 2H, $J$ = 7.0 Hz), 4.96 (s, 2H), 5.77 (br s, 2H), 7.32 (d, 2H, $J$ = 7.1 Hz) and 7.80 (d, 2H, $J$ = 7.1 Hz); $^{13}$C NMR δ 11.7, 14.1, 21.6, 62.0, 70.8, 111.9, 128.1, 130.0, 131.8, 145.4, 153.0, 159.2, 164.4 and 165.7; mass spectrum (MALDI-TOF) *m/z* 366.1167 $(M+H)^+$ ($C_{16}H_{20}N_3O_5S$ requires 366.1125).

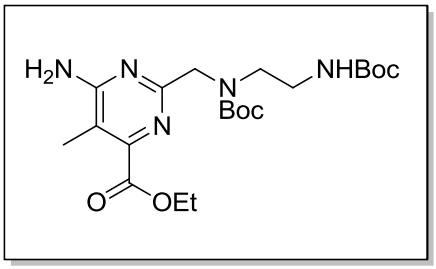


**Ethyl 6-Amino-2-((*tert*-butoxycarbonyl(2-(*tert*-butoxycarbonylamino)ethyl)amino)methyl)-5-methylpyrimidine-4-carboxylate (2.10).**[12,13,18] To a stirred solution of 410 mg (1.22 mmol) of **2.09** in 6 mL of $CH_3CN$ was added 189 mg (2.44 mmol) of $NaHCO_3$ and 0.71 mL (4.88 mmol) of *N*-Boc-ethylenediamine at 25 $^oC$. The solution was stirred at 25 $^oC$ for 24, filtered through a Celite® pad and the pad was washed with $CH_3CN$. The filtrate was concentrated under diminished pressure to give a colorless oil. The oil was dissolved in 6 mL $CH_2Cl_2$ and to the solution was added 532 mg (2.44 mmol) of $Boc_2O$ and 0.68 mL (4.88 mmol) of $Et_3N$ at 25 $^oC$. The solution was stirred at 25 $^oC$ for 24 h and then concentrated under diminished pressure. The residue was purified by flash chromatography on a silica gel column (15 x 3 cm). Elution with 90:10 $CH_2Cl_2$–MeOH gave **2.10** as a colorless foam: yield 438 mg (79% over 2 steps); silica gel TLC $R_f$ 0.61 (90:10 $CH_2Cl_2$–MeOH); $^1H$ NMR ($CDCl_3$) δ 1.37 (t, 3H, $J$ = 7.0 Hz), 1.41 (s, 9H), 1.43 (s, 9H), 2.16 (m, 2H), 3.20 (br s, 2H), 3.39, (m, 2H), 4.31 (m, 1H), 4.39 (q, 2H, $J$ = 7.0 Hz), 4.91 (br s, 1H) and 5.41 (br s, 2H); $^{13}C$ NMR δ 13.4, 14.1, 28.1, 31.9, 38.3, 51.2, 55.6, 62.0, 70.8, 126.1, 127.5, 113.9, 128.5, 145.5, 157.7, 163.3 and 175.3; mass spectrum (FAB), *m/z* 454.2674 ($M^+$) ($C_{21}H_{35}N_5O_6$ requires 454.2666).

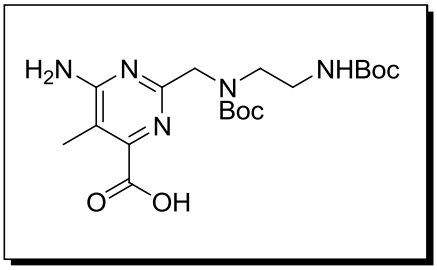


**6-Amino-2-((*tert*-butoxycarbonyl(2-(*tert*-butoxycarbonylamino)ethyl)amino)methyl)-5-methylpyrimidine-4-carboxylic acid (2.11).**[12,13,17] To a stirred solution of 151 mg (0.33 mmol) of **2.10** in 3 mL of 3:1:1 THF–MeOH–$H_2O$ was added 0.66 mL (0.66 mmol) of 1 N aq LiOH at 0 $^oC$. The solution was allowed to warm to room temperature and was stirred at 25 $^oC$ for 3 h and then concentrated under diminished pressure. The residue was partitioned between $H_2O$ and 4:1 $CHCl_3$–2-propanol (7 mL each). The aqueous phase was extracted with two 7-mL portions of 4:1 $CHCl_3$–2-propanol. The aqueous phase was then acidified to pH ~4 with 1 N aq HCl at 0 $^oC$ and then extracted with five 7-mL portions of 4:1 $CHCl_3$–2-propanol. The organic extract combined was concentrated under diminished pressure. The residue was purified by flash chromatography on a silica gel column (7 x 3 cm). Elution with 88:10:2 $CH_2Cl_2$–MeOH–acetic acid gave **2.11** as a colorless foam: yield 129 mg (92%); silica gel TLC $R_f$ 0.58 (90:10 $CH_2Cl_2$–MeOH); $^1H$ NMR ($D_2O$) δ 1.34 (s, 9H), 1.38 (s, 9H), 2.05 (s, 3H), 3.06 (m, 2H), 3.31 (m, 2H), 4.26 (s, 2H), 6.90 (br s, 1H) and 7.19 (s, 2H); $^{13}C$ NMR ($D_2O$) δ 12.3, 28.7, 28.9, 48.2, 51.9, 52.9, 63.1, 79.2, 108.7, 154.2, 155.7, 156.3, 163.8, 164.7 and 167.3; mass spectrum (FAB), *m/z* 426.2356 ($M^+$) ($C_{19}H_{31}N_5O_6$ requires 426.2353).

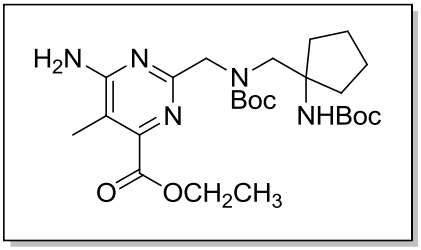


**Ethyl 6-Amino-2-((*tert*-butoxycarbonyl((1-(*tert*-butoxycarbonylamino)cyclopentyl)methyl)amino)methyl)-5-methylpyrimidine-4-carboxylate (2.12a).** To a stirred solution of 67 mg (0.18 mmol) of **2.09** in 1 mL of $CH_3CN$ was added 31 mg (0.37 mmol) of $NaHCO_3$ and 118 mg (0.55 mmol) of amine **a** at 25 $^oC$. The solution was stirred at 25 $^oC$ for 24 h, filtered through a Celite® pad, the pad was washed with $CH_3CN$ and concentrated under diminished pressure. The residue was dissolved in 1 mL of $CH_2Cl_2$ and was added 79 mg (0.36 mmol) of $(Boc)_2O$ and 0.10 mL of $Et_3N$ at 25 $^oC$. The solution was stirred at 25 $^oC$ for 24 h and then concentrated under diminished pressure. The residue was purified by flash chromatography on a silica gel column (12 x 3 cm). Elution with 95:5 $CH_2Cl_2$–MeOH gave **2.12a** as a colorless oil: yield 61 mg (67%); silica gel TLC $R_f$ 0.63 (95:5 $CH_2Cl_2$–MeOH); $^1H$ NMR ($CDCl_3$) δ 1.22 (s, 9H), 1.28 (s, 9H), 1.36 (t, 3H, $J$ = 7.1 Hz), 1.44 (s, 3H), 1.67-1.97 (m, 8H), 2.19 (s, 2H), 4.35 (s, 2H), 4.37 (q, 2H, $J$ = 7.1 Hz), 5.30 (br s, 2H) and 5.71 (br s, 1H). $^{13}C$ NMR δ 11.6, 14.1, 23.5, 28.1, 28.3, 35.8, 55.4, 55.5, 61.8, 65.2, 79.4, 80.1, 109.6, 153.6, 155.2, 156.8, 163.1, 165.2 and 166.1; mass spectrum (FAB), *m/z* 507.3063 ($M^+$) ($C_{25}H_{41}N_5O_6$ requires 507.3057).

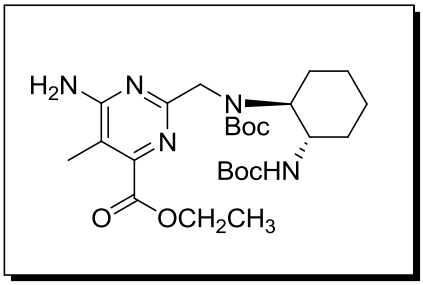


**Ethyl 6-Amino-2-((*tert*-butoxycarbonyl((1*S*,2*S*)-2-(*tert*-butoxycarbonylamino)cyclohexyl)amino)methyl)-5-methylpyrimidine-4-carboxylate (2.12b).** To a stirred solution of 70 mg (0.19 mmol) of **2.09** in 1 mL of $CH_3CN$ was added 32 mg (0.38 mmol) of $NaHCO_3$ and 123 mg (0.57 mmol) of amine **b** at 25 $^oC$. The solution was stirred at 25 $^oC$ for 24 h, filtered through a Celite® pad, the pad was washed with $CH_3CN$ and concentrated under diminished pressure. The residue was dissolved in 1 mL of $CH_2Cl_2$ and was added 83 mg (0.38 mmol) of $(Boc)_2O$ and 0.11 mL of $Et_3N$ at 25 $^oC$. The solution was stirred at 25 $^oC$ for 24 h and then concentrated under diminished pressure. The residue was purified by flash chromatography on a silica gel column (12 x 3 cm). Elution with 95:5 $CH_2Cl_2$–MeOH gave **2.12b** as colorless oil: yield 154 mg (quant.); silica gel TLC $R_f$ 0.67 (95:5 $CH_2Cl_2$–MeOH); $[\alpha]^{25}_D$ +46.4$^o$ $^1$H NMR ($CDCl_3$) δ 1.37 (s, 9H), 1.43 (s, 9H), 1.46 (t, 3H, *J* = 7.1 Hz), 1.49 (s, 3H), 1.26-2.29 (m, 8H), 2.19 (s, 2H), 3.24 (m, 1H), 4.38 (q, 2H, *J* = 7.1 Hz) 4.88 (m, 1H), 5.30 (br s, 2H) and 5.71 (br s, 1H). $^{13}$C NMR δ 11.5, 14.1, 24.8, 27.3, 28.3, 28.5, 32.9, 55.0, 61.9, 63.4, 64.8, 66.6, 79.1, 85.1, 109.9, 146.7, 156.4, 157.5, 163.7 and 164.1; mass spectrum (FAB), *m/z* 507.3040 ($M^+$) ($C_{25}H_{41}N_5O_6$ requires 507.3057).

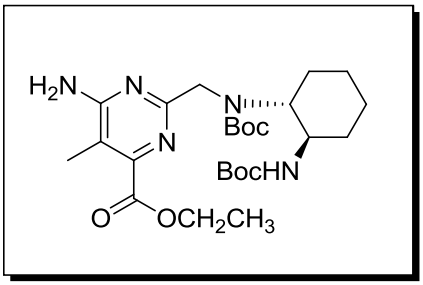


**Ethyl 6-Amino-2-((*tert*-butoxycarbonyl((1*R*,2*R*)-2-(*tert*-butoxycarbonylamino)cyclohexyl)amino)methyl)-5-methylpyrimidine-4-carboxylate (2.12c).** To a stirred solution of 70 mg (0.19 mmol) of **2.09** in 1 mL of $CH_3CN$ was added 32 mg (0.38 mmol) of $NaHCO_3$ and 123 mg (0.57 mmol) of amine **c** at 25 $^oC$. The solution was stirred for 24 h at 25 $^oC$, filtered through a Celite® pad, the pad was washed with $CH_3CN$ and concentrated under diminished pressure. The residue was dissolved in 1 mL of $CH_2Cl_2$ and was added 83 mg (0.38 mmol) of $(Boc)_2O$ and 0.11 mL of $Et_3N$ at 25 $^oC$. The solution was stirred at 25 $^oC$ for 24 h and then concentrated under diminished pressure. The residue was purified by flash chromatography on a silica gel column (12 x 3 cm). Elution with 95:5 $CH_2Cl_2$–MeOH gave **2.12c** as a colorless oil: yield 100 mg (quant.); silica gel TLC $R_f$ 0.67 (95:5 $CH_2Cl_2$–MeOH); $[\alpha]^{25}_D$ -42.7$^o$ $^1$H NMR ($CDCl_3$) δ 1.37 (s, 9H), 1.43 (s, 9H), 1.46 (t, 3H, *J* = 7.1 Hz), 1.49 (s, 3H), 1.26-2.29 (m, 8H), 2.19 (s, 2H), 3.24 (m, 1H), 4.38 (q, 2H, *J* = 7.1 Hz) 4.88 (m, 1H), 5.30 (br s, 2H) and 5.71 (br s, 1H). $^{13}$C NMR δ 11.5, 14.1, 24.8, 27.3, 28.3, 28.5, 32.9, 55.0, 61.9, 63.4, 64.8, 66.6, 79.1, 85.1, 109.9, 146.7, 156.4, 157.5, 163.7 and 164.1; mass spectrum (FAB), *m/z* 507.3040 ($M^+$) ($C_{25}H_{41}N_5O_6$ requires 507.3057).

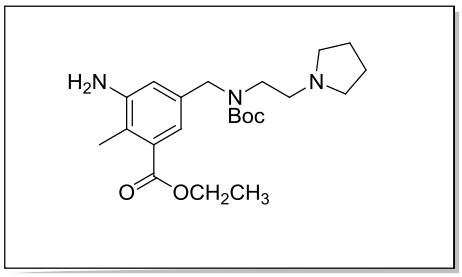


**Ethyl 3-Amino-5-(((*tert*-butoxycarbonyl)(2-(pyrrolidin-1-yl)ethyl)amino)methyl)-2-methylbenzoate (2.12d)** To a stirred solution of 200 mg (0.49 mmol) of **2.09** and 83 mg (0.986 mmol) of $NaHCO_3$ in 10 mL of $CH_3CN$ was added 233 µL (210 mg, 1.97 mmol) of amine **d** at 25 °C and the solution was stirred for 12 h. The mixture was filtered through a pad of Celite®, the pad was washed with $CH_3CN$ and concentrated under diminished pressure. The residue was dissolved in 7 mL of $CH_2Cl_2$ and subsequently treated with 240 mg (0.99 mmol) of $Boc_2O$ and 206 µL (150 mg, 1.48 mmol) of $Et_3N$ at 25 °C and stirred for 12 h. The solution was then concentrated under diminished pressure and purified by flash chromatography on a silica gel column (10 x 4 cm); elution with 9:1 $CH_2Cl_2$–MeOH gave **2.12d** as a colorless foam: yield 127 mg (64%); silica gel TLC $R_f$ 0.53 (9:1 $CH_2Cl_2$–MeOH); $^1$H NMR ($CDCl_3$) δ 1.31 (s, 9H), 1.38 (t, 3H, $J$ = 7.0 Hz), 3.13 (m, 6H), 2.34 (s, 3H), 3.13 (m, 4H), 3.61 (m, 2H), 3.82 (m, 2H), 4.40 (q, 2H, $J$ = 7.1 Hz), 4.46 (s, 2H) and 6.22 (br s, 2H); $^{13}$C NMR ($CDCl_3$) δ 13.4, 14.1, 24.5, 28.4, 40.0, 50.1, 56.9, 60.9, 79.8, 118.9, 123.8, 132.2, 146.1, 154.3, 167.5; mass spectrum (FAB), *m/z* 405.2619 ($M^+$) ($C_{22}H_{35}N_3O_4$ requires 405.2628).

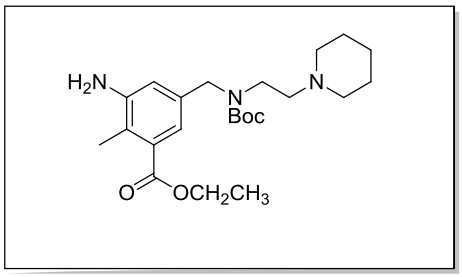


**Ethyl 3-Amino-5-(((*tert*-butoxycarbonyl)(2-(piperidin-1-yl)ethyl)amino)methyl)-2-methylbenzoate (2.12e).** To a stirred solution of 200 mg (0.55 mmol) of **2.09** and 91 mg (1.09 mmol) of $NaHCO_3$ in 10 mL of $CH_3CN$ was added 233 µL (1.64 mmol) of amine **e** at 25 $^oC$ and the solution was stirred for 12 h. The mixture was filtered through a pad of Celite®, the pad was washed with $CH_3CN$ and concentrated under diminished pressure. The residue was dissolved in 7 mL of $CH_2Cl_2$ and subsequently treated with 240 mg (1.09 mmol) of $Boc_2O$ and 300 µL (227 mg, 2.18 mmol) of $Et_3N$ at 25 $^oC$ and stirred for 12 h. The solution was then concentrated under diminished pressure and purified by flash chromatography on a silica gel column (10 x 4 cm); elution with 9:1 $CH_2Cl_2$–MeOH gave **2.12e** as a colorless foam: yield 134 mg (42%); silica gel TLC $R_f$ 0.54 (9:1 $CH_2Cl_2$–MeOH); $^1H$ NMR ($CDCl_3$) δ 1.31 (s, 9H), 1.38 (t, 3H, $J$ = 7.0 Hz), 3.13 (m, 6H), 2.34 (s, 3H), 3.13 (m, 6H), 3.61 (m, 2H), 3.82 (m, 2H), 4.40 (q, 2H, $J$ = 7.0 Hz), 4.46 (s, 2H) and 6.22 (br s, 2H); $^{13}C$ NMR ($CDCl_3$) δ 13.4, 14.1, 24.5, 25.9, 28.4, 40.0, 50.1, 56.9, 60.9, 79.8, 118.9, 123.8, 132.2, 146.1, 154.3, 167.5; mass spectrum (FAB), *m/z* 418.2801 ($M^+$) ($C_{23}H_{37}N_3O_4$ requires 418.2784).

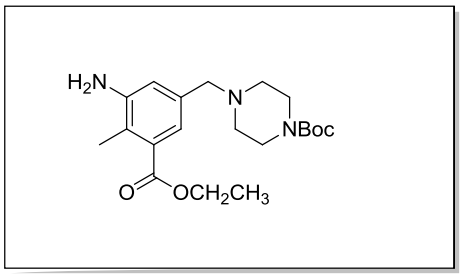


***Tert*-butyl 4-(3-amino-5-(ethoxycarbonyl)-4-methylbenzyl)piperazine-1-carboxylate (2.12f)** To a stirred solution of 200 mg (0.49 mmol) of **2.09** and 83 mg (0.99 mmol) of $NaHCO_3$ in 10 mL of $CH_3CN$ was added 233 µL (210 mg, 1.97 mmol) of amine **f** at 25 $^oC$ and the solution was stirred for 12 h. The mixture was filtered through a pad of Celite®, the pad was washed with $CH_3CN$ and concentrated under diminished pressure. The residue was dissolved in 7 mL of $CH_2Cl_2$ and subsequently treated with 240 mg (0.99 mmol) of $Boc_2O$ and 206 µL (150 mg, 1.48 mmol) of $Et_3N$ at 25 $^oC$ and stirred for 12 h. The solution was then reconcentrated under diminished pressure and purified by flash chromatography on a silica gel column (10 x 4 cm); elution with 9:1 $CH_2Cl_2$–MeOH gave **2.12f** as a colorless foam: yield 127 mg (64%); silica gel TLC $R_f$ 0.53 (9:1 $CH_2Cl_2$–MeOH); $^1H$ NMR ($CDCl_3$) δ 1.29 (t, 3H, $J$ = 7.0 Hz), 1.38 (s, 9H), 2.34 (s, 3H), 2.50 (t, 4H, $J$ = 6.5 Hz), 3.20 (t, 4H), $J$ = 6.5 Hz), 3.65 (s, 2H), 4.33 (q, 2H), 6.27 (br s, 2H), 6.69 (s, 1H) and 7.1 (s, 1H); $^{13}C$ NMR ($CDCl_3$) δ 13.4, 14.1, 28.4, 46.2, 54.4, 60.9, 64.5, 79.8, 120.1, 124.2, 132.1, 146.0, 154.7 and 167.8; mass spectrum (FAB), *m/z* 377.2304 ($M^+$) ($C_{20}H_{31}N_3O_4$ requires 377.2315).

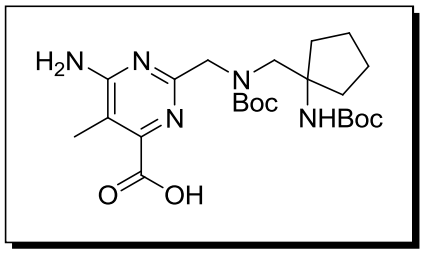


**6-Amino-2-((*tert*-butoxycarbonyl((1-(*tert*-butoxycarbonylamino)cyclopentyl)methyl)amino)methyl)-5-methylpyrimidine-4-carboxylic acid (2.13a).** To a stirred solution of 59 mg (0.12 mmol) of **2.12a** in 1 mL of 3:1:1 THF–MeOH–$H_2O$ was added 0.24 mL (0.24 mmol) of 1 N aq LiOH at 0 $^oC$. The solution was allowed to warm to room temperature and was stirred at 25 $^oC$ for 4 h. The solution was concentrated under diminished pressure and the residue was partitioned between $H_2O$ and $CH_2Cl_2$ (~5 mL each). The aqueous phase was extracted with four 5-mL portions of $CH_2Cl_2$. The organic extract combined was concentrated under diminished pressure. The residue was purified by flash chromatography on a silica gel column (12 x 3 cm). Elution with 95:5 $CH_2Cl_2$–MeOH gave **2.13a** as a colorless foam: yield 48 mg (83%); silica gel TLC $R_f$ 0.55 (95:5 $CH_2Cl_2$–MeOH); $^1H$ NMR ($CDCl_3$) δ 1.22 (s, 9H), 1.26 (s, 9H), 1.44 (s, 3H), 1.65-1.95 (m, 8H), 2.20 (s, 2H), 4.35 (s, 2H), 5.30 (br s, 2H), 5.71 (br s, 1H) and 7.10 (br s, 1H). $^{13}C$ NMR δ 11.6, 23.5, 28, 28.3, 35.8, 55.4, 55.5, 65.2, 79.4, 80.1, 109.6, 153.6, 155.2, 156.8, 163.1, 165.2 and 166.1; mass spectrum (FAB), *m/z* 479.2721 ($M^+$) ($C_{23}H_{37}N_5O_6$ requires 479.2744).

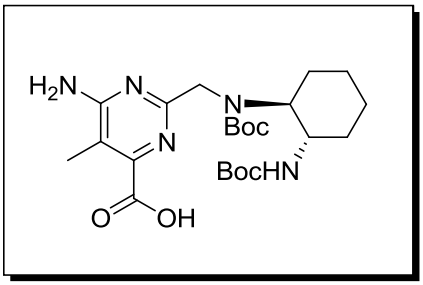


**6-Amino-2-((*tert*-butoxycarbonyl((1*S*,2*S*)-2-(*tert*-butoxycarbonylamino)cyclohexyl)amino)methyl)-5-methylpyrimidine-4-carboxylic acid (2.13b).** To a stirred solution of 171 mg (0.19 mmol) of **2.12b** in 3 mL of 3:1:1 THF–MeOH–$H_2O$ was added 0.38 mL (0.38 mmol) of 1 N aq LiOH at 0 $^oC$. The solution was allowed to warm to room temperature and was stirred at 25 $^oC$ for 4 h. The solution was concentrated under diminished pressure and the residue was partitioned between $H_2O$ and $CH_2Cl_2$ (~5 mL each). The aqueous phase was extracted with four 5-mL portions of $CH_2Cl_2$. The organic extract combined was concentrated under diminished pressure. The residue was purified by flash chromatography on a silica gel column (12 x 3 cm). Elution with 95:5 $CH_2Cl_2$–MeOH gave **2.13b** as a colorless foam: yield 60 mg (66%); silica gel TLC $R_f$ 0.57 (95:5 $CH_2Cl_2$–MeOH); $[\alpha]^{25}_D$ +62.3$^o$ $^1$H NMR ($CDCl_3$) δ 1.37 (s, 9H), 1.43 (s, 9H), 1.49 (s, 3H), 1.26-2.29 (m, 8H), 2.19 (s, 2H), 3.24 (m, 1H), 4.88 (m, 1H), 5.30 (br s, 2H), 5.71 (br s, 1H) and 9.21 (br s, 1H). $^{13}$C NMR δ 11.5, 24.8, 27.3, 28.3, 28.5, 32.9, 55.0, 63.4, 64.8, 66.6, 79.1, 85.1, 109.9, 146.7, 156.4, 157.5, 163.7 and 164.1; mass spectrum (FAB), *m/z* 479.2722 ($M^+$) ($C_{23}H_{37}N_5O_6$ requires 479.2744).

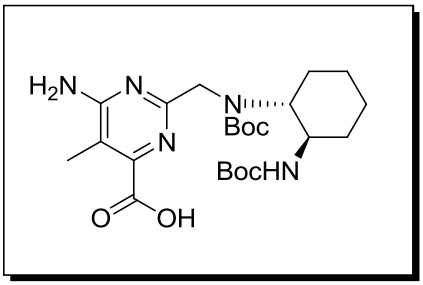


**6-Amino-2-((*tert*-butoxycarbonyl((1*R*,2*R*)-2-(*tert*-butoxycarbonylamino)cyclohexyl)amino)methyl)-5-methylpyrimidine-4-carboxylic acid (2.13c).** To a stirred solution of 95 mg (0.18 mmol) of **2.12c** in 3 mL of 3:1:1 THF–MeOH–$H_2O$ was added 0.36 mL (0.36 mmol) of 1 N aq LiOH at 0 $^oC$. The solution was allowed to warm to room temperature and was stirred at 25 $^oC$ for 4 h. The solution was concentrated under diminished pressure and the residue was partitioned between $H_2O$ and $CH_2Cl_2$ (~5 mL each). The aqueous phase was extracted with four 5-mL portions of $CH_2Cl_2$. The organic extract combined was concentrated under diminished pressure. The residue was purified by flash chromatography on a silica gel column (12 x 3 cm). Elution with 95:5 $CH_2Cl_2$–MeOH gave **2.13c** as a colorless foam: yield 35 mg (41%); silica gel TLC $R_f$ 0.57 (95:5 $CH_2Cl_2$–MeOH); $[\alpha]^{25}_D$ +60.2$^o$ $^1$H NMR ($CDCl_3$) δ 1.37 (s, 9H), 1.43 (s, 9H), 1.49 (s, 3H), 1.26-2.29 (m, 8H), 2.19 (s, 2H), 3.24 (m, 1H), 4.88 (m, 1H), 5.30 (br s, 2H), 5.71 (br s, 1H) and 9.21 (br s, 1H). $^{13}$C NMR δ 11.5, 24.8, 27.3, 28.3, 28.5, 32.9, 55.3, 63.4, 64.8, 66.5, 79.0, 85.1, 109.8, 146.6, 156.4, 157.4, 163.2 and 164.2; mass spectrum (FAB), *m/z* 479.2722 ($M^+$) ($C_{23}H_{37}N_5O_6$ requires 479.2744).

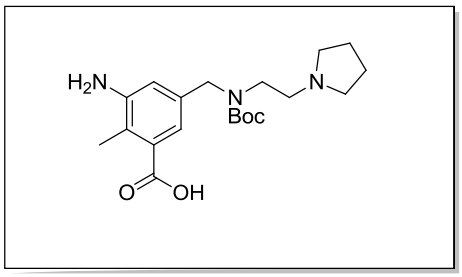


**3-Amino-5-(((*tert*-butoxycarbonyl)(2-(pyrrolidin-1-yl)ethyl)amino)methyl)-2-methylbenzoic acid (2.13d).** To a stirred solution of 127 mg (0.314 mmol) of **2.12d** in 3 mL of 3:1:1 THF–MeOH–$H_2O$ was added 0.42 mL (0.42 mmol) of 1 N aq LiOH at 0 $^oC$. The solution was allowed to warm to room temperature and was stirred at 25 $^oC$ for 3 h. The solution was concentrated under diminished pressure and the residue partitioned between $H_2O$ and 4:1 $CHCl_3$–2-propanol (7 mL each). The aqueous phase was extracted with two 7-mL portions of 4:1 $CHCl_3$–2-propanol. The aqueous phase was then acidified to pH ~3 with 1 N aq HCl at 0 $^oC$ and then extracted with five 7-mL portions of 4:1 $CHCl_3$–2-propanol. The organic extract combined was concentrated under diminished pressure. The residue was purified by flash chromatography on a silica gel column (6 x 4 cm); elution with 88:10:2 $CH_2Cl_2$–MeOH–acetic acid gave **2.13d** as a colorless foam: yield 36 mg (30%); silica gel TLC $R_f$ 0.21 (9:1 $CH_2Cl_2$–MeOH); $^1H$ NMR ($CDCl_3$) δ 1.30 (m, 4H), 1.31 (s, 9H), 3.13 (m, 6H), 3.13 (m, 6H), 3.61 (m, 2H), 3.82 (m, 2H), 4.46 (s, 2H), 5.08 (br s, 1H), 6.02 (br s, 1H) and 6.22 (br s, 2H); $^{13}C$ NMR ($CDCl_3$) δ 13.4, 24.5, 25.9, 28.4, 40.0, 79.8, 118.9, 123.8, 132.2, 146.1, 154.3, 167.5; mass spectrum (FAB), *m/z* 377.2304 ($M^+$) ($C_{20}H_{31}N_3O_4$ requires 377.2315).

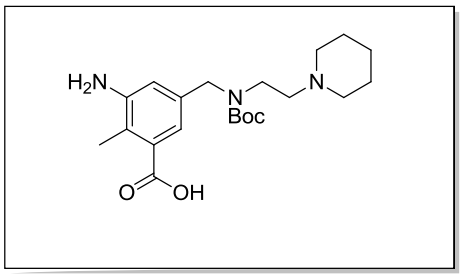


**3-Amino-5-(((*tert*-butoxycarbonyl)(2-(piperidin-1-yl)ethyl)amino)methyl)-2-methylbenzoic acid (2.13e).** To a stirred solution of 134 mg (0.23 mmol) of **2.12e** in 3 mL of 3:1:1 THF–MeOH–$H_2O$ was added 0.46 mL (0.46 mmol) of 1 N aq LiOH at 0 $^oC$. The solution was allowed to warm to room temperature and was stirred at 25 $^oC$ for 3 h. The solution was concentrated under diminished pressure and the residue partitioned between $H_2O$ and 4:1 $CHCl_3$–2-propanol (7 mL each). The aqueous phase was extracted with two 7-mL portions of 4:1 $CHCl_3$–2-propanol. The aqueous phase was then acidified to pH ~3 with 1 N aq HCl at 0 $^oC$ and then extracted with five 7-mL portions of 4:1 $CHCl_3$-2-propanol. The organic extract combined was concentrated under diminished pressure. The residue was purified by flash chromatography on a silica gel column (6 x 4 cm); elution with 88:10:2 $CH_2Cl_2$–MeOH–acetic acid gave **2.13e** as a colorless foam: yield 34 mg (27%); silica gel TLC $R_f$ 0.23 (9:1 $CH_2Cl_2$–MeOH); $^1H$ NMR ($CDCl_3$) δ 1.30 (m, 4H), 1.31 (s, 9H), 2.81-3.13 (m, 6H), 2.34 (s, 3H), 3.13 (m, 6H), 3.61 (m, 2H), 3.82 (m, 2H), 4.46 (s, 2H), 5.08 (br s, 1H) and 6.22 (br s, 2H); $^{13}C$ NMR ($CDCl_3$) δ 13.4, 24.5, 25.9, 28.4, 40.0, 50.1, 56.9, 79.8, 118.9, 123.8, 132.2, 146.1, 154.3, 167.5; mass spectrum (FAB), *m/z* 491.2466 ($M^+$) ($C_{21}H_{33}N_3O_4$ requires 491.2477).

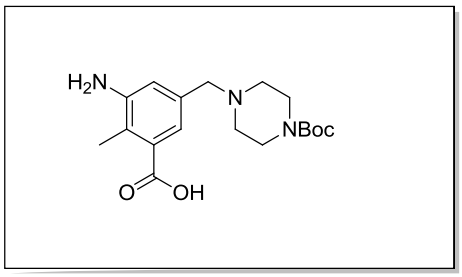


**3-Amino-5-((4-(*tert*-butoxycarbonyl)piperazin-1-yl)methyl)-2-methylbenzoic acid (2.13f).** To a stirred solution of 127 mg (0.337 mmol) of **2.12f** in 3 mL of 3:1:1 THF–MeOH–$H_2O$ was added 0.67 mL (0.67 mmol) of 1 N aq LiOH at 0 $^oC$. The solution was allowed to warm to room temperature and was stirred at 25 $^oC$ for 3 h. The solution was concentrated under diminished pressure and the residue partitioned between $H_2O$ and 4:1 $CHCl_3$–2-propanol (7 mL each). The aqueous phase was extracted with two 7-mL portions of 4:1 $CHCl_3$–2-propanol. The aqueous phase was then acidified to pH ~3 with 1 N aq HCl at 0 $^oC$ and then extracted with five 7-mL portions of 4:1 $CHCl_3$–2-propanol. The organic extract combined was concentrated under diminished pressure. The residue was purified by flash chromatography on a silica gel column (7 x 4 cm); elution with 88:10:2 $CH_2Cl_2$–MeOH–acetic acid gave **2.13f** as a colorless foam: yield 57 mg (48%); silica gel TLC $R_f$ 0.16 (9:1 $CH_2Cl_2$–MeOH); $^1H$ NMR ($CDCl_3$) δ 1.38 (s, 9H), 2.34 (s, 3H), 2.50 (t, 4H, $J$ = 6.5 Hz), 3.20 (t, 4H, $J$ = 6.5 Hz), 3.65 (s, 2H), 5.03 (br s, 1H) 6.27 (br s, 2H), 6.69 (s, 1H) and 7.1 (s, 1H); $^{13}C$ NMR ($CDCl_3$) δ 13.4, 28.4, 46.2, 54.4, 64.5, 79.8, 120.1, 124.2, 132.1, 146.0, 154.7 and 167.8; mass spectrum (FAB), *m/z* 349.1994 ($M^+$) ($C_{18}H_{27}N_3O_4$ requires 349.2002).

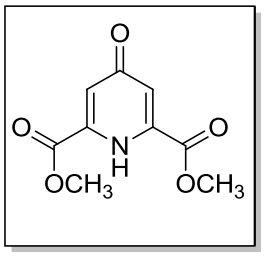

**Dimethyl chelidamate (2.14).**[53] To a stirred solution of 5.0 g (24.9 mmol) of chelidamic acid monohydrate in 50 mL of MeOH was added 9.9 mL (137 mmol) of $SOCl_2$ at 0 $^oC$. The reaction mixture was allowed to warm to room temperature and was stirred at 25 $^oC$ for 72 h. The reaction mixture was concentrated under diminished pressure and the residue was mixed well with 54 ml of an 8% (w/v) aq $NH_4O_2CCH_3$ solution at 0 $^oC$. The resulting mixture was filtered and subsequent crystallization from MeOH gave **2.14** as colorless crystals: yield 3.71 g (71%); mp 169-170 $^oC$, lit.[53] mp 170-171 $^oC$; silica gel TLC $R_f$ 0.27 (95:5 $CH_2Cl_2$-MeOH); $^1H$ NMR ($CDCl_3$) δ 3.98 (s, 6H), 7.42 (br s, 1H) and 7.78 (s, 2H). $^{13}C$ NMR ($CDCl_3$) δ 52.0, 92.8, 148.0, 164.9 and 187.2; mass spectrum (MALDI-TOF), *m/z* 212.0693 $(M+H)^+$ ($C_9H_{10}NO_5$ requires 212.0561).

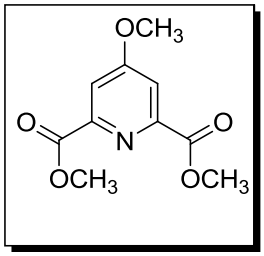

**Dimethyl 4-methoxypyridine-2,6-dicarboxylate (2.15).**[53] To a stirred solution of 3.71 g (17.6 mmol) of **2.13** in 30 mL of DMF was added 4.86 g (12.6 mmol) of $K_2CO_3$ and 50. mL (53.0 mmol) of $(CH_3)_2SO_4$ at 25 $^oC$. The reaction mixture was stirred at 25 $^oC$ for 24 h and then concentrated under diminished pressure to give a colorless solid.

The solid was partitioned between $CH_2Cl_2$ and $H_2O$ (75-mL each) and the aqueous phase was extracted with four 50-mL portions of $CH_2Cl_2$. The combined organic layer was dried ($MgSO_4$) and concentrated under diminished pressure. Crystallization from acetone gave **2.15** as colorless needles: yield 1.90 g (48%); mp 126 $^oC$, lit.[53] 123-124 $^oC$; silica gel TLC $R_f$ 0.43 (95:5 $CH_2Cl_2$–MeOH); $^1H$ NMR ($CDCl_3$) δ 3.98 (s, 3H), 4.01 (s, 6H) and 7.82 (s, 2H). $^{13}C$ NMR ($CDCl_3$) δ 53.5, 56.3, 114.3, 149.9, 165.3 and 167.8; mass spectrum (MALDI-TOF), *m/z* 226.0762 $(M+H)^+$ ($C_{10}H_{12}NO_5$ requires 226.0717).

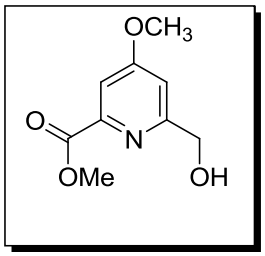


**Methyl 6-hydroxymethyl-4-methoxypyridine-2-carboxylate (2.16).**[19,53] To a stirred solution of 1.90 g (8.44 mmol) of **2.15** in 160 mL of MeOH and 30 mL of $CH_2Cl_2$ was added 543 mg (14.3 mmol) of $NaBH_4$ at 0 $^oC$. The solution was allowed to warm to room temperature and was stirred for 3 h, neutralized to pH ~7 with 1 N HCl and then concentrated under diminished pressure. The resulting solution was extracted with four 50-mL portions of $CH_2Cl_2$. The combined organic layer was dried ($MgSO_4$) and concentrated under diminished pressure. The residue was purified by flash chromatography on a silica gel column (20 x 4 cm). Elution with 95:5 $CH_2Cl_2$–MeOH gave **2.16** as a colorless solid: yield 1.40 g (84%); mp 124-126 $^oC$, lit.[19] mp 127.3-127.5 $^oC$; silica gel TLC $R_f$ 0.29 (95:5 $CH_2Cl_2$–MeOH); $^1H$ NMR ($CDCl_3$) δ 3.92 (s, 3H), 3.99 (s, 3H), 4.80 (s, 2H), 4.5 (br s, 1H) 7.03 (s, 1H) and 7.58 (s, 1H). $^{13}C$ NMR ($CDCl_3$) δ

53.2, 55.9, 64.8, 109.4, 111.0, 148.2, 162.3, 165.5 and 167.3; mass spectrum (MALDI-TOF), *m/z* 198.0770 $(M+H)^+$ ($C_9H_{12}NO_4$ requires 198.0768).

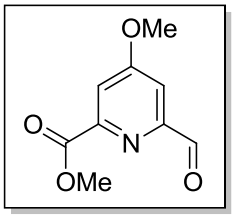


**Methyl 6-formyl-4-methoxypyridine-2-carboxylate (2.17).**[19] To a stirred solution of 1.40 g (7.10 mmol) of **2.16** in 50 mL of $CH_2Cl_2$ was added 6.17 g (71.0 mmol) of activated $MnO_2$ at 25 $^oC$. The mixture was stirred at 25 $^oC$ for 12 h, then filtered through a Celite® pad and the pad was washed with $CH_2Cl_2$. The filtrate was concentrated under diminished pressure and the residue was purified by flash chromatography on a silica gel column (15 x 4 cm). Elution with 95:5 $CH_2Cl_2$–MeOH gave **2.17** as a colorless solid: yield 883 mg (64%); mp 116-117 $^oC$, lit.[19] 116.3-117.1 $^oC$; silica gel TLC $R_f$ 0.47 (95:5 $CH_2Cl_2$–MeOH); $^1H$ NMR ($CDCl_3$) δ 3.98 (s, 3H), 4.05 (s, 3H), 7.61 (s, 1H), 7.85 (s, 1H) and 10.13 (s, 1H); $^{13}C$ NMR ($CDCl_3$) δ 51.3, 55.7, 109.1, 113.4, 149.8, 152.7, 161.2, 165.4 and 191.5; mass spectrum (MALDI-TOF), *m/z* 196.0540 $(M+H)^+$ ($C_9H_{10}NO_4$ requires 196.0612).

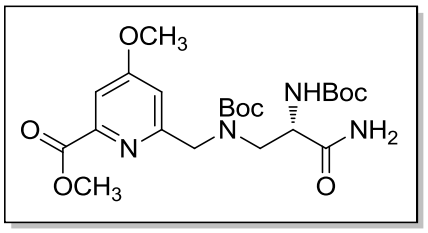


**(*S*)-methyl 6-(((3-amino-2-(*tert*-butoxycarbonylamino)-3-oxopropyl)(*tert*-butoxycarbonyl)amino)methyl)-4-methoxypicolinate (2.18).** A solution of 491 mg (2.05 mmol) of **2.05** in 25 mL MeOH was passed through a Dowex 1 x 2 ($^-$OH form) ion exchange column and concentrated under diminished pressure to regenerate **2.04** as a colorless oil in quantitative yield. To the oil was added 2.0 g of 4Å powdered molecular sieves and a solution of 400 mg (2.05 mmol) of **2.17** in 20 mL $CH_3CN$ at 25 $^oC$. The mixture was stirred at 25 $^oC$ for 24 h, filtered through a Celite® pad and the pad was washed with $CH_3CN$. The filtrate was concentrated under diminished pressure and the residue was dissolved in 30 mL MeOH, treated with a catalytic amount of 10% Pd/C and stirred under a $H_2$ atmosphere at 25 $^oC$ for 24 h. The mixture was filtered through a Celite® pad, the pad was washed with MeOH and concentrated under diminished pressure. The residue was dissolved in 25 mL of $CH_2Cl_2$ and to the solution was added 895 mg (4.10 mmol) of $(Boc)_2O$ and and 1.14 mL (8.2 mmol) $Et_3N$ at 25 $^oC$. The solution was stirred for 24 h at 25 $^oC$ and then concentrated under diminished pressure to give crude **2.18** as a yellow oil. The oil was purified by flash chromatography on a silica gel column (25 x 4 cm). Elution with 9:1 $CH_2Cl_2$–MeOH gave **2.18** as a colorless foam: yield 793 mg (80%); silica gel $R_f$ 0.50 (9:1 $CH_2Cl_2$–MeOH); $^1$H NMR ($CDCl_3$) δ 1.39 (s, 9H), 1.40 (s, 9H), 3.47 (m, 1H), 3.89 (s, 3H), 3.91 (s, 3H), 3.9-4.0 (m, 2H), 4.2-4.8 (m, 2H), 5.61 (s, 1H), 6.85 (d, 1H), 7.51 (d, 1H), 7.93 (br s, 1H) and 8.47 (br s, 1H). 28.4, 28.6,

50.7, 51.2, 53.5, 54.4, 56.6, 80.4, 81.8, 111.2, 111.4, 149.8, 157.3, 162.1, 162.7, 166.7, 168.8 and 175.4; mass spectrum (FAB), *m/z* 483.2477 $(M+H)^+$ ($C_{22}H_{35}N_4O_8$ requires 483.2457).

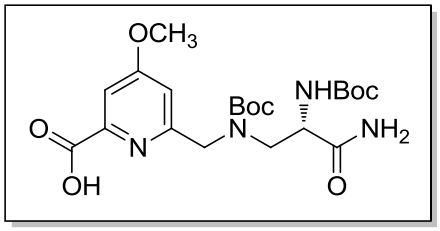


**(*S*)-6-(((3-amino-2-(*tert*-butoxycarbonylamino)-3-oxopropyl)(*tert*-butoxycarbonyl)amino)methyl)-4-methoxypicolinic acid (2.19).** To a stirred solution of 161 mg (0.33 mmol) of **2.18** in 5.6 mL of 3:1:1 THF–MeOH–$H_2O$ was added 0.66 mL of 1 N aq LiOH at 0 $^oC$. The solution was allowed to warm to room temperature and was stirred at 25 $^oC$ for 3 h. The solution was acidified to pH ~4.0 with 1 N aq HCl and concentrated under diminished pressure. The residue was dissolved in 10 mL $H_2O$ and extracted with four 20-mL portions of $CH_2Cl_2$. The organic layers were combined and concentrated under diminished pressure. The residue was purified by flash chromatography on a silica gel column (15 x 2 cm). Elution with 9:1 $CH_2Cl_2$–MeOH gave **2.19** as a colorless foam: yield 90 mg (58%); silica gel $R_f$ 0.50 (9:1 $CH_2Cl_2$–MeOH); $^1H$ NMR ($D_2O$) δ 1.41 (s, 9H), 1.40 (s, 9H), 3.39 (t, 1H), 3.91 (s, 3H), 3.9-4.2 (m, 2H), 4.4-5.0 (m, 2H), 5.85 (d, 1H), 6.87 (d, 1H), 7.58 (d, 1H), 7.93 (br s, 1H) and 8.47 (br s, 1H) 9.23 (br s, 1H); $^{13}C$ NMR ($CDCl_3$) δ 27.7, 27.9, 49.6, 53.7, 53.9, 55.6, 79.8, 80.5, 110.2, 110.5, 148.9, 156.5, 160.8, 161.5, 165.4, 167.7 and 174.4; mass spectrum (MALDI-TOF), *m/z* 470.2357 $(M+H)^+$ ($C_{21}H_{33}N_4O_8$ requires 470.2378).

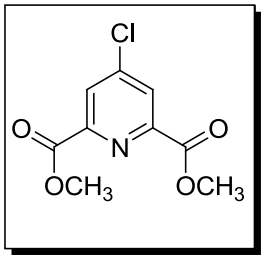


**Dimethyl 4-chloropyridine-2,6-dicarboxylate (2.20).**[54] To a stirred solution of 10.0 g (59.7 mmol) of chelidamic acid monohydrate in 100 mL $CCl_4$ was added 33.1 g (159 mmol) of $PCl_5$ at 25 $^oC$. The solution was heated at reflux at 85 $^oC$ and stirred for 15 h. The solution was allowed to cool to 40 $^oC$ and 30 mL of MeOH was slowly added. The solution was heated to reflux at 70 $^oC$ and stirred for 3 h. The mixture was cooled to 0 $^oC$ and filtered. Crystallization from MeOH gave **2.20** as colorless needles: yield 6.63 g (58%); mp 142 $^oC$, lit.[54] 141-142 $^oC$; silica gel TLC $R_f$ 0.67 (95:5 $CH_2Cl_2$–MeOH); $^1H$ NMR ($CDCl_3$) δ 3.97 (s, 3H) and 8.24 (s, 2H); $^{13}C$ NMR ($CDCl_3$) δ 55.7, 128.5, 147.0, 149.6 and 164.2; mass spectrum (MALDI-TOF), *m/z* 230.0236 $(M+H)^+$ ($C_9H_9NO_4Cl$ requires 230.0222).

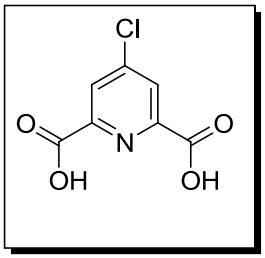


**4-Methoxypyridine-2,6-dicarboxylic acid (2.21).**[19,53,54] A suspension of 6.63 g (28.9 mmol) of **2.20** in 72 mL (72.0 mmol) of 1 N aq NaOH was heated to 80 $^oC$ and stirred for 4 h. The solution was cooled to 0 $^oC$ and acidified to pH ~4 with 1 N aq HCl. The precipitate was collected and dried to give **2.21** as a colorless solid: yield 6.80 g

(quant.); mp 266 °C, lit.[52] 265-267 °C; mass spectrum (MALDI-TOF), *m/z* 201.9919 $(M+H)^+$ ($C_7H_4NO_4Cl$ requires 201.9909).

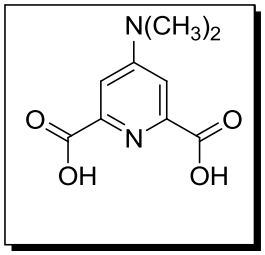


**4-Dimethylaminopyridine-2,6-carboxylic acid (2.22).**[54] A suspension of 3.83 g (19.0 mmol) of **2.21** in 135 mL of 40% (w/w) aq *N*,*N*-dimethylamine solution was heated in a sealed vessel to 135 °C and stirred for 24 h. The solution was cooled to 0 °C and acidified to pH ~3 with conc. aq $H_2SO_4$. The precipitate was collected and dried to give **2.22** as a colorless solid: yield 3.72 g (97%); mp 262 °C, lit.[54] mp 260-262 °C; mass spectrum (MALDI-TOF), *m/z* 211.0779 $(M+H)^+$ ($C_9H_{11}N_2O_4$ requires 211.0721).

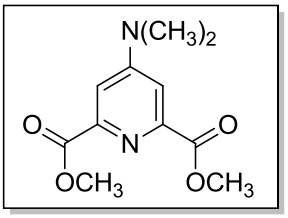


**Dimethyl 4-dimethylaminepyridine-2,6-dicarboxylate (2.23).**[54] To a stirred suspension of 2.40 g (11.4 mmol) of **2.22** in 90 mL of MeOH was added 8.3 mL (114 mmol) of $SOCl_2$ at 0 °C. The solution was heated to reflux at 75 °C and stirred for 5 h and then concentrated under diminished pressure. The residue was mixed well with 90 mL of 8% (w/w) aq solution of $NH_4O_2CCH_3$ at 0 °C and the precipitate was collected and

dried. The crude material was crystallized from acetone to give **2.23** as colorless needles: yield 2.11 g (78%); mp 168 °C, lit.[54] 168-170 °C; silica gel TLC $R_f$ 0.51 (95:5 $CH_2Cl_2$–MeOH); $^1$H NMR ($CDCl_3$) δ 3.13 (s, 6H), 3.98 (s, 6H) and 7.51 (s, 2H); $^{13}$C ($CDCl_3$) δ 39.4, 53.0, 110.2, 148.5, 155.7 and 166.2; mass spectrum (MALDI-TOF), *m/z* 239.1079 $(M+H)^+$ ($C_{11}H_{15}N_2O_4$ requires 239.1034).

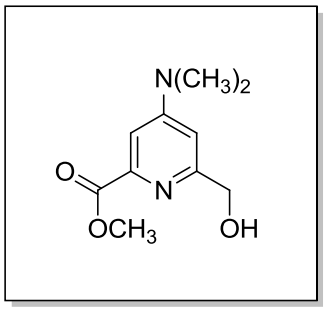


**Methyl 4-((Dimethyl)amino)-6-(hydroxymethyl)picolinate (2.24).**[13,18,54] To a stirred solution of 1.00 g (4.20 mmol) of **2.23** in 16 mL of $CH_2Cl_2$ and 78 mL of MeOH was added 270 mg (7.14 mmol) of $NaBH_4$ at 0 °C. The solution was allowed to warm to room temperature and was stirred at 25 °C for 4 h. The reaction mixture was then acidified to pH 3 using 1 N aq HCl and then concentrated under diminished pressure. The resulting solution was extracted with four 50-mL portions of $CH_2Cl_2$. The combined organic layer was dried ($MgSO_4$) and concentrated under diminished pressure. The residue was purified by flash chromatography on a silica gel column (20 x 4 cm). Elution with 95:5 $CH_2Cl_2$–MeOH gave **2.24** as a colorless solid: yield 665 mg (75%); mp 79-81 °C, lit.[54] mp 81-82 °C; silica gel TLC $R_f$ 0.28 (95:5 $CH_2Cl_2$–MeOH); $^1$H NMR ($CDCl_3$) δ 3.01 (s, 6 H), 3.89 (s, 3H), 4.32 (s, 2H), 5.23 (br s, 1H), 7.03 (s, 1H) and 7.58 (s, 1H); $^{13}$C NMR ($CDCl_3$) δ 41.3, 52.7, 55.4, 64.6, 108.9, 110.1, 148.2, 165.2 and 167.1; mass spectrum (MALDI-TOF), *m/z* 211.1112 $(M+H)^+$ ($C_{10}H_{15}N_2O_3$ requires 211.1084).

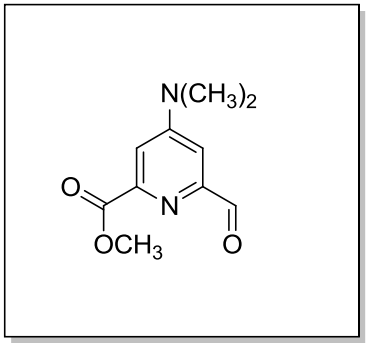


**Methyl 4-((Dimethyl)amino)-6-formylpicolinate (2.25).** [13,18,54] To a stirred solution of 213 mg (1.01 mmol) of **2.24** in 15 mL of $CH_3CN$ was added 878 mg (10.10 mmol) of $MnO_2$ at 25 $^oC$. The reaction mixture was heated to 45 $^oC$ for 24 h, allowed to cool to room temperature, then filtered through a pad of Celite® and the pad was washed with $CH_3CN$. The filtrate was concentrated under diminished pressure and the residue was purified by flash column chromatography on a silica gel column (10 x 3 cm); elution with 95:5 $CH_2Cl_2$–MeOH gave **2.25** as a colorless solid: yield 56 mg (26%); mp 116.0-117.0 $^oC$, lit.[54] 117.0-117.5 $^oC$; silica gel TLC $R_f$ 0.43 (95:5 $CH_2Cl_2$–MeOH); $^1H$ NMR ($CDCl_3$) δ 2.88 (s, 6H), 3.79 (s, 3H), 6.98 (s, 1H), 7.24 (s, 1H) and 9.81 (s, 1H); $^{13}C$ ($CDCl_3$) δ 38.9, 52.5, 105.3, 110.7, 148.1, 152.4, 154.8, 165.3 and 193.3; mass spectrum (MALDI-TOF), *m/z* 209.0964 $(M+H)^+$ ($C_{10}H_{13}N_2O_3$ requires 209.0928).

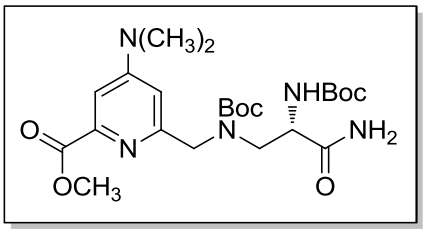


**(*S*)-Methyl 6-(((3-Amino-2-(*tert*-butoxycarbonylamino)-3-oxopropyl)(*tert*-butoxycarbonyl)amino)methyl)-4-dimethylaminopicolinate (2.26).** A solution of

100 mg (0.42 mmol) of **2.05** in 10 mL MeOH was passed through a Dowex 1 x 2 ($^-$OH form) ion exchange column and concentrated under diminished pressure to regenerate **2.04** as a colorless oil in quantitative yield. To the oil was added 0.42 g of 4Å powdered molecular sieves and a solution of 87 mg (0.42 mmol) of **2.25** in 5 mL $CH_3CN$ at 25 $^oC$. The mixture was stirred at 25 $^oC$ for 24 h, filtered through a Celite® pad and washed with $CH_3CN$. The filtrate was concentrated under diminished pressure and the residue was dissolved in 20 mL MeOH, treated with a catalytic amount of 10% Pd/C and stirred under a $H_2$ atmosphere at 25 $^oC$ for 24 h. The mixture was filtered through a Celite® pad, the pad was washed with MeOH and then concentrated under diminished pressure. The residue was dissolved in 15 mL of $CH_2Cl_2$ and to the solution was added 183 mg (0.84 mmol) of $(Boc)_2O$ and and 0.23 mL (1.68 mmol) of $Et_3N$ at 25 $^oC$. The solution was stirred at 25 $^oC$ for 24 h and then concentrated under diminished pressure. The residue was purified by flash chromatography on a silica gel column (16 x 2 cm). Elution with 95:5 $CH_2Cl_2$–MeOH gave **2.26** as a colorless foam: yield 82 mg (39%); silica gel $R_f$ 0.53 (9:1 $CH_2Cl_2$–MeOH); $^1$H NMR ($CDCl_3$) δ 1.29 (s,18H), 2.94 (s, 6H), 3.41 (m, 2H), 3.71 (m, 3H), 4.2-4.9 (m, 3H), 5.99 (s, 1H), 6.36 (s, 1H), 6.36 (s, 1H), 7.17 (s, 1H) and 8.59 (s 1H); $^{13}$C NMR ($CDCl_3$) δ 27.9, 28.0, 39.0, 51.1, 52.2, 52.4, 53.7, 79.0, 80.2, 106.4, 107.4, 146.9, 155.2, 155.6, 158.5, 158.9, 166.0 and 172.6; mass spectrum (FAB), *m/z* 497.2880 $(M+H)^+$, ($C_{23}H_{38}N_5O_7$ requires 497.2851).

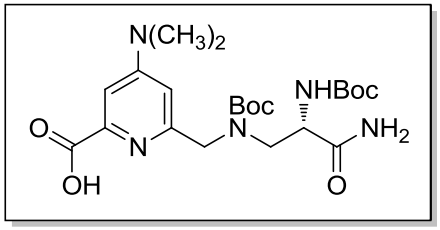


**(*S*)-6-(((3-Amino-2-((*tert*-butoxycarbonyl)amino)-3-oxopropyl)(*tert*-butoxycarbonyl)amino)methyl)-4-(dimethylamino)picolinic acid (2.27).** To a stirred solution of 145 mg (0.36 mmol) of **2.26** in 8 mL of 3:1:1 THF–MeOH–$H_2O$ was added 0.7 mL of 1 N aq LiOH at 0 $^oC$. The solution was allowed to warm to room temperature and was stirred at 25 $^oC$ for 3 h. The solution was acidified to pH ~4.0 with 1 N aq HCl and concentrated under diminished pressure. The residue was dissolved in 10 mL $H_2O$ and extracted with four 20-mL portions of $CH_2Cl_2$. The organic layers were combined and concentrated under diminished pressure. The residue was purified by flash chromatography on a silica gel column (15 x 2 cm). Elution with 9:1 $CH_2Cl_2$–MeOH gave **2.27** as a colorless foam: yield 80 mg (53%); silica gel $R_f$ 0.48 (9:1 $CH_2Cl_2$–MeOH); $^1H$ NMR ($D_2O$) δ 1.41 (s, 9H), 1.40 (s, 9H), 2.96 (s, 6H), 3.14 (t, 1H), 3.51-3.90 (m, 4H), 5.64 (br s, 1H), 6.87 (d, 1H), 7.58 (d, 1H), 7.93 (br s, 1H), 8.47 (br s, 1H) and 9.01 (br s, 1H); mass spectrum (FAB), *m/z* 483.2704 $(M+H)^+$, ($C_{22}H_{36}N_5O_7$ requires 483.2695).

**Incorporation of pyrimidoblamic acid analogues (2.11, 2.13a-2.13f, 2.19, 2.27) Figure 2.04, Schemes 2.01-2.06) into novel deglycoBLM $A_6$ analogues (2.32-2.40, Figure 2.06)**

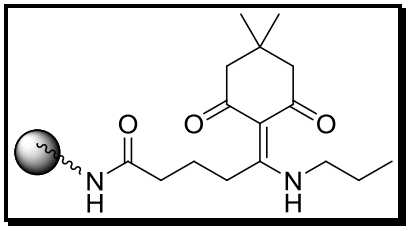

**Procedure for the functionalization of resin (2.27).**[14] 100 mg of resin (0.048 mmol) (NOVASYNTG amino Resin, 0.048 mmol/g loading capcaity) was added in a solid phase test tube. The beads were rinsed with DMF (3 x 4 mL), and DCM (3 x 4 mL) 10 min each and then washed with DMF (3 x 4 mL). A solution containing 42.5 mg (0.144 mmol) of DDE-linker, 54 mg (0.144 mmol) of HBTU, and 50 μL (0.288 mmol) of DIPEA in 1.5 mL of DMF was added to the test tube containing beads and stirred overnight. The resin was filtered and washed with (3 x 3 mL) DMF, (3 x 3 mL) DCM, (3 x 3 mL) MeOH. The resulting resin was qualitatively tested by the Kaiser Test. The resin was dried under vacuum overnight.

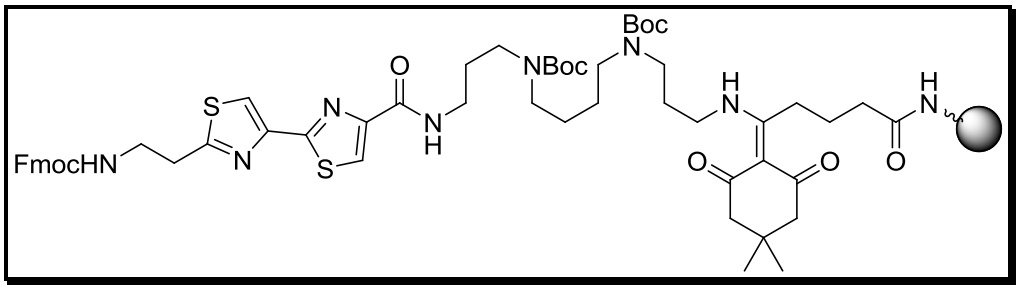

**General Procedure for the Attachment of Bithiazole to the Solid Support (2.28).**[14] To a suspension containing 100 mg (0.48 mmol/g) of NovaSyn TentaGel amino functionalized resin was added a solution containing 170 mg (0.439 mmol) of Boc-

protected permine[26] and 96 uL (71 mg, 0.548 mmol) Hunig's base in 4 mL DMF. After 24 h, the resin was filtered, and washed for 30 s each with three 5-mL potions of DMF, three 5-mL portions of $CH_2Cl_2$, and three 5-mL portions of MeOH and then three 5-mL portions of DMF. A solution containing 69 mg (0.144 mmol) fmoc-bithiazole, 54 mg (0.144 mmol) of HBTU, and 50 uL of Hunig's base in 4 mL DMF was added. After 30 min, the resin was filtered, washed for 30 s each with three 5-mL potions of DMF, three 5-mL portions of $CH_2Cl_2$, and three 5-mL portions of MeOH. The resulting resin was dried under diminished pressure over KOH pellets. Quantatative Fmoc cleavage analysis indicated a loading of 0.18 mm/g (60% over three steps).

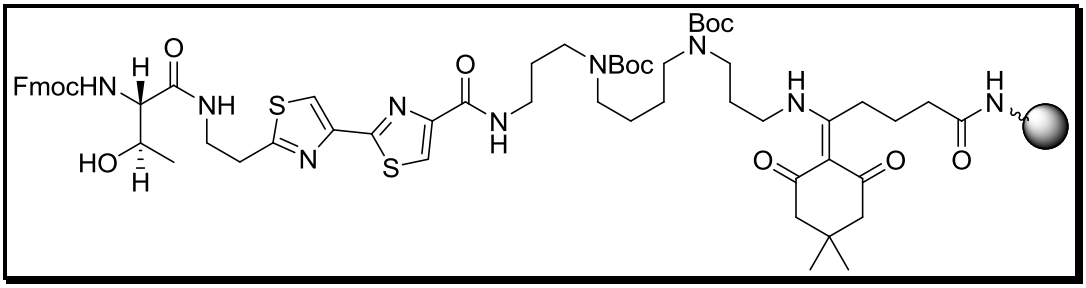


**General Procedure for the Attachement of Threonine to the Resin-Bound Dipeptide (2.29).**[14] To a suspension containing 100 mg bithiazole-functionalized resin was added sequentially for 5 min each, three 4-mL solutions containing 20% piperidine in DMF. The resulting resin was washed for 30 s each with three 10-mL portions of DMF, three 10-mL portions of $CH_2Cl_2$, and then three 10-mL portions of DMF. A solution containing 49 mg (0.144 mmol) of Fmoc-threonine, 54 mg (0.144 mmol) of HBTU, 19 mg (0.144 mmol) of HOBt, and 28 uL (37 mg, 0.288 mmol) of Hunig's base in 4 mL of DMF was added. After 30 min the resin was filtered and washed with three 5-mL portions of DMF, three 5-mL portions of $CH_2Cl_2$, and again with three 5-mL portions of MeOH. The

resulting resin was dried under diminished pressure over KOH pellets. Quantitative Fmoc cleavage analysis indicated a loading of 0.18 mmol/g (93%).

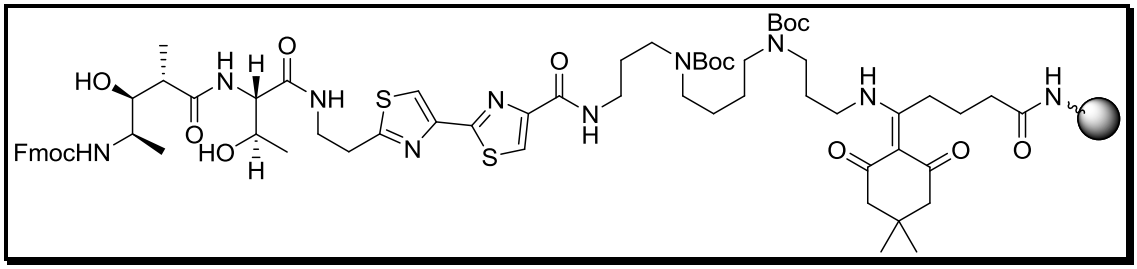

**General Procedure for the Attachment of Methylvalerate to the Resin-Bound Tripeptide (2.30).**[14] To a suspension containing 100 mg of the derivatized resin was added successively three 1.0-mL solutions containing 20% piperidine in DMF. The resulting resin was washed for 30 s each with three 5-mL portions of DMF, three 5-mL portions of $CH_2Cl_2$, and then three 5-mL portions of DMF. A solution containing 53 mg (0.144 mmol) of Fmoc-methylvalerate, 55 mg (0.144 mmol) of HBTU, 19 mg (0.144 mmol) of HOBt and 27 uL (37 mg, 0.288 mmol) of Hunig's base in 1 mL DMF was added. After 30 min, the resin was filtered and washed with three 5-mL portions of DMF, three 5-mL portions of $CH_2Cl_2$, and again with three 5-mL portions of MeOH. The resulting resin was dried under diminished pressure over KOH pellets. Quantitative Fmoc cleavage analysis indicated a loading of 0.17 mmol/g (90%).

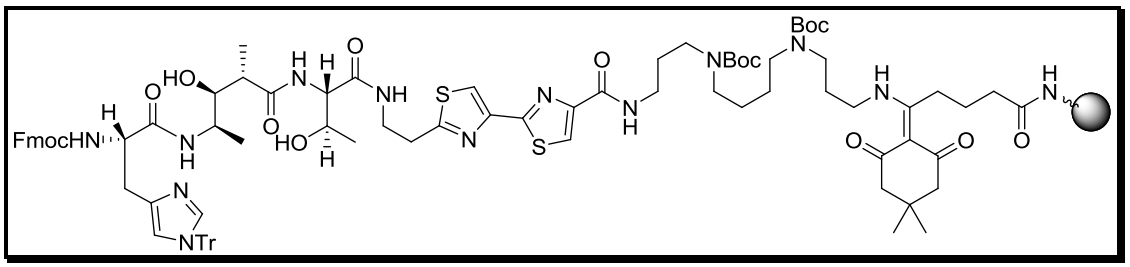

**General Procedure for the Attachment of Histidine to the Resin-Bound Tetrapeptide (2.31).**[14] To a suspension containing 60 mg of the derivatized resin was added successively three 1.0-mL solutions containing 20% piperidine in DMF. The resulting resin was washed for 30 s each with three 5-mL portions of DMF, three 5-mL portions of $CH_2Cl_2$, and then three 5-mL portions of DMF. A solution containing 89 mg (0.144) of Fmoc-trityl-histidine, 55 mg (0.144 mmol) of HATU, 20 mg (0.144 mmol) of HOAt, and 27 uL (37 mg, 0.144 mmol) of Hunig's base in 1-mL of DMF was added. After 30 min, the resin was filtered and washed for 30 s each with three 5-mL portions of DMF, three 5-mL portions of $CH_2Cl_2$, and then three 5-mL portions of MeOH. The resulting resin was dried under diminished pressure over KOH pellets. Quantitative Fmoc cleavage analysis indicated a loading of 0.16 mmol/g (90%).

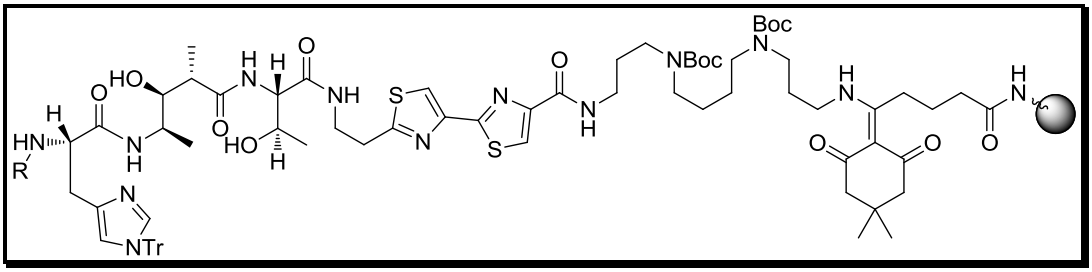


**General Procedure for the Synthesis of Deglycobleomycin $A_6$ (Analogues) (2.32-3.40).**[14] To a suspension containing 40 mg of the pentapeptide derivatized resin was added successively, three 1.0-mL solutions containing 20% piperidine in DMF. The resulting resin was washed for 30 s each with three 5-mL portions of DMF, three 5-mL portions of $CH_2Cl_2$, and then three 5-mL portions of DMF. The resin was then added to a 10 mL round bottom flask containing 1-mL of DMF and cooled to 0 $^oC$ for 10 min. A mixture containing 16-20 mg (0.072. mmol) of a Boc-pyrimidoblamic acid analogue

**2.11, 2.13a-2.13f, 2.19, 2.27** and 27 mg (0.072 mmol) of BOP was added to the resin with an additional 1-mL of DMF. The reaction mixture was cooled for an additional 10 min followed by the addition of 13 µL (27 mg, 0.144 mmol) of Hunig's base. After 16 h, the resin was filtered and washed for 30 s each with three 5-mL portions of DMF, three 5-mL portions of $CH_2Cl_2$, and then three 5-mL portions of MeOH. The resulting resin was dried under diminished pressure over KOH pellets.

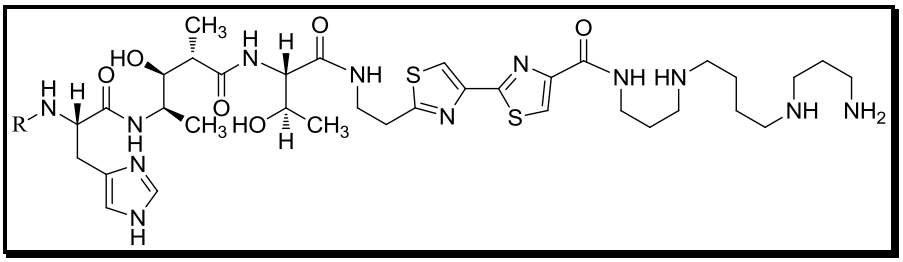

**General Procedure for the Cleavage of Deglycobleomycin $A_6$ (Analogues) from the Resin.**[14] To a suspension containing 30 mg of resin-bound fully protected deglycobleomycin $A_6$ (analogue) was added a solution containing 200 µL of triisopropylsilane and 200 µL of $(CH_3)_2S$. After 10 min, 4 mL of TFA was added to the suspension. After 4 h, the resin was filtered and washed with five 3-mL portions of $CH_2Cl_2$, and five 3-mL portions of DMF. The resulting resin was treated successively with four 1-mL portions of a 2% hydrazine in DMF solution over 40 min. The eluate was collected and concentrated under diminished pressure at <30 $^oC$. The resulting oil was dissolved in 5-mL of a 0.1% aq TFA solution, frozen and lyophilized to give the crude residue.

**Fully Synthesized DeglycoBLM $A_6$ Analogues Altered at the Pyrimidoblamic aAcid Moiety (Figure 2.06)**

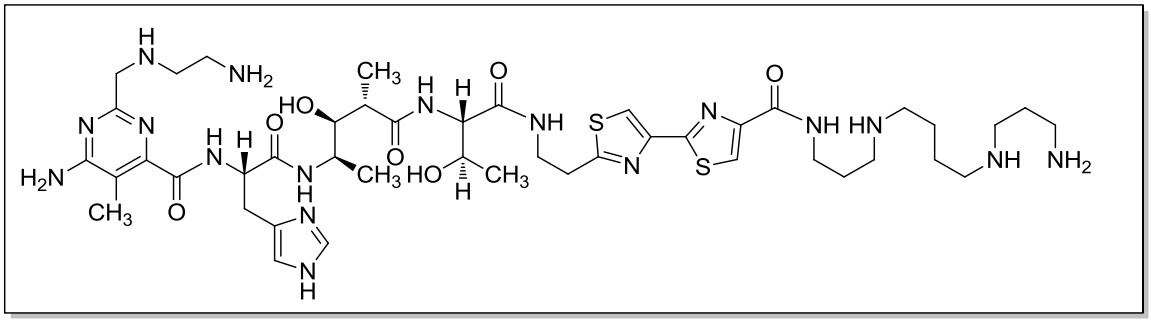

**DelcycoBLM $A_6$ Analogue 2.32.** The crude residue was dissolved in 0.1% aq TFA to give a solution containing 1 mg/mL of the fully deprotected deglycoBLM $A_6$ analogue **2.32**. The solution was purified on an All-Tech $C_{18}$ (10 x 250 mm, 5 µm) reversed phase semi-preparative HPLC column using 0.1% aq TFA and $CH_3CN$ mobile phases. A linear gradient was employed (99:1 0.1% aq TFA–$CH_3CN$ → 50:50 0.1% aq TFA–$CH_3CN$) over a period of 30 min at a flow rate of 3.5 mL/min. Fractions containing the desired product eluted at 14.1 min and were collected, frozen, and lyophilized to give **2.32** as a colorless solid: yield 2.26 mg (88% over two steps); mass spectrum (TOF ESI), *m/z* 1013.5170 ($M^+$) ($C_{44}H_{71}N_{17}O_7S_2$ requires 1013.5164).

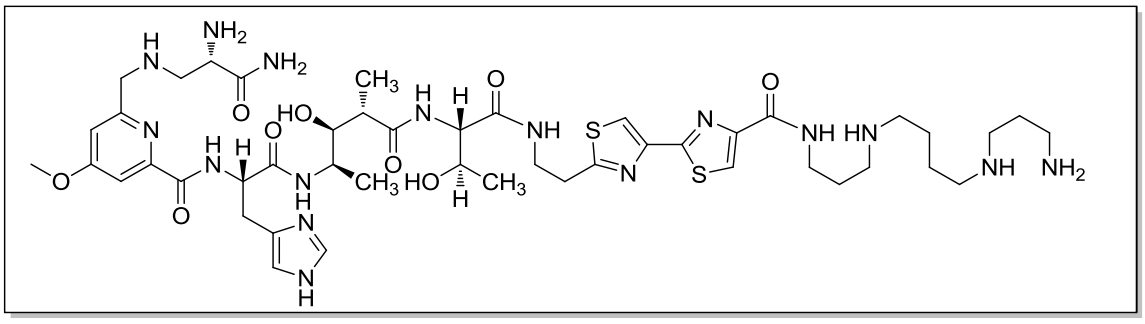

**DelcycoBLM $A_6$ Analogue 2.33.** The crude residue was dissolved in 0.1% aq TFA to give a solution containing 1 mg/mL of the fully deprotected deglycoBLM $A_6$ analogue **2.33**. The solution was purified on an All-Tech $C_{18}$ (10 x 250 mm, 5 µm) reversed phase semi-preparative HPLC column using 0.1% aq TFA and $CH_3CN$ mobile phases. A linear gradient was employed (99:1 0.1% aq TFA–$CH_3CN$ → 50:50 0.1% aq TFA–$CH_3CN$) over a period of 30 min at a flow rate of 3.5 mL/min. Fractions containing the desired product eluted at 13.9 min and were collected, frozen, and lyophilized to give **2.33** as a colorless solid: yield 1.28 mg (45% over two steps); mass spectrum (TOF ESI), *m/z* 10056.5130 ($M^+$) ($C_{46}H_{72}N_{16}O_9S_2$ requires 1056.5110).

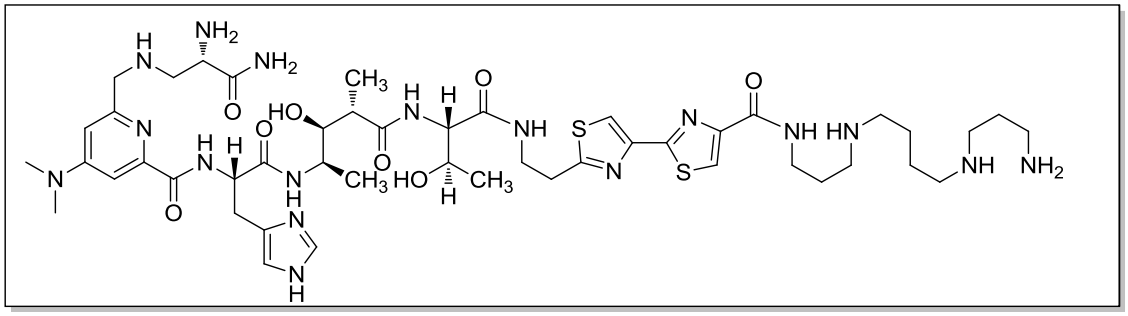

**DelcycoBLM $A_6$ Analogue 2.34.** The crude residue was dissolved in 0.1% aq TFA to give a solution containing 1 mg/mL of the fully deprotected deglycoBLM $A_6$ analogue **2.34**. The solution was purified on an All-Tech $C_{18}$ (10 x 250 mm, 5 µm) reversed phase semi-preparative HPLC column using 0.1% aq TFA and $CH_3CN$ mobile phases. A linear gradient was employed (99:1 0.1% aq TFA–$CH_3CN$ → 50:50 0.1% aq TFA–$CH_3CN$) over a period of 30 min at a flow rate of 3.5 mL/min. Fractions containing the desired product eluted at 13.8 min and were collected, frozen, and lyophilized to give **2.34** as a colorless solid: yield 1.37 mg (55% over two steps); mass spectrum (TOF ESI), *m/z* 1069.5434 ($M^+$) ($C_{46}H_{72}N_{16}O_9S_2$ requires 1069.5426).

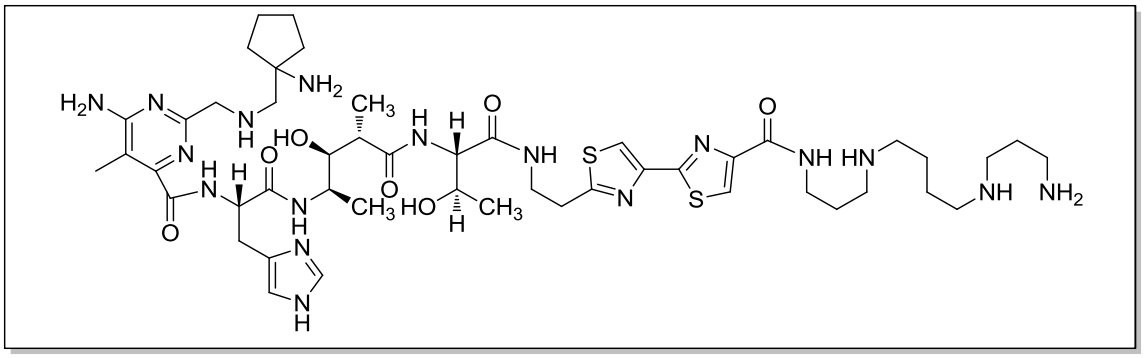

**DelcycoBLM $A_6$ Analogue 2.35.** The crude residue was dissolved in 0.1% aq TFA to give a solution containing 1 mg/mL of the fully deprotected deglycoBLM $A_6$ analogue **2.35**. The solution was purified on an All-Tech $C_{18}$ (10 x 250 mm, 5 µm) reversed phase semi-preparative HPLC column using 0.1% aq TFA and $CH_3CN$ mobile phases. A linear gradient was employed (99:1 0.1% aq TFA–$CH_3CN$ → 50:50 0.1% aq TFA–$CH_3CN$) over a period of 30 min at a flow rate of 3.5 mL/min. Fractions containing the desired product eluted at 14.2 min and were collected, frozen, and lyophilized to give **2.35** as a colorless solid: yield 1.78 mg (65% over two steps); mass spectrum (TOF ESI), *m/z* 1067.5650 ($M^+$) ($C_{48}H_{77}N_{17}O_7S_2$ requires 1067.5633).

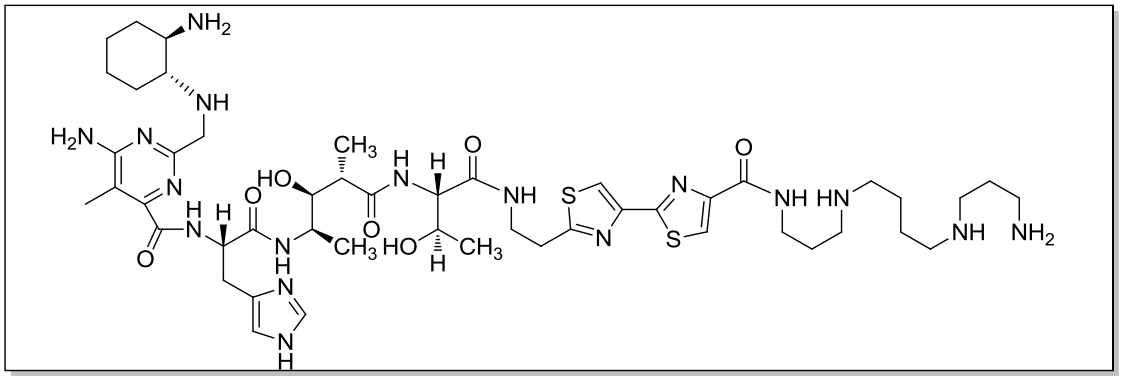

**DelcycoBLM $A_6$ Analogue 2.36.** The crude residue was dissolved in 0.1% aq TFA to give a solution containing 1 mg/mL of the fully deprotected deglycoBLM $A_6$ analogue

**2.36**. The solution was purified on an All-Tech $C_{18}$ (10 x 250 mm, 5 µm) reversed phase semi-preparative HPLC column using 0.1% aq TFA and $CH_3CN$ mobile phases. A linear gradient was employed (99:1 0.1% aq TFA–$CH_3CN$ → 50:50 0.1% aq TFA–$CH_3CN$) over a period of 30 min at a flow rate of 3.5 mL/min. Fractions containing the desired product eluted at 14.2 min and were collected, frozen, and lyophilized to give **2.36** as a colorless solid: yield 1.33 mg (50% over two steps); mass spectrum (TOF ESI), *m/z* 1067.5651 ($M^+$) ($C_{48}H_{77}N_{17}O_7S_2$ requires 1067.5633).

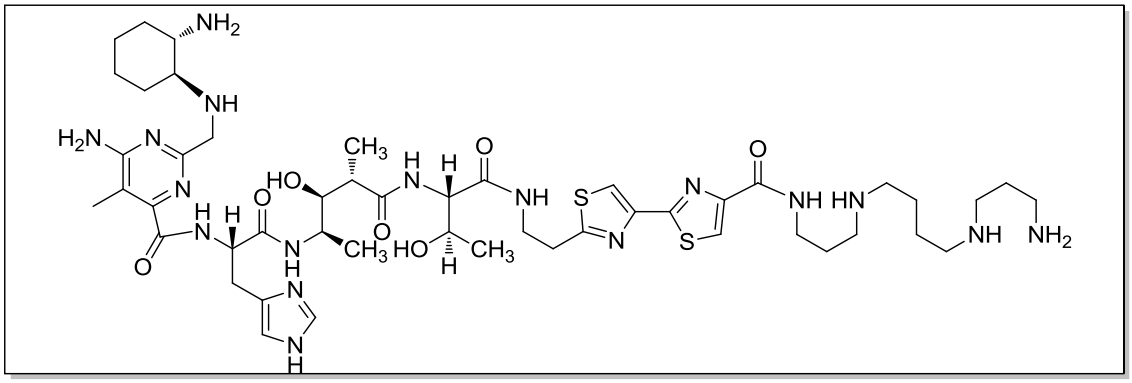

**DelcycoBLM $A_6$ Analogue 2.37.** The crude residue was dissolved in 0.1% aq. TFA to give a solution containing 1 mg/mL of the fully deprotected deglycoBLM $A_6$ analogue **2.37**. The solution was purified on an All-Tech $C_{18}$ (10 x 250 mm, 5 µm) reversed phase semi-preparative HPLC column using 0.1% aq TFA and $CH_3CN$ mobile phases. A linear gradient was employed (99:1 0.1% aq TFA–$CH_3CN$ → 50:50 0.1% aq TFA–$CH_3CN$) over a period of 30 min at a flow rate of 3.5 mL/min. Fractions containing the desired product eluted at 14.2 min and were collected, frozen, and lyophilized to give **2.37** as a colorless solid: yield 1.55 mg (61% over two steps); mass spectrum (TOF ESI), *m/z* 1067.5654 ($M^+$) ($C_{48}H_{77}N_{17}O_7S_2$ requires 1067.5633).

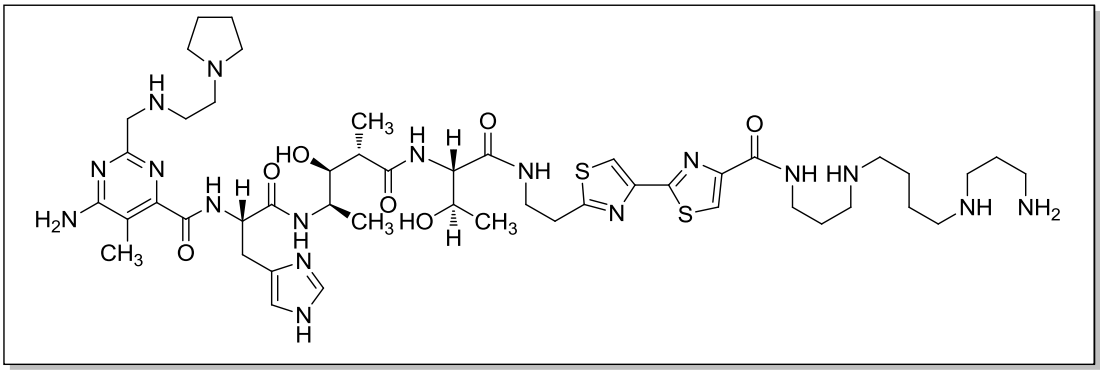

**DelcycoBLM $A_6$ Analogue 2.38.** The crude residue was dissolved in 0.1% aq. TFA to give a solution containing 1 mg/mL of the fully deprotected deglycoBLM $A_6$ analogue **2.38**. The solution was purified on an All-Tech $C_{18}$ (10 x 250 mm, 5 µm) reversed phase semi-preparative HPLC column using 0.1% aq TFA and $CH_3CN$ mobile phases. A linear gradient was employed (99:1 0.1% aq TFA–$CH_3CN$ → 50:50 0.1% aq TFA–$CH_3CN$) over a period of 30 min at a flow rate of 3.5 mL/min. Fractions containing the desired product eluted at 14.2 min and were collected, frozen, and lyophilized to give **2.38** as a colorless solid: yield 1.78 mg (66% over two steps); mass spectrum (TOF ESI), *m/z* 1067.5643 ($M^+$) ($C_{48}H_{77}N_{17}O_7S_2$ requires 1067.5633).

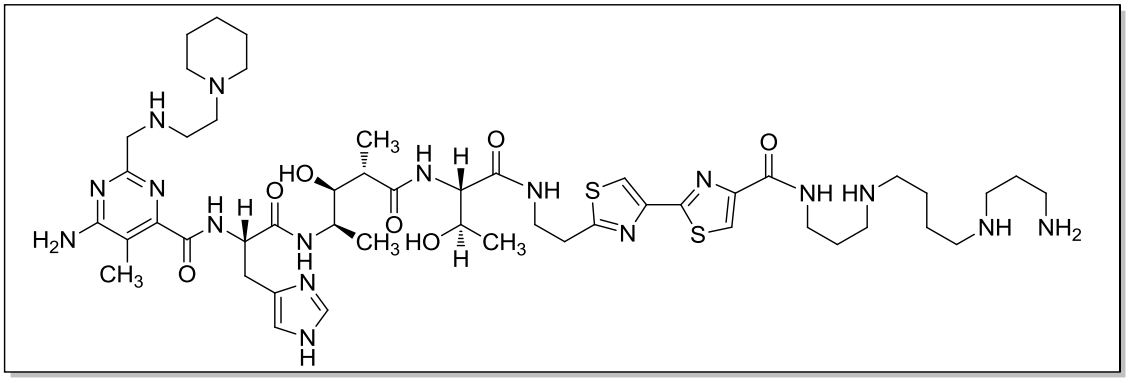

**DelcycoBLM $A_6$ Analogue 2.39.** The crude residue was dissolved in 0.1% aq TFA to give a solution containing 1 mg/mL of the fully deprotected deglycoBLM $A_6$ analogue **2.39**. The solution was purified on an All-Tech $C_{18}$ (10 x 250 mm, 5 µm) reversed phase

semi-preparative HPLC column using 0.1% aq TFA and $CH_3CN$ mobile phases. A linear gradient was employed (99:1 0.1% aq TFA–$CH_3CN$ → 50:50 0.1% aq TFA–$CH_3CN$) over a period of 30 min at a flow rate of 3.5 mL/min. Fractions containing the desired product eluted at 14.2 min and were collected, frozen, and lyophilized to give **2.39** as a colorless solid: yield 1.69 mg (69% over two steps); mass spectrum (TOF ESI), *m/z* 1081.5788 ($M^+$) ($C_{48}H_{77}N_{17}O_7S_2$ requires 1081.5790).

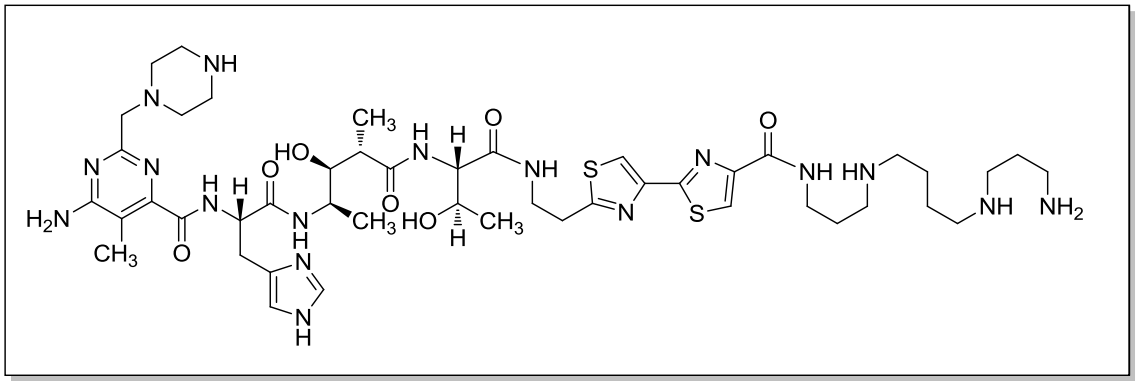

**DelcycoBLM $A_6$ Analogue 2.40.** The crude residue was dissolved in 0.1% aq TFA to give a solution containing 1 mg/mL of the fully deprotected deglycoBLM $A_6$ analogue **2.40**. The solution was purified on an All-Tech $C_{18}$ (10 x 250 mm, 5 µm) reversed phase semi-preparative HPLC column using 0.1% aq TFA and $CH_3CN$ mobile phases. A linear gradient was employed (99:1 0.1% aq TFA–$CH_3CN$ → 50:50 0.1% aq TFA–$CH_3CN$) over a period of 30 min at a flow rate of 3.5 mL/min. Fractions containing the desired product eluted at 14.2 min and were collected, frozen, and lyophilized to give **2.40** as a colorless solid: yield 1.88 mg (75% over two steps); mass spectrum (TOF ESI), *m/z* 1039.5328 ($M^+$) ($C_{46}H_{73}N_{17}O_7S_2$ requires 1039.5320)

# Chapter 3

## 3.01 Introduction

Surface plasmon resonance (SPR) biosensor techniques can directly provide essential kinetic and even mechanistic information for the study and characterization of small molecule–nucleic acid interactions. The method is label free and can monitor the interactions in real time. Both dynamic and steady-state information can be obtained for a variety of rates and binding affinities.[56] SPR biosensor techniques are the fundamental principle of many "lab-on-a-chip" sensors and work by measuring the oscillations or difference in collective oscillations of free electron gas density, or "plasmons". A plasmon is a quantum of plasma oscillation analogous to the way in which photons or phonons are quantizations of electromagnetic and mechanical vibrations. However the photon is an elementary particle, whereas the plasmon remains a quasiparticle. When the affinity of two ligands must be determined by surface plasmon resonance (i.e. small molecule–nucleic acid interactions), the binding constant must be measured and can be found using the dynamical SPR model and the standard equation (Equation 3.11).

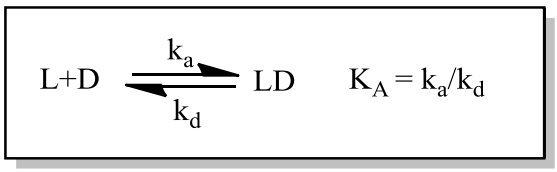


**Equation 3.01** Binding constant determination by ligand interaction

In a biosensor evaluation of a ligand (L) and a nucleic acid binding site (D) the components bind to give a complex (LD), where either D or L must be immobilized/functionalized on the surface of a chip.[56] This is easily achieved with nucleic acids which can be biotinylated at either the 5′ or 3′ terminus, used in conjunction

with a chip surface that has been coated with streptavidin (Figure 3.01). It has also been shown to be possible to immobilize biotinylated small molecules which have the ability to bind specific oligonucleotides and motifs.[57]

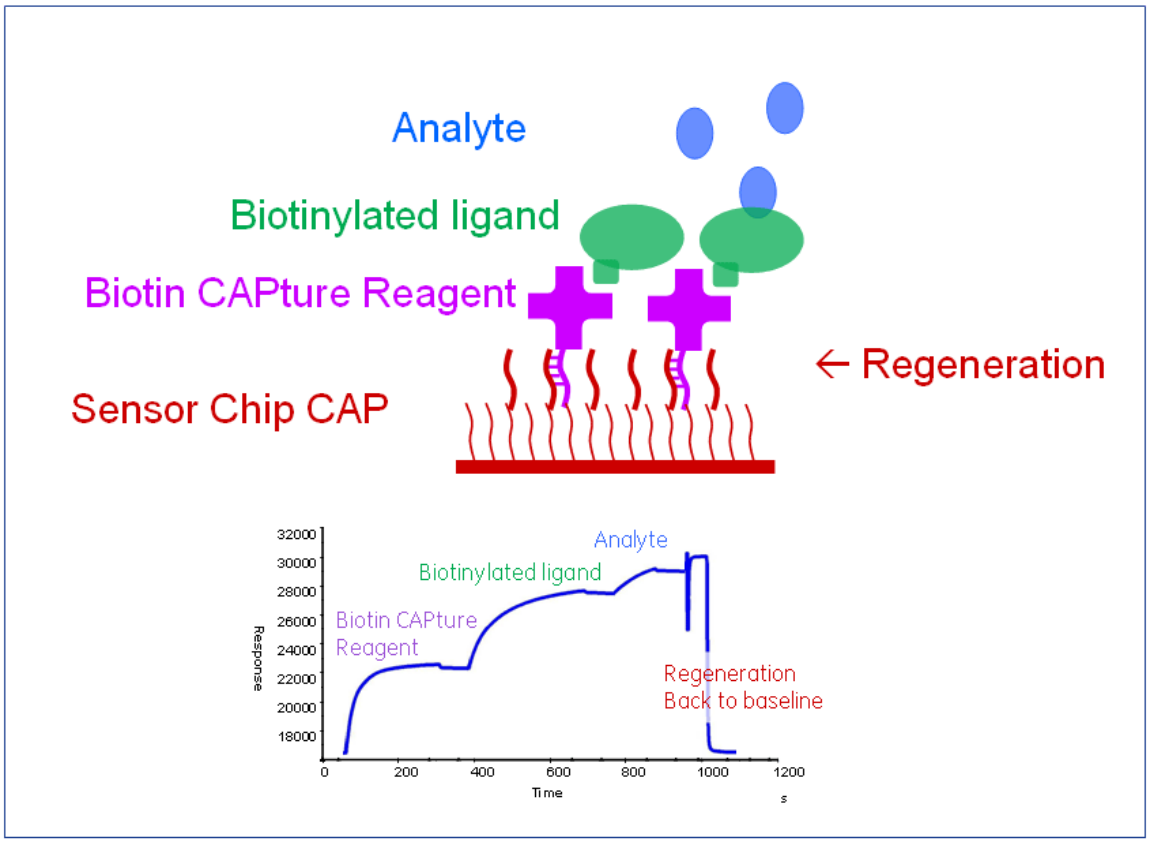


**Figure 3.01** Example of a streptavadin-biotin capture biosensor chip[58]

To date, much is already known about the bithiazole DNA binding domain of bleomycin as well as its binding specificity and strong preference for 5′-CT and 5′-CG rich sequences.[10,17] Previous studies done to identify DNA binding motifs of bleomycin have been based primarily on cleavage assays of oligonucleotides and the investigation and characterization of the degradation products produced. However, there has been little supporting literature[59,60] reporting the use of SPR as a tool to delineate such a unique DNA binding profile (Figure 3.02).

When binding constant determination is possible within the parameters of the two

ligands (and instrumentation limits), the resulting output is a sensorgram. When the two ligands interact through a microflow system an increase in SPR signal, expressed in "response units (RU)" is observed. When the complex of the two ligands becomes disassociated a decrease in RU is observed. From the two observable events, the on-($k_a$) and off-($k_d$) rates as well as the equilibrium constant ($K_D$) can be calculated. The valuable kinetic information obtained can provide mechanistic conclusions about the system.

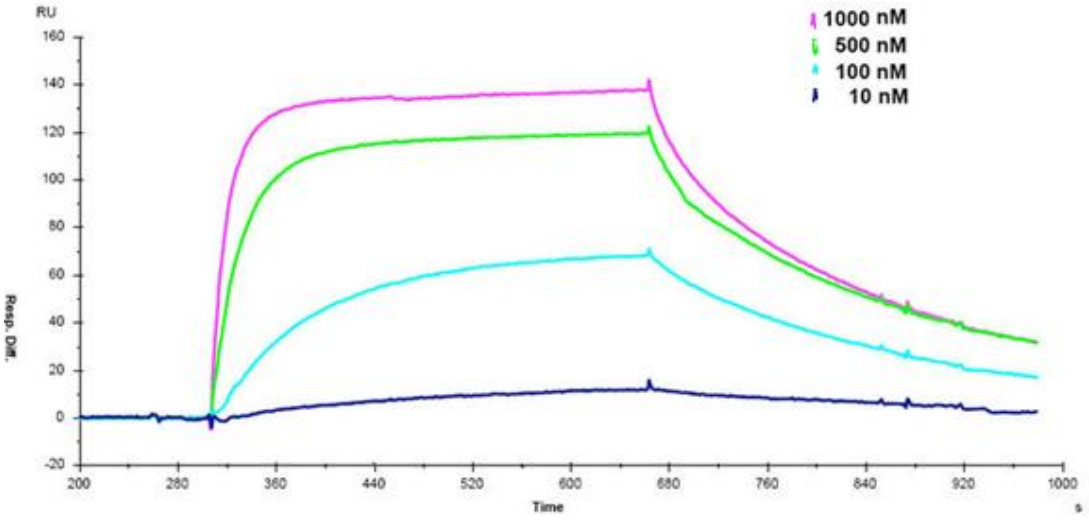


**Figure 3.02** A typical sensorgram model (As output from a typical biacore instrument)

The antitumor activity of bleomycin is understood to derive its ability to cleave DNA,[61] and possibly RNA as well.[62-65] Until very recently, almost all studies of BLM-mediated DNA cleavage were carried out using an excess of metalloBLM. However, one unique characteristic of bleomycin is its atypically low clinical dose (~5 μmol). Accordingly, it seemed logical to inquire whether the preferential binding motifs observed previously (where a large excess of bleomycin was present) were unchanged when a large excess of DNA relative to bleomycin was employed and studied.

## 3.02 Results

Many derivatized apo-(metal free) BLMs and metalloBLMs were prepared for the study of DNA binding dynamics, in accordance with previous literature for functionalizing BLMs.[66] Usually, the final product was obtained in no more than two steps and in good yield (Schemes 3.01-3.05). Often the necessary transformations occurred in a single step (many metalloBLMs) and in quantitative yield following simple mixing and lyophilization (Scheme 3.01). Functionalization of BLM $A_5$ generally proceeded by generating the Cu(II) conjugate, thereby leaving a single reactive exposed amine at the C-terminus. This was the methodology followed for N-acetyl BLM $A_5$ presented in Scheme 3.02, as well as for the biotinylation of several BLMs (Scheme 3.04). N-acetylation of BLM $A_2$ required no such chelation to a Cu(II), as the amine contained in the β-aminoalanineamide side chain of the pyrimidoblamic acid moiety (one of the N-terminal metal ion binding sites contained within bleomycin), was the free amine intended to undergo the acetylation (Schemes 3.02 and 3.05). Additionally the synthesis of the *N*-biotinyloxysuccinimide **3.14** (needed for the biotin functionalization of BLM $A_5$) is shown below in Scheme 3.03.

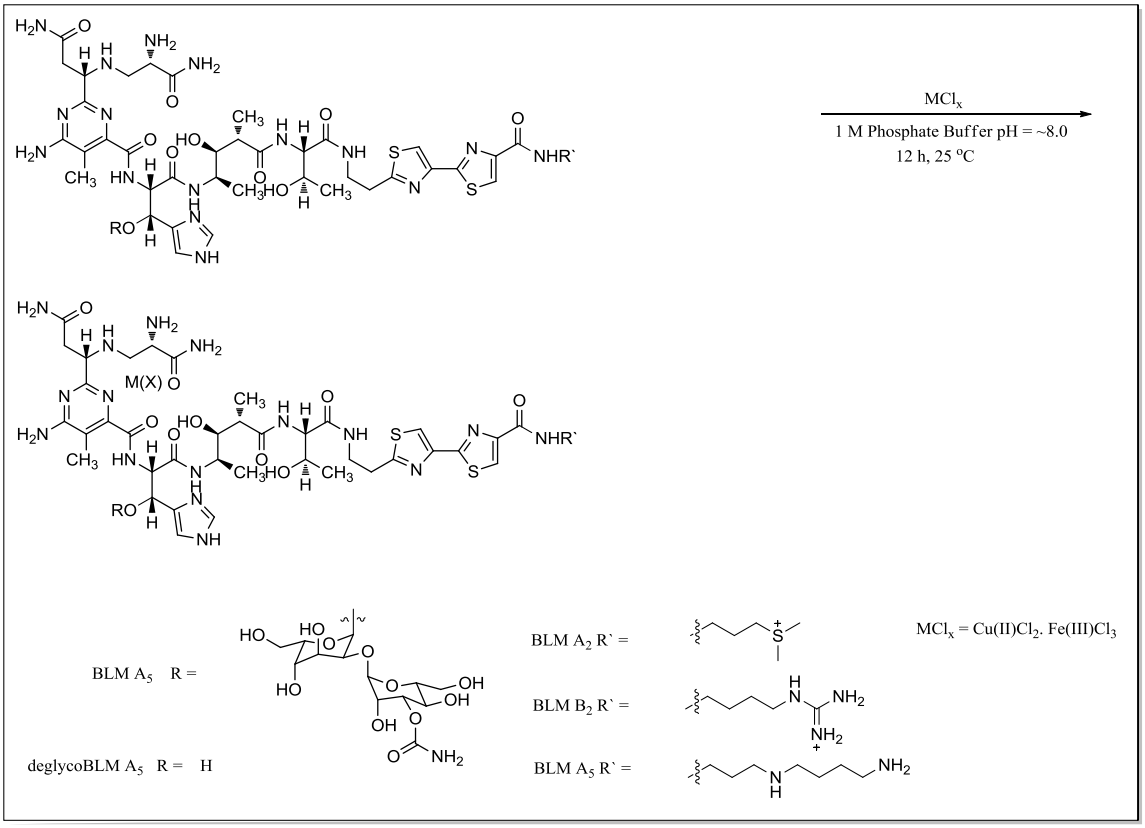


**Scheme 3.01** General synthetic scheme employed for several metalloBLMs

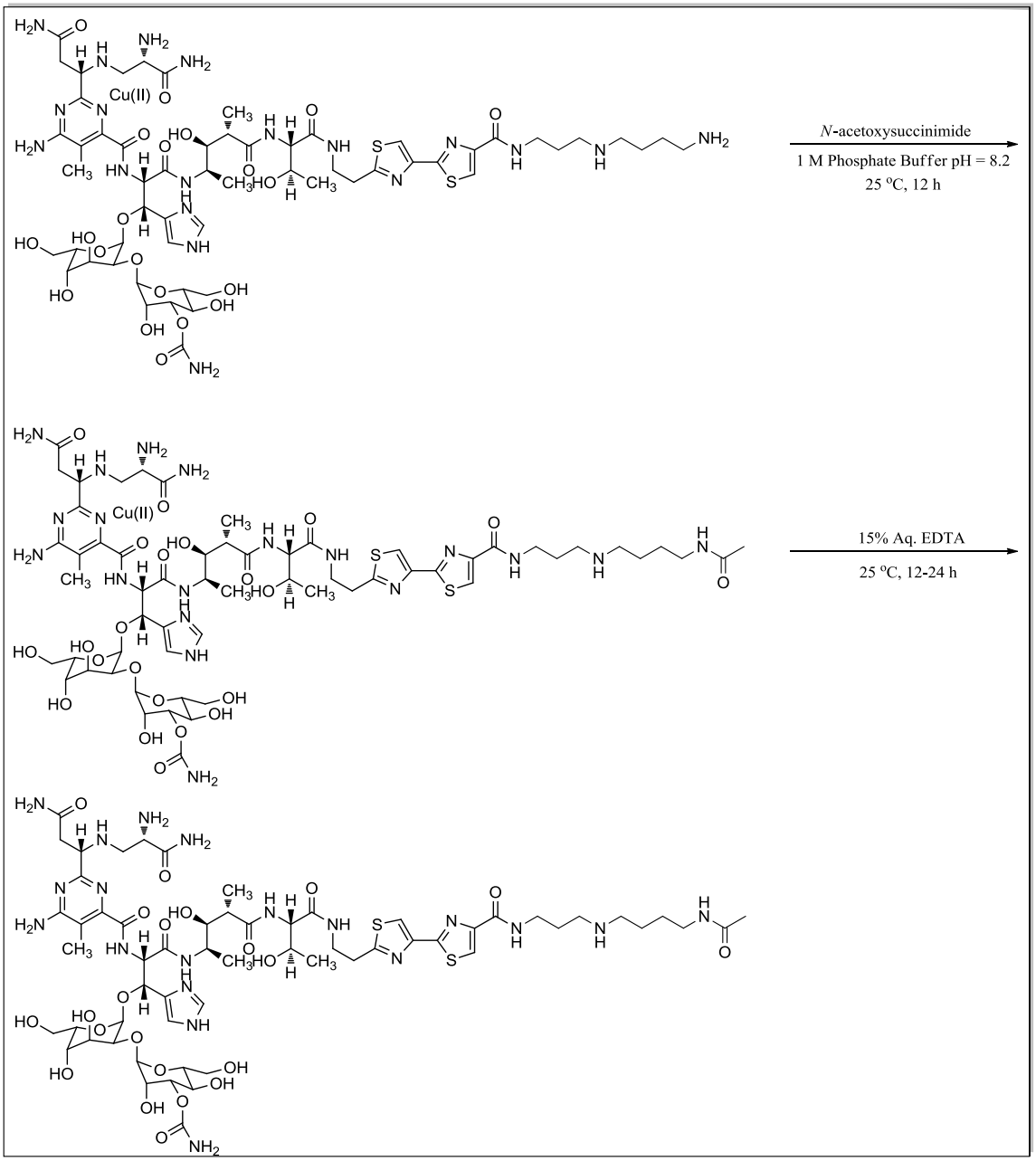


**Scheme 3.02** Synthetic route employed for N-acetyl BLM $A_5$


**Scheme 3.03** Synthetic route employed for the *N*-biotinyloxysuccinimide[66]

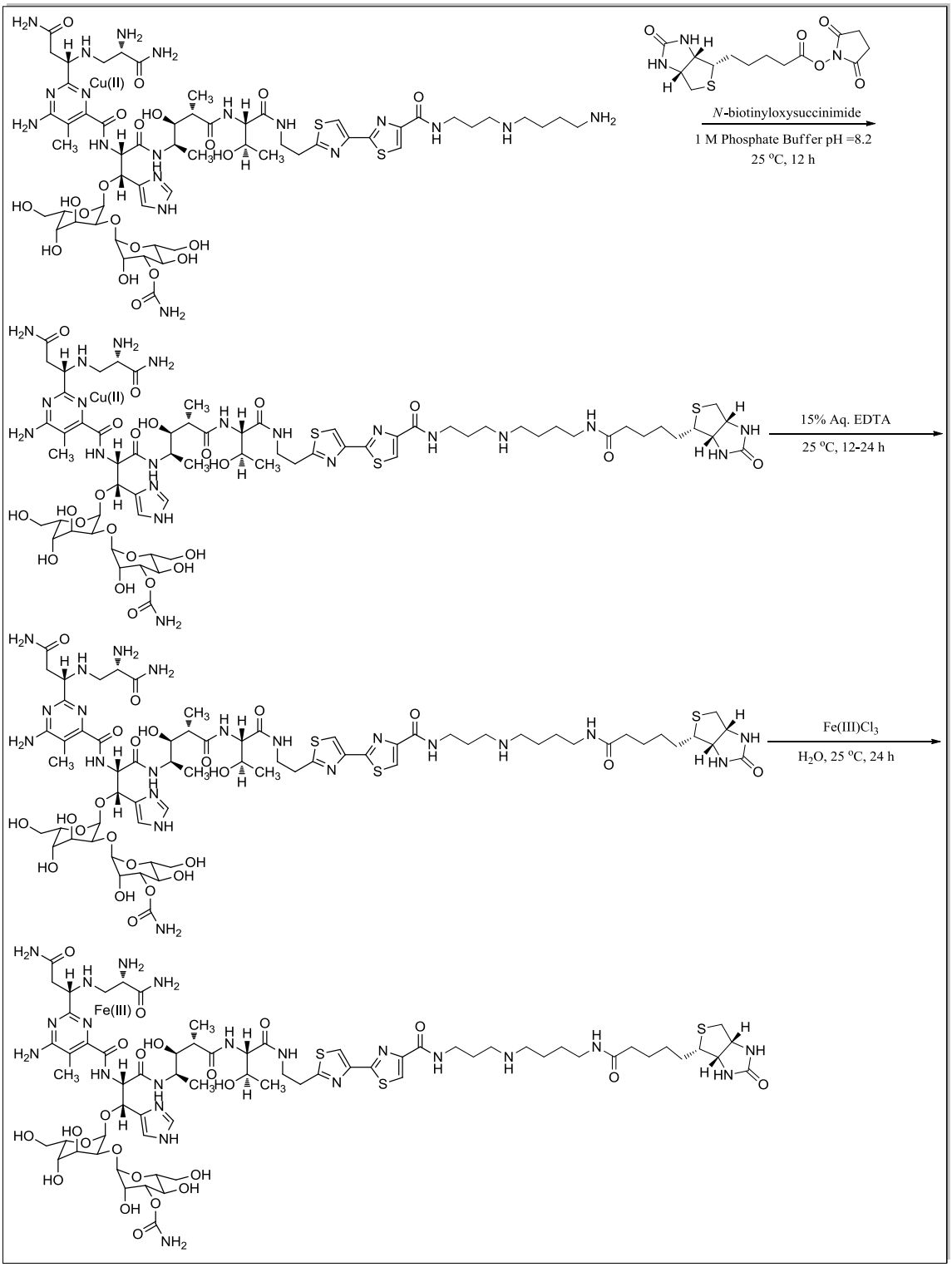


**Scheme 3.04** Synthetic route employed for the preparation of biotinylated BLMs

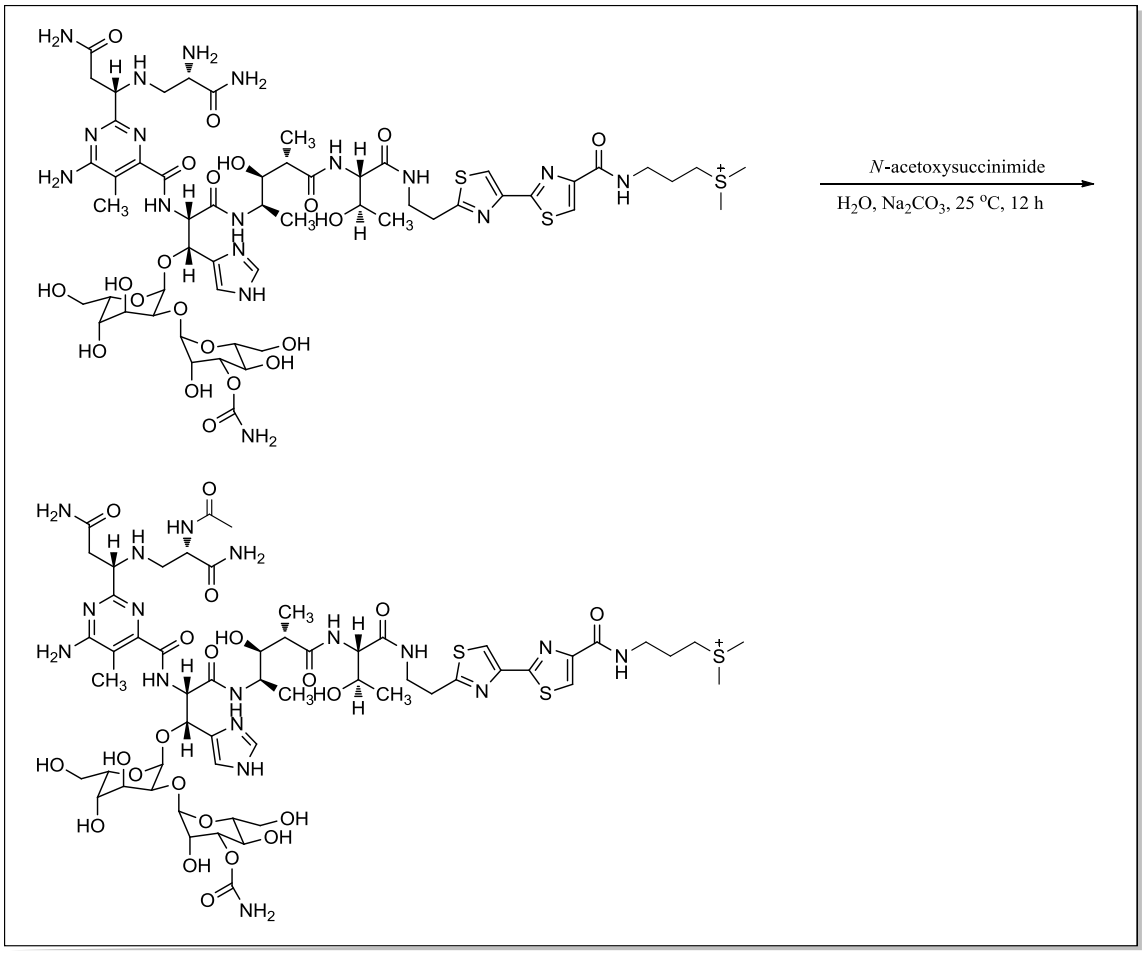


**Scheme 3.05** Synthetic route employed for N-acetyl BLM $A_2$

Previous studies, including the microbubble–BLM experiments[67] lacked the ability to quantitatively measure nucleic acid binding by BLM. Binding of BLM to B-form DNA is accompanied by fluorescence quenching of the bithiazole moiety.[68,69] However this potential method for quantification has not been independently validated and does not predict binding affinities for non-B-form DNAs.[70,71] To overcome the quantification obstacle and permit assessment of the dynamics of BLM binding to selected hairpin DNAs (whose sequences were chosen for strong BLM binding),[72-74] surface plasmon resonance (SPR) was employed. This method has been the choice of many studies to assess the interaction of other ligands with nucleic acid moieties.[75-77]

The primary focus of this SPR study was hairpin DNA **2** (Figure 3.203, which was shown in a previous study to bind BLM $A_5$ more strongly than most of the other hairpin DNAs investigated.[73,74]

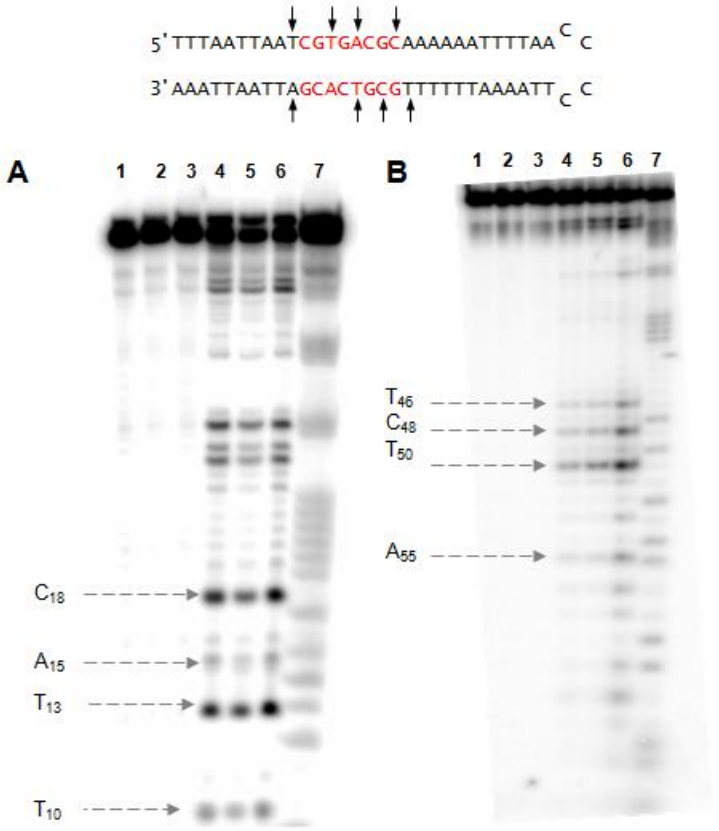


**Figure 3.03** A) Sequence-selective cleavage of [5′-$^{32}$P]-end labeled 64-nt hairpin DNA 2 by BLM $A_5$. Lane 1, radiolabeled 2 alone; lane 2, 20 $\mu$M $Fe^{2+}$; lane 3, 20 $\mu$M BLM $A_5$; lane 4, 5 $\mu$M Fe(II)•BLM $A_5$; lane 5, 10 $\mu$M Fe(II)•BLM $A_5$; lane 6, 20 $\mu$M Fe(II)•BLM $A_5$; lane 7, G+A lane. B) Sequence-selective cleavage of [3′-$^{32}$P]-end labeled 64-nt hairpin DNA 2 by BLM $A_5$. Lane 1, radiolabeled 2 alone; lane 2, 10 $\mu$M $Fe^{2+}$; lane 3, 10 $\mu$M BLM $A_5$; lane 4, 1 $\mu$M Fe(II)•BLM $A_5$; lane 5, 5 $\mu$M Fe(II)•BLM $A_5$; lane 6, 10 $\mu$M Fe(II)•BLM $A_5$; lane 7, G+A lane.

The 5′-$^{32}$P end-labeled DNA **2** exhibited cleavage at numerous sites when treated with Fe(II)•BLM $A_5$ and Fe(II)•deglycoBLM $A_5$. The cleavage sites for the two BLM congeners were quite similar,[74,75] but Fe(II)•BLM $A_5$ was found to be more potent as a

DNA cleaving agent. Summarized in Figure 3.03 are the sites of cleavage by Fe(II)•BLM $A_5$ of the same hairpin DNA, radiolabeled at the 3′- and 5′- ends. Treatment of the same 5′-$^{32}$P end-labeled hairpin DNA with Fe(II)•BLM $B_2$ gave similar results, with similar cleavage intensities seen with Fe(II)•BLM $A_5$.[78]

Hairpin DNA **2** was attached to a BIAcore sensor chip through a biotin moiety that was connected through a six carbon alkyl chain tether at the 5′-end.[79] The alkyl tether enables a more "free-flowing" DNA due to its flexibility and one that more sensibly mimics a purely solution phase interaction. It is also conveniently commercially available as a feature in custom oligonucleotide functionalizations. Initially the $K_A$ values obtained for Fe(III)•BLM $B_2$, Fe(III)•deglycoBLM $A_5$, and BLM $A_5$ were measured to assess the relative affinities for metalloBLMs , that were incapable of DNA cleavage. For all of the BLM samples, a single strong binding mode was noted. When the BLM samples were measured at 25 $^{o}$C and 10 mM NaCl, the $K_A$ values were found to be approximately 3.2 x $10^6$, 3.0 x $10^6$ and 1.5 x $10^6$ $M^{-1}$, respectively, for the above BLMs. Therefore the relative affinities of these metalloBLMs for hairpin DNA **2** (BLM $B_2 \approx$ deglycoBLM $A_5 >$ BLM $A_5$) was not in the same order as the respective potencies of cleavage of the DNA by the corresponding Fe(II) derivatives (BLM $B_2 \approx$ BLM $A_5 >$ deglycoBLM $A_5$). However the actual cleavage sites for all three BLMs were quite similar.

These experiments establish that the relative efficiency of cleavage of a strongly bound hairpin DNA by a metalloBLM is not controlled simply by BLM–DNA affinity. This observation is also supported by the finding that there was a single strong binding site for Fe(III)•BLM $B_2$ but there were multiple cleavage sites observed, two of which involved strong cleavage. BLM $B_2$ has been shown to cleave chromosomal DNA

efficiently in cultured human cell lines.[80] The interaction of BLM $B_2$ with DNA **2** was characterized more carefully. An SPR sensorgram shown in Figure 3.04 summarizes the interaction at 25 and 10 mM NaCl concentrations, respectively.

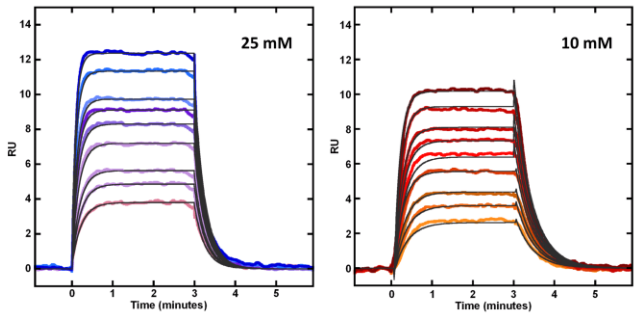


**Figure 3.04** SPR sensorgrams for the interaction of Fe(III)•BLM $B_2$ with DNA **2** at 25 mM (left panal) and 10 mM (right panel) NaCl concentrations at 25 $^{o}$C. The individual sensorgrams (colored) represent responses at BLM $B_2$ concentrations of 50, 75, 100, 150, 200, 250, 300, 400 and 500 nM (bottom to top). Global kinetic fit (black solid lines) with a 1:1 binding model was performed using BIAcore T200 Evaluation Software to obtain kinetic association and dissociation rate constants.

Shown in Figure 3.22 is an SPR sensorgram of the binding of Fe(III)•BLM $B_2$ to immobilized hairpin DNA **2** at 25 $^{o}$C. The concentrations of metalloBLM employed were 50-500 nM. The $K_A$ calculated for this interaction was found to be 3.9 x $10^6$ $M^{-1}$. The on-rate $k_a$ was determined to be 0.074 $s^{-1}$. A summary of the data calculated at the two salt concentrations used and two temperatures is displayed in Table 1. Similar results for the on-rates increased 2.5–3-fold at the higher temperature (25 $^{o}$C). Accordingly $K_A$ was ~3 times larger at the lower temperature (15 $^{o}$C) due to the change in off-rate. Small, consistent changes in measured parameters were a direct result of the changes in salt concentrations (10 mM-25 mM NaCl).

**Table 3.01** Binding of Fe(III)•BLM $B_2$ to DNA 2[a]

| | $k_a$ ($M^{-1}s^{-1}$) | $k_d$ ($s^{-1}$) | $K_A$ ($M^{-1}$) | $K_D$ (nM) | $K_A$ ($M^{-1}$, steady-state) |
|---|---|---|---|---|---|
| 15 °C | | | | | |
| 10 mM NaCl | $1.78 \times 10^5$ | 0.017 | $10.5 \times 10^6$ | 95 | $9.4 \times 10^6$ ; $0.20 \times 10^6$ |
| 25 mM NaCl | $3.45 \times 10^5$ | 0.023 | $15.2 \times 10^6$ | 66 | $9.3 \times 10^6$ ; $0.38 \times 10^6$ |
| 25 °C | | | | | |
| 10 mM NaCl | $1.35 \times 10^5$ | 0.042 | $3.2 \times 10^6$ | 312 | $3.1 \times 10^6$ |
| 25 mM NaCl | $2.85 \times 10^5$ | 0.074 | $3.9 \times 10^6$ | 256 | $3.4 \times 10^6$ |

[a]50, 75, 100, 150, 200 and 250 nM concentrations of Fe (III)•BLM $B_2$. Quite similar results were obtained when higher (300 – 500 nM) concentrations were employed. Based on reproducibility of results, the errors in the strong binding constants and kinetics constants are ±15% and close to 50% for the weaker binding constants.

The structural components in hairpin DNA **2** or Fe(III)•BLM $B_2$ which cause these changes in affinity and dynamics of interaction are not entirely clear at this time but could be revealed by further alterations in the BLM congeners or the hairpin DNA itself. An unanticipated result was the dramatically lower affinity of apo-(metal free) BLM $B_2$ for DNA **2** ($K_A = 2.2 \times 10^4$ $M^{-1}$ at 10 mM NaCl and 25 °C). However this result was in qualitative agreement with a previous study that used fluorescence quenching of the bithiazole (DNA binding domain) of bleomycin as an end point for assessing DNA binding in the presence of Fe(II) and Cu(II).[69]

As is presented in Figure 3.03, for Fe(III)•BLM $B_2$, the Fe(II)•BLMs investigated each cleaved hairpin DNA **2** at multiple sites, and with somewhat different efficiencies. The cleavage sites seen in Figure 3.03 were obtained under single hit kinetic conditions; therefore it is logical to conclude that it may be possible for metalloBLMs to bind hairpin DNAs in multiple different ways, each of which would give a distinct DNA cleavage pattern. In order to assess whether it is possible to detect more than one binding mode by SPR, the data obtained from the sensorgrams was subjected to a steady-state analysis.

This was done using additional concentrations of Fe(III)•BLM $B_2$ up to 1 µM (Figure 3.03) The Figure below shows the SPR equilibrium binding plots for Fe(III)•BLM $B_2$ with DNA **2** at two salt concentrations (10 and 25 mmol) at 25 $^{o}$C. The steady-state analysis used the same experimental data shown above, but up to a higher concentration (1 µM). The strong binding constant determined (3.4 x $10^6$ at 25 mM NaCl and 3.1 x $10^6$ mM NaCl) and the kinetic binding constant determined (3.9 x $10^6$ at 25 mM NaCl and 3.2 x $10^6$ at 10 mMol NaCl) were in good agreement.

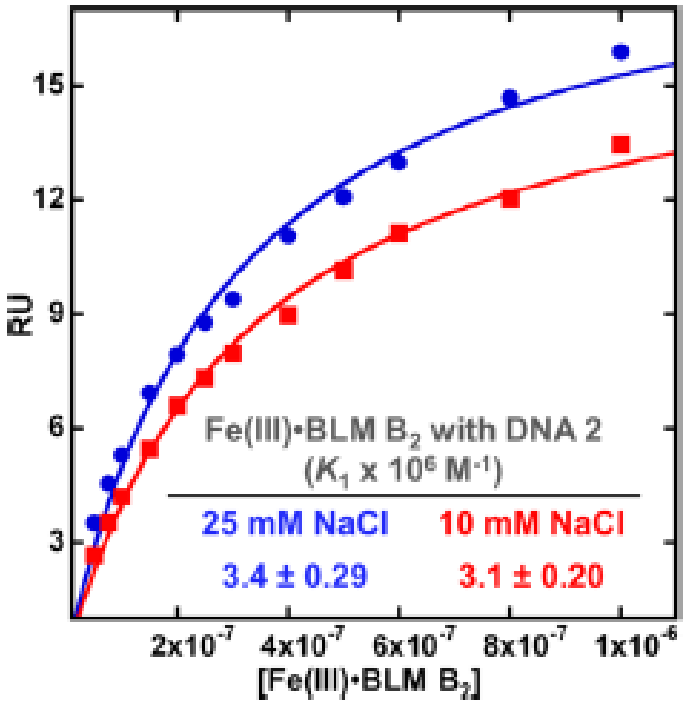


**Figure 3.05** SPR equilibrium binding plots of Fe(III)•BLM $B_2$ with DNA **2** at 10 mM and 25 mM NaCl concentrations and 25 $^{o}$C. The steady-state response values were fitted as a function of free ligand concentration to a single-site interaction model. The binding affinities are listed in Table 3.01.

Figure 3.06 below displays the SPR equilibrium binding plots for Fe(III)•BLM $B_2$ and DNA 2 at the two salt concentrations and at 15 $^{o}$C. Comparing the steady-state

analysis and experimental data shown above shows that there is good agreement of the strong binding constant and the kinetic binding constant ($3.4 \times 10^6$ vs $3.9 \times 10^6$ $M^{-1}$ at 25 mM NaCl and $3.2 \times 10^6$ vs $3.1 \times 10^6$ $M^{-1}$ at 10 mM NaCl). By using the steady-state model, it was possible to estimate a value for the second binding mode which was found to have quite fast kinetics. It was found that the second binding mode was 10-20+ times weaker than the primary binding mode and could only be determined with a large margin of error (~40%).The estimated values of the steady-state binding constants for Fe(III)•BLM $B_2$ and immobilized hairpin DNA **2** at 10 mM NaCl and 15 $^oC$ were $9.4 \times 10^6$ and $0.20 \times 10^6$ $M^{-1}$ for the strong and weak binding sites, respectively. Given that there are multiple cleavage sites observed for Fe•BLM on DNA **2**, there probably exist multiple weaker binding sites for Fe(III)•BLM $B_2$ as well. However, they have not been established as it is difficult to achieve saturation and maximum stoichiometry.

The presence of one strong binding site as well as multiple weaker binding sites for Fe(III)•BLM $B_2$ was observed for other DNAs in addition to DNA **2**, and was reported previously (Figure 3.06).[72,73] Shown below, DNAs **4** and **5** exhibited similar characteristics (a single strong binding site as one or more weaker binding sites. DNA **5** actually showed numerous strong cleavage sites, even though there was only a single strong binding site expected.

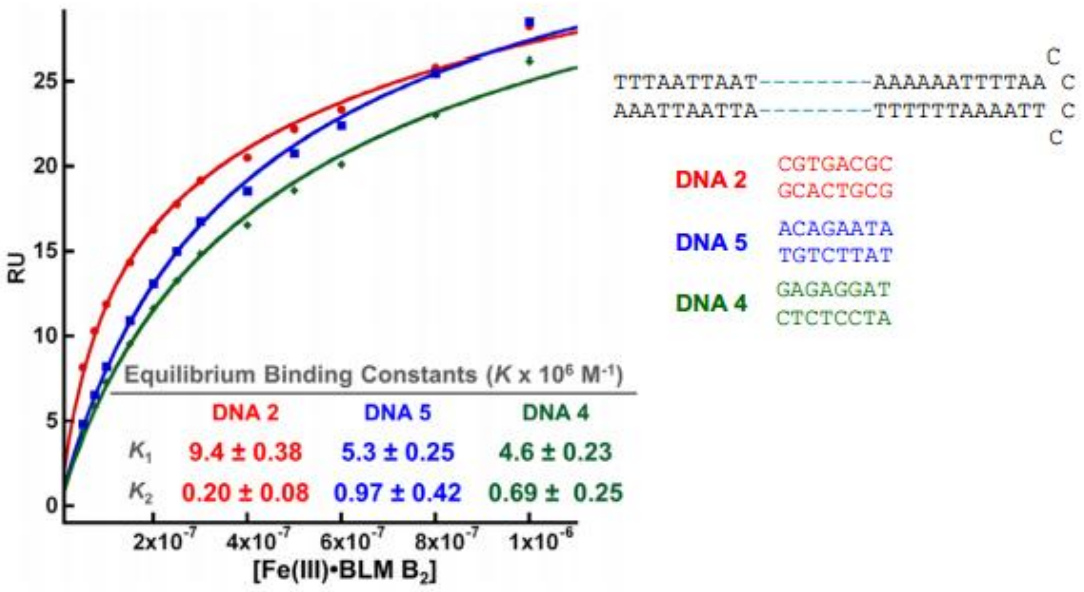


**Figure 3.06** SPR steady-state equilibrium binding plots of Fe(III)•BLM $B_2$ with different DNA sequences at 10 mM NaCl and 15 °C. The steady-state response values were fitted as a function of free ligand concentration to a two-site interaction model. The equilibrium binding affinities are listed in the inset

Also shown in a previous study, was evidence that a 16-nt hairpin DNA cleaved stoichiometrically of Fe(II)•BLM did not undergo significant cleavage in the presence of an additional one equivalent of some selected, strongly bound 64-nt hairpin DNA.[78] This observation suggests that association of BLM with a strongly bound DNA substrate, effectively precludes the binding to other DNA species. In an attempt to gain further insight into the mechanistic nature of hairpin DNA **2** cleavage, several competition experiments in which $^{32}$P-radiolabeled samples of DNA **2** (or another 16-nt hairpin DNA of comparable specific activity) were treated with Fe(II)•BLM in the presence of an unlabeled DNA substrate as a competitor species. As shown in Figure 3.06 above, the Fe(II)•BLM $B_2$-mediated cleavage of hairpin DNA **2** was minimally affected by the use of eight additional equivalents of the unlabeled 16-nt DNA. However, the presence of a single equivalent of DNA **2** precluded cleavage of the radiolabeled 16-nt hairpin DNA.

These findings suggest that, even when not bound to the established strong binding sites of DNA, Fe(II)•BLM must remain in proximity to this DNA. This results in selective preferential cleavage at weakly bound sites in the same hairpin DNA in spite of available cleavage sites in another DNA.

### 3.03 Discussion

The characterization of the binding and cleavage by Fe•BLM of a hairpin DNA substrate, which was selected for strong binding affinity to BLM was successful. The hairpin DNA is cleaved on both arms by three different BLM species, all with similar sequence preferences but with different efficiencies. Throughout the above study it was clearly shown that the relative efficiencies of DNA cleavage do not simply correlate with relative binding affinities. This indicates that affinity is only one single factor in understanding and defining the cleavage efficiency of BLM on a DNA substrate. SPR analysis of BLM binding to the immobilized hairpin DNA has recently permitted the dynamics of binding to be defined.[56]

In addition to immobilizing the 16-nt hairpin DNA **2** substrate, the system was also attempted in reverse. The BLMs employed were functionalized with a biotin moiety, which then allowed the immobilization of the biotinylated-BLM on the SPR sensor chip (streptavidin derivatized). This change in experimental parameters led to irreproducible results and very large margins of error. While this approach (having an excess of BLM in the presence of a DNA substrate) is a traditional model for the study of BLM–nucleic acid interaction[16,81-86] it proved unsuccessful for measuring steady-state binding profiles of BLM.

In summary, the binding constants identified by SPR analysis showed that the on-rate, ($k_a$ values) were essentially unchanged when temperature decreased from 25 $^{o}$C to 15 $^{o}$C, while the off-rate ($k_d$ values) decreased approximately three fold at both salt concentrations studied. Both the kinetic and steady-state binding constants were in agreement and the steady-state analysis allowed for the detection of at least one weaker

binding mode for Fe(III)•BLM $B_2$ to hairpin DNA **2** (as well as DNA **4** and DNA **5**). While the mode of binding to DNA by BLM has been studied previously,[85,87-90] the dynamics of interaction have not. The work presented herein significantly expands our understanding of the quantitative parameters and dynamics of BLM binding to DNA substrates and the overall relationship between DNA binding and cleavage by metalloBLMs.

### 3.04 Experimental

**General Methods:** All solvents used were of analytical grade. Anhydrous solvents were of DriSolv® quality and purchased from VWR. All experiments were run under a dry nitrogen atmosphere in flame-dried glassware. All other chemicals were purchased from Aldrich and used without further purification. Flash chromatography was carried out using Silicycle 200-400 mesh silica gel. Analytical TLC was carried out using 0.25 mm EM silica gel 60 $F_{250}$ plates that were visualized by UV irradiation (254 nm). HPLC separations were performed on an Agilent 1100 series HPLC system using a diode array detector. The crude products were purified on an Alltech Alltima $C_{18}$ reversed phase semi-preparative (250 x 10 mm, 5 μm) HPLC column using aq 0.1% TFA and $CH_3CN$ mobile phases. UV-Vis spectrophotometric analysis and quantifications were done using a Beckman DU Series 500 UV/Vis spectrophotometer equipped with a single cell module. $^1H$ and $^{13}C$ NMR spectra were recorded on a 400 MHz Varian Liquid-State NMR in chloroform-*d* (unless otherwise noted). Chemical shifts were reported in parts per million (ppm, δ) referenced to the residual $^1H$ resonance of the solvent ($CDCl_3$, 7.26 ppm). $^{13}C$ spectra were referenced to the residual $^{13}C$ resonance of the solvent ($CDCl_3$, 77.0 ppm). Splitting patterns were designated as follows: s, singlet; br, broad; d, doublet; dd, doublet of doublets; t, triplet; q, quartet; m, multiplet. High resolution mass spectra were obtained in the Arizona State University CLAS High Resolution Mass Spectrometry Laboratory or in the Michigan State University Mass Spectrometry Facility.

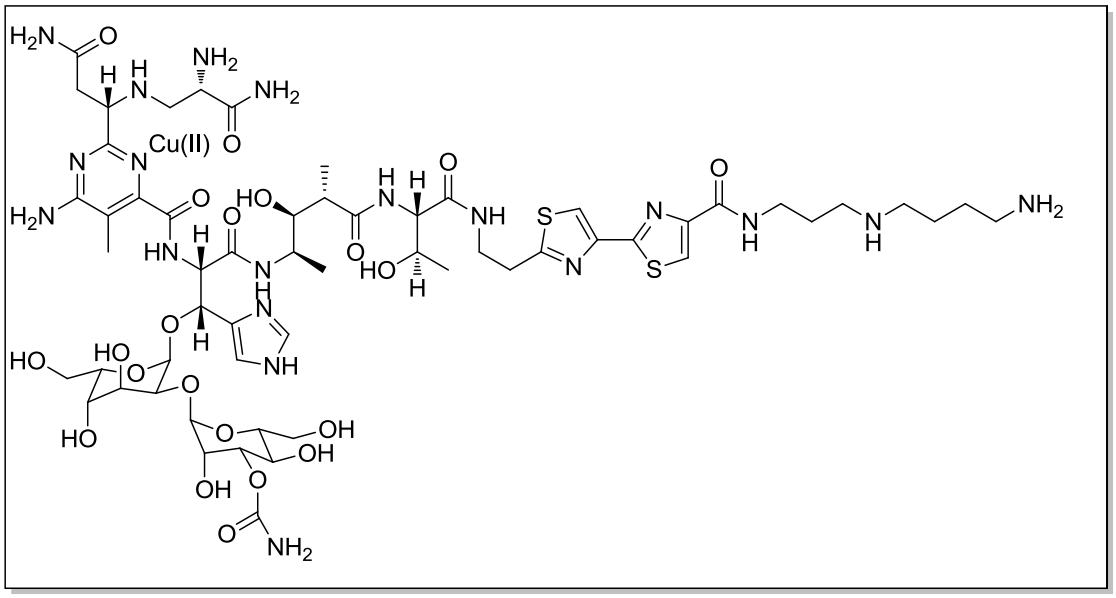

**Cu(II)•Bleomycin $A_5$ (3.01).** Bleomycin $A_5$ (2.00 mg, 1.39 μmol) of was dissolved in 495 μL (1.46 μmol) of 2.944 mM aq $CuCl_2$ at 25 $^oC$ and stirred for 24 h. The solution was frozen and lyophilized to give Cu(II)•bleomycin $A_5$ **(3.01)** as a blue solid: yield 2.09 mg (quant.); mass spectrum (MALDI-TOF $ES^+$), *m/z* 1439.5910 $(M\text{-}Cu)^+$ ($C_{57}H_{89}N_{19}O_{21}S_2$ requires 1439.5922).

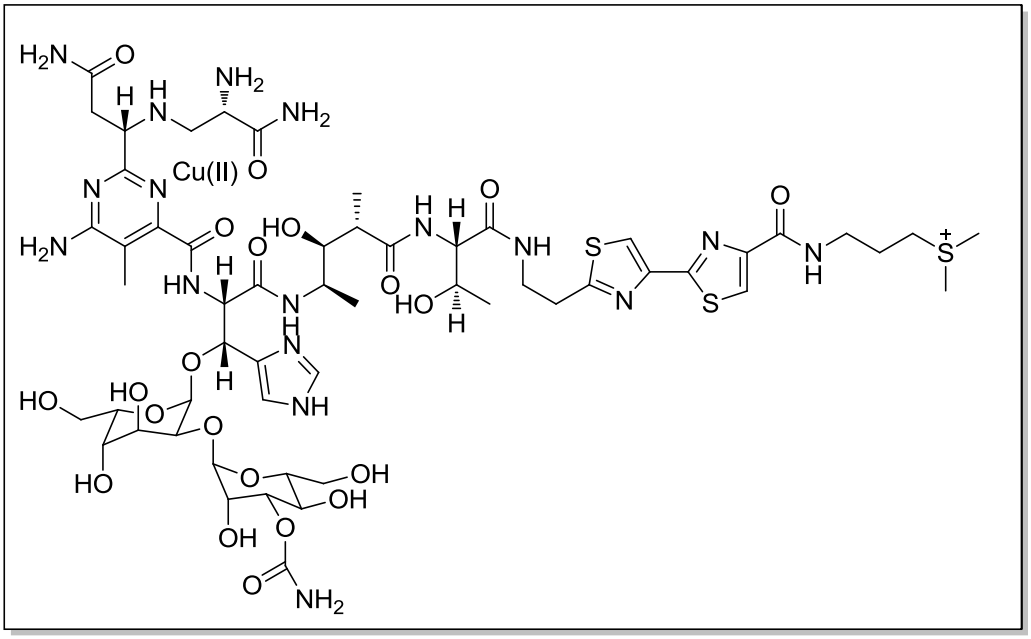

**Cu(II)•Bleomycin $A_2$ (3.02).** Bleomycin $A_2$ (2.00 mg (1.41 μmol) of was dissolved in 504 μL (1.48 mmol) of 2.944 mM aq $CuCl_2$ at 25 $^oC$ and stirred for 24 h. The solution was frozen and lyophilized to give Cu(II)•bleomycin $A_2$ **(3.02)** as a blue solid: yield 2.09 mg (quant.); mass spectrum (MALDI-TOF $ES^+$), *m/z* 1414.5180 $(M\text{-}Cu)^+$ ($C_{55}H_{84}N_{17}O_{21}S_3$ requires 1414.5184).

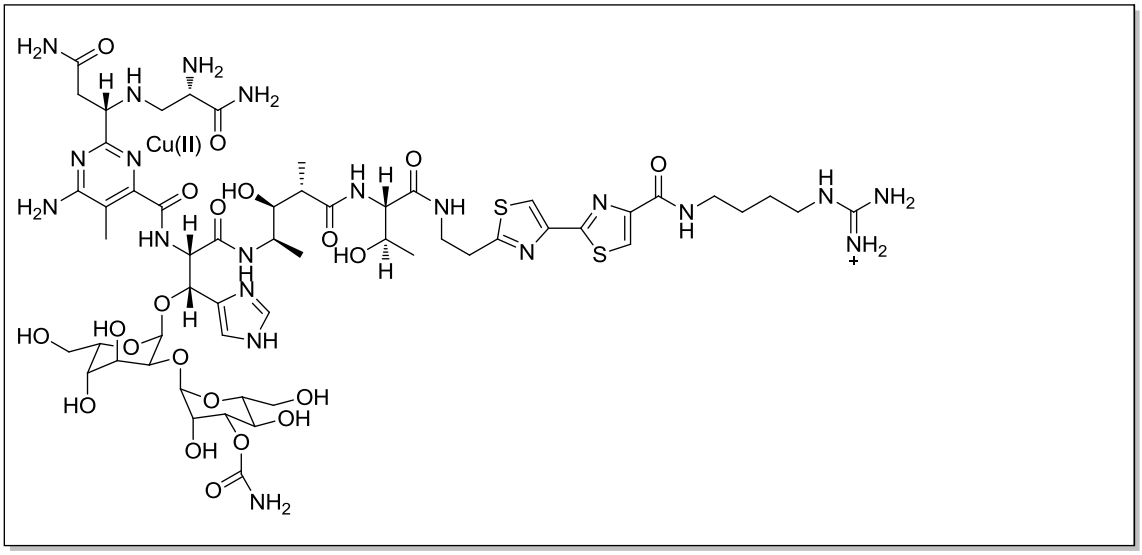


**Copper(II)•Bleomycin $B_2$ (3.03).** Bleomycin $B_2$ (2.00 mg  1.40 μmol) of was dissolved in 504 μL (1.48 μmol) of 2.944 M aq $CuCl_2$ at 25 $^oC$ and stirred for 24 h. The solution was frozen and lyophilized to give Cu(II)•bleomycin $B_2$ **(3.03)** as a blue solid: yield 2.09 mg (quant.); mass spectrum (MALDI-TOF $ES^+$), *m/z* 1488.4930 $(M\text{-}Cu)^+$ ($C_{55}H_{85}N_{20}O_{21}S_2$ requires 1488.4930).

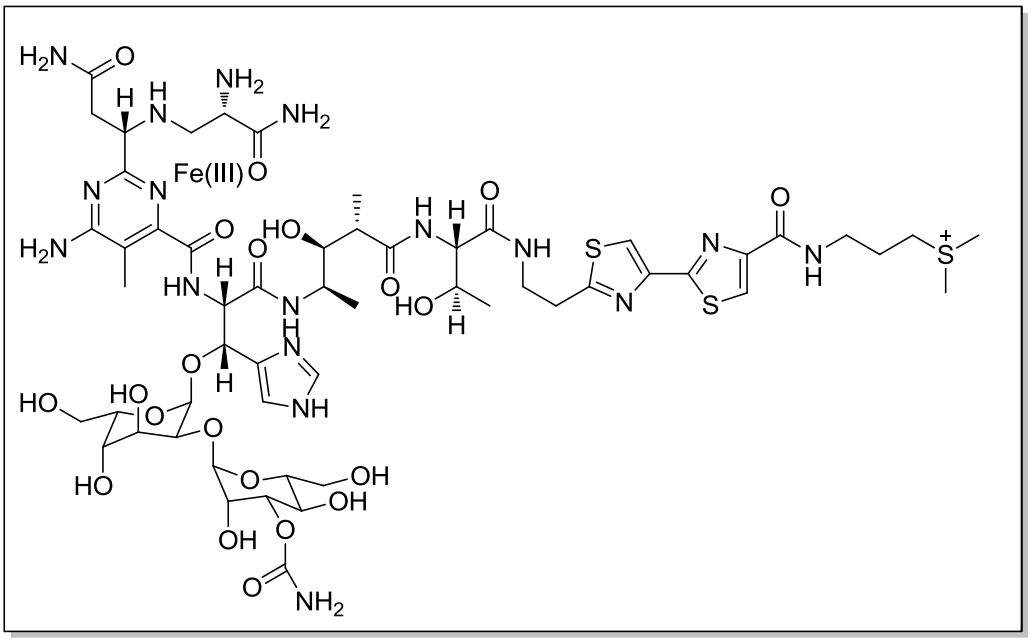


**Fe(III)•Bleomycin $A_2$ (3.04).** Bleomycin $A_2$ **(**2.00 mg, 1.41 μmol) of was treated with 504 μL (1.48 μmol) of a 2.944 mM aq $FeCl_3 \cdot 6H_2O$ at 25 $^oC$ and stirred for 24 h. The solution was lyophilized to give Fe(III)•bleomycin $A_2$ **(3.04)** as a yellow solid: yield 2.08 mg (quant.); mass spectrum (MALDI-TOF $ES^+$), *m/z* 1414.5180 $(M\text{-}Fe)^+$ ($C_{57}H_{86}N_{17}O_{22}S_3$ requires 1414.5184).

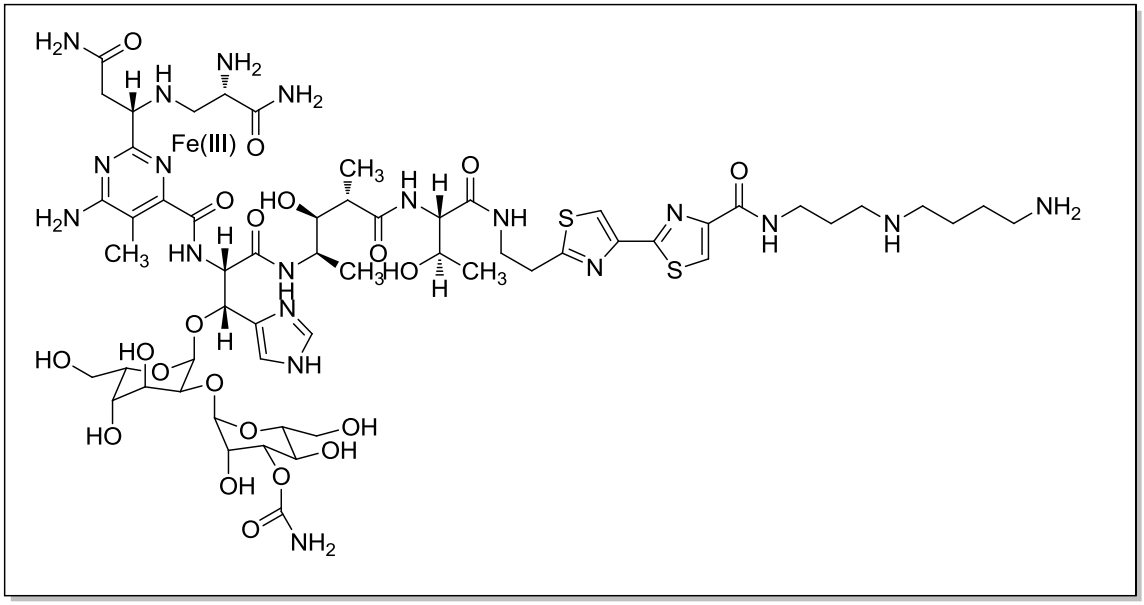

**Fe(III)•Bleomycin $A_5$ (3.05).** Bleomycin $A_5$ (2.00 mg, 1.34 μmol) of was treated with 495 μL (1.46 μmol) of a 2.944 mM aq $FeCl_3 \cdot 6H_2O$ at 25 $^oC$ for 24 h, frozen and then lyophilized to give Fe(III)•Bleomycin $A_5$ **(3.05)** as a yellow solid: yield 2.08 mg (quant.) mass spectrum (MALDI-TOF $ES^+$), *m/z* 1495.5280 $(M\text{-}Fe)^+$ ($C_{57}H_{89}N_{19}O_{21}S_2$ requires 1495.5271).

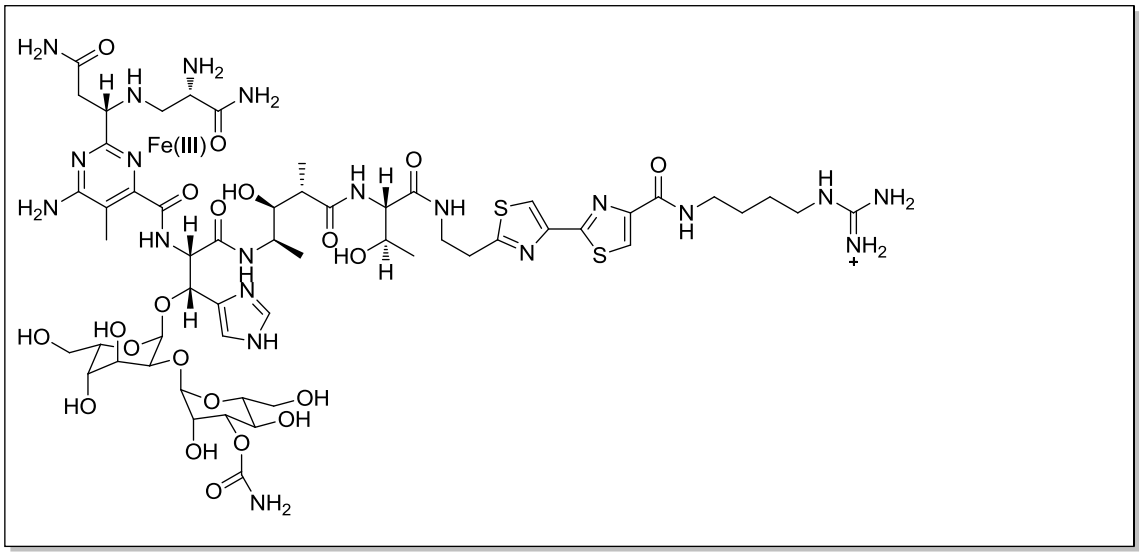


**Fe(III)•Bleomycin $B_2$ (3.06).** Bleomycin $B_2$ (2.00 mg, 1.40 μmol) was treated with 500 μL (1.47 μmol) of 2.944 mM aq $FeCl_3 \cdot 6H_2O$ at 25 $^oC$ for 24 h. The solution was frozen and then lyophilized to give Fe(III)•bleomycin $A_2$ **(3.06)** as a yellow solid: yield 2.08 mg (quant.); mass spectrum (MALDI-TOF $ES^+$), *m/z* 1414.5180 $(M\text{-}Fe)^+$ ($C_{57}H_{86}N_{17}O_{22}S_3$ requires 1414.5184).

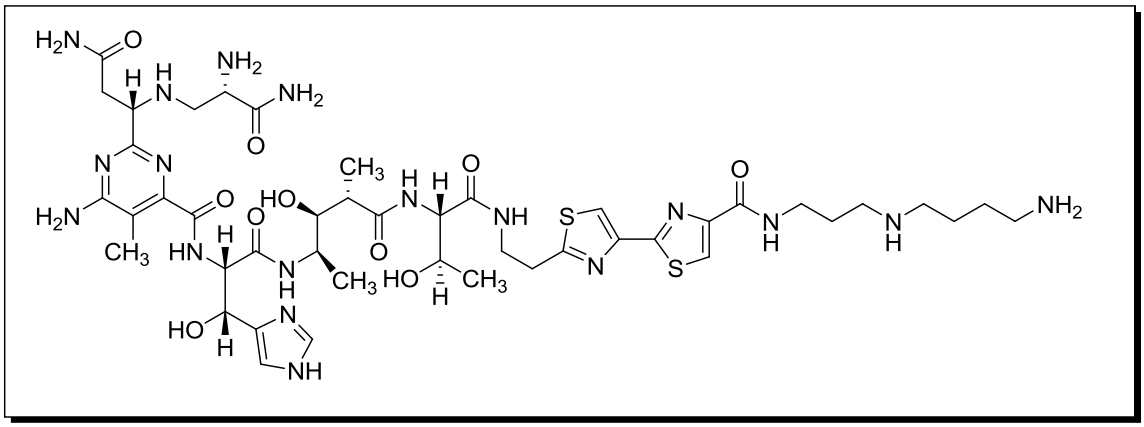

**Deglycobleomycin $A_5$ (3.07).** Cu(II)•deglycobleomycin $A_5$ (4.00 mg, 3.52 μmol) was treated with 0.5 mL of 15% aq EDTA at 25 $^{o}$C for 24 h and then lyophilized.

The reaction mixture was purified on an Alltech $C_{18}$ reversed phase semi-preparative (250 x 10 mm, 5 μm) HPLC column using 0.1% aq TFA and $CH_3CN$ mobile phases. A linear gradient was employed (99:1 0.1% aq TFA–$CH_3CN$ → 65:35 0.1% aq TFA–$CH_3CN$) over a period of 35 min at a flow rate of 3 mL/min. Fractions containing the desired product eluted at 14.4 min and were collected, frozen and lyophilized to afford a colorless solid: yield 2.15 mg (57%); mass spectrum (MALDI-TOF $ES^+$), *m/z* 1072.4797 $(M)^+$ ($C_{44}H_{68}N_{18}O_{10}S_2$ requires 1072.4807).

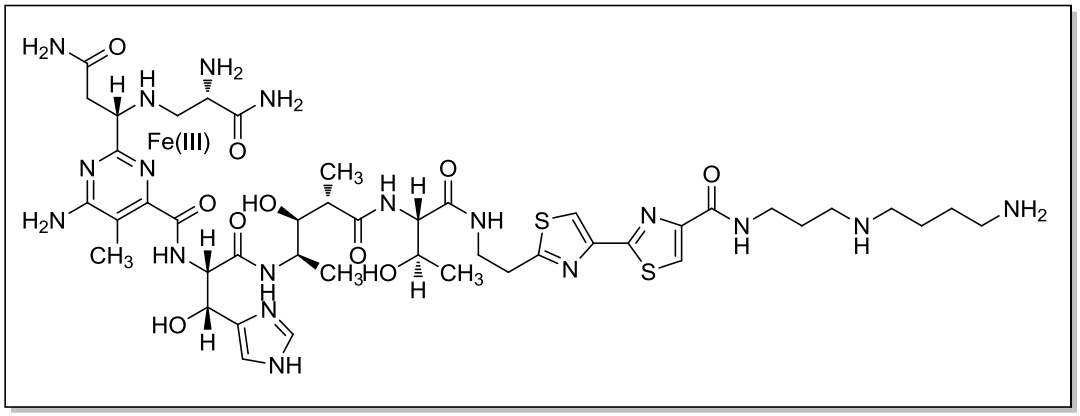

**Fe(III)•Deglycobleomycin $A_5$ (3.08).** Deglycobleomycin $A_5$ **(**1.76 mg, 1.64 μmol)

was treated with 583 μL (1.72 μmol) of a 2.944 mM aq solution of $FeCl_3 \cdot 6H_2O$ at 25 $^oC$ for 24 h. The solution was frozen and then lyophilized to give Fe(III)•Deglycobleomycin $A_5$ **(3.08)** as a yellow solid: yield 1.86 mg (quant.); mass spectrum (MALDI-TOF $ES^+$), *m/z* 1072.4850 $(M\text{-}Fe)^+$ ($C_{44}H_{68}N_{18}O_{10}S_2$ requires 1072.4837).

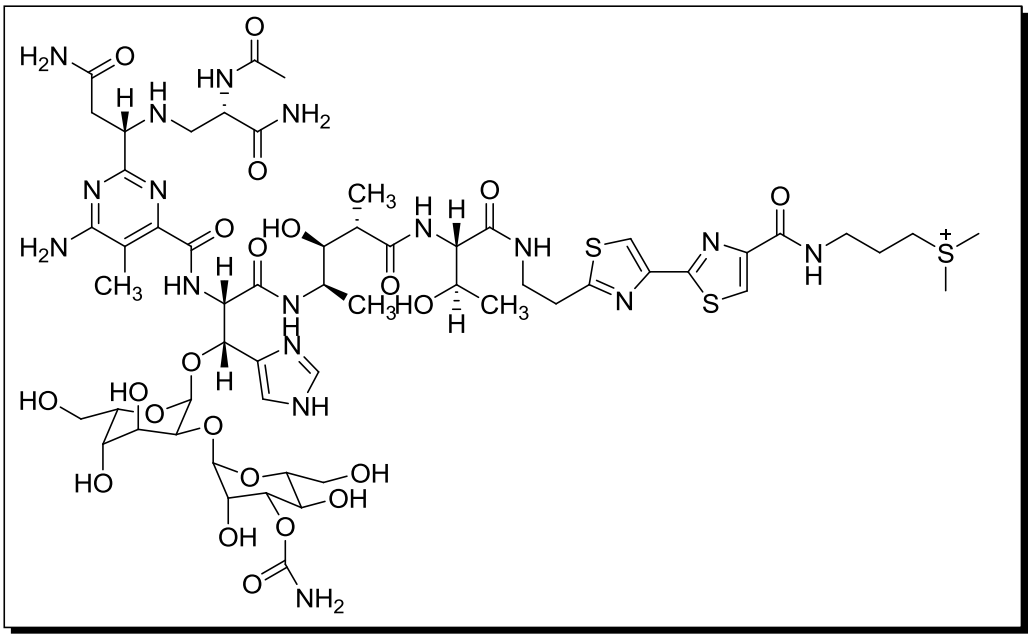

**N-acetyl bleomycin $A_2$ (3.09).** To a stirred solution of 4.50 mg (3.20 μmol) of bleomycin $A_2$ in 1.0 mL $H_2O$ was added 1.5 mg (9.50 μmol) of *N*-acetoxysuccinimide and a catalytic amount of $Na_2CO_3$ at 25 $^oC$, the reaction mixture was stirred for 12 h. The reaction mixture was purified on an Alltech $C_{18}$ reversed phase semi-preparative (250 x 10 mm, 5 μm) HPLC column using 0.1% aq TFA and $CH_3CN$ mobile phases. A linear gradient was employed (99:1 0.1% aq TFA–$CH_3CN$ → 63:37 0.1% aq TFA–$CH_3CN$) over a period of 20 min at a flow rate of 3 mL/min. Fractions containing the desired product eluted at 15.2 min and were collected, frozen and lyophilized to afford a colorless

solid: yield 2.34 mg (50%); mass spectrum (MALDI-TOF $ES^+$), *m/z* 1456.5280 $(M\text{-}Fe)^+$ ($C_{57}H_{86}N_{17}O_{22}S_3$ requires 1456.5290).

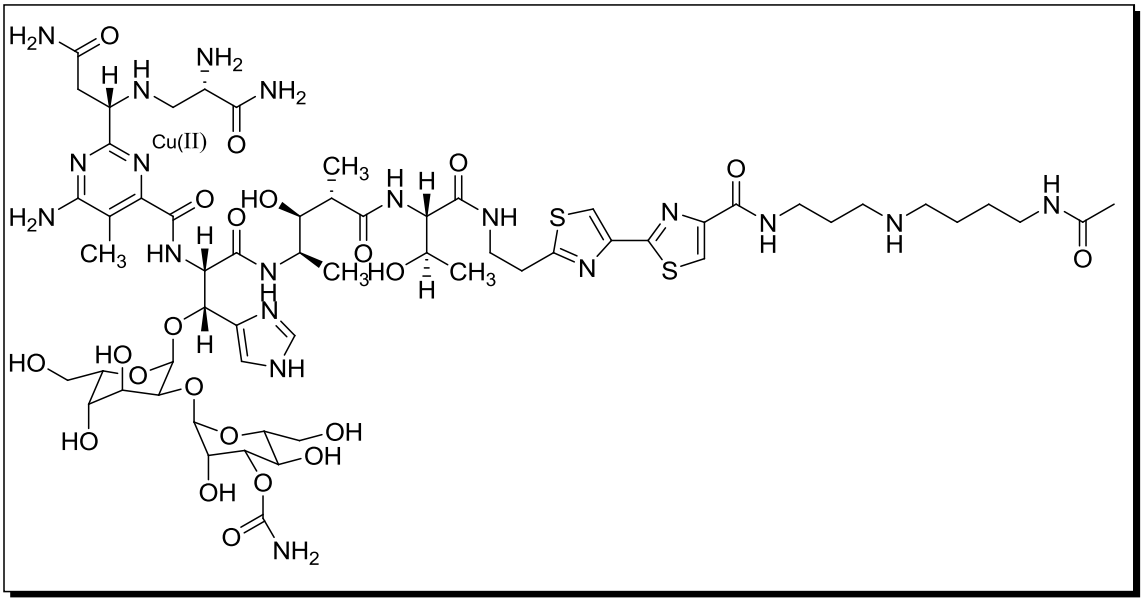


**Cu(II)•N-acetyl bleomycin $A_5$ (3.10).** To a stirred solution of 11.0 mg (7.30 μmol) of Cu(II)•bleomycin $A_5$ **(3.01)** in 2.0 mL of 1 M phosphate buffer pH = 8.2 was added 3.50 mg (22.0 μmol) of *N*-acetoxysuccinimide at 25 $^oC$, the reaction mixture was stirred for 12 h. The reaction mixture was purified on an Alltech $C_{18}$ reversed phase semi-preparative (250 x 10 mm, 5 μm) HPLC column using 0.1% aq TFA and $CH_3CN$ mobile phases. A linear gradient was employed (99:1 0.1% aq TFA–$CH_3CN$ → 63:37 0.1% aq TFA–$CH_3CN$) over a period of 20 min with a flow rate of 3 mL/min. Fractions containing the desired product eluted at 15.1 min and were collected, frozen and lyophilized to afford a blue solid: yield 4.84 mg (45%); mass spectrum (MALDI-TOF $ES^+$), *m/z* 1444.5344 $(M\text{-}Fe)^+$ ($C_{59}H_{91}N_{19}O_{22}S_2$ requires 1444.5323).

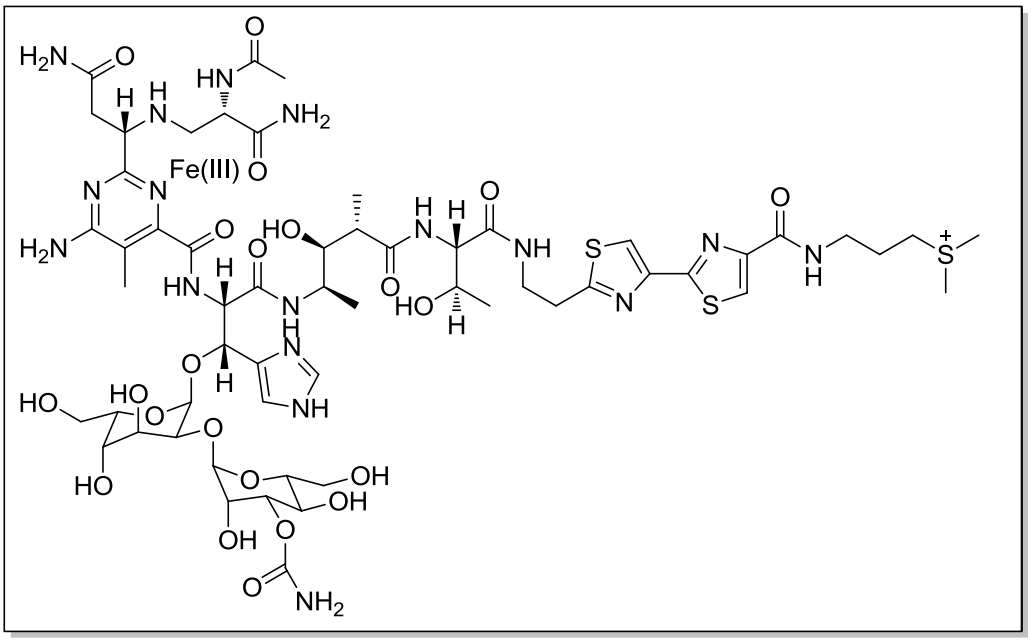


**Fe(III)•N-acetyl bleomycin $A_2$ (3.11).** N-acetyl BLM $A_2$ **(2.09)**, (0.51 mg, 0.35 µmol) was treated with 125 µL (0.37 µmol) of a 2.944 mM aq $FeCl_3 \cdot 6H_2O$ solution at 25 $^oC$ for 12 h. The mixture was frozen and then lyophilized to afford Fe(III)•N-acetyl bleomycin $A_2$ **(3.11)** as a yellow solid: yield 0.53 mg (quant); mass spectrum (TOF $ES^+$), *m/z* 1456.5280 $(M\text{-}Fe)^+$ ($C_{57}H_{86}N_{17}O_{22}S_3$ requires 1456.5290).

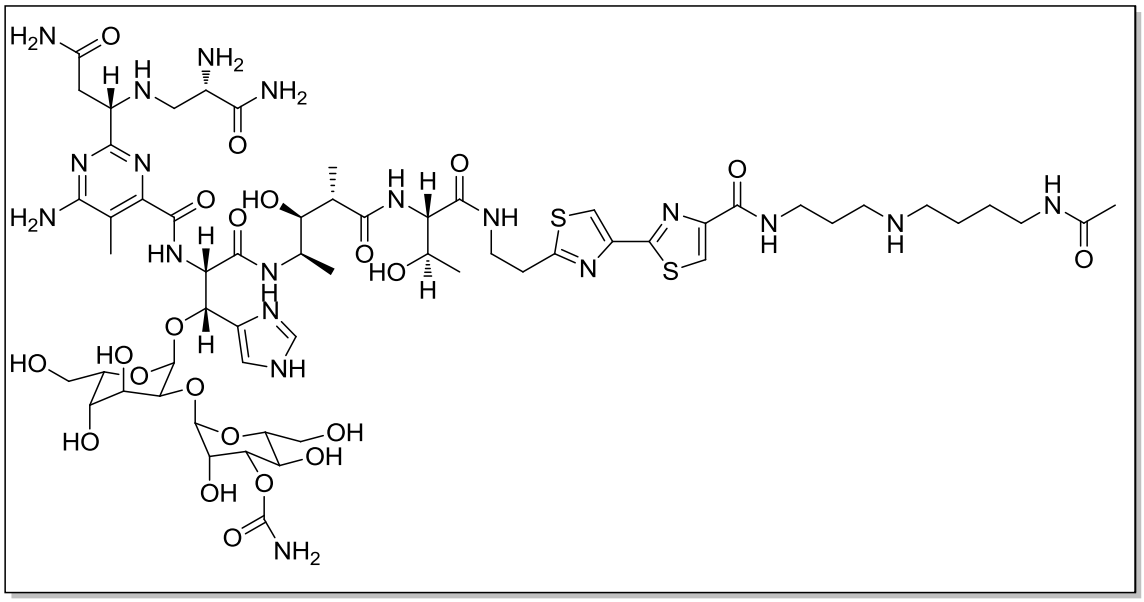

**N-acetyl bleomycin $A_5$ (3.12).** N-acetyl Cu(II)•bleomycin $A_5$ (**3.10)**, 2.00 mg (1.29 μmol) of was treated with 1.5 mL of a 15% aq EDTA solution at 25 $^{o}$C, the reaction mixture was stirred for 12 h. The crude reaction mixture was purified on an Alltech $C_{18}$ reversed phase semi preparative (250 x 10 mm, 5 μm) HPLC column using 0.1% aq TFA and $CH_3CN$ mobile phases. A linear gradient was employed (99:1 0.1% aq TFA–$CH_3CN$ → 63:37 0.1% aq TFA–$CH_3CN$) over a period of 20 min at a flow rate of 3.0 mL/min. Fractions containing the desired product eluted at 18.3 min and were collected, frozen and lyophilized to afford a colorless solid: yield 1.91 mg (99%); mass spectrum (MALDI-TOF $ES^+$), *m/z* 1481.6020 ($M^+$) ($C_{59}H_{91}N_{19}O_{22}S_2$ requires 1481.6027).

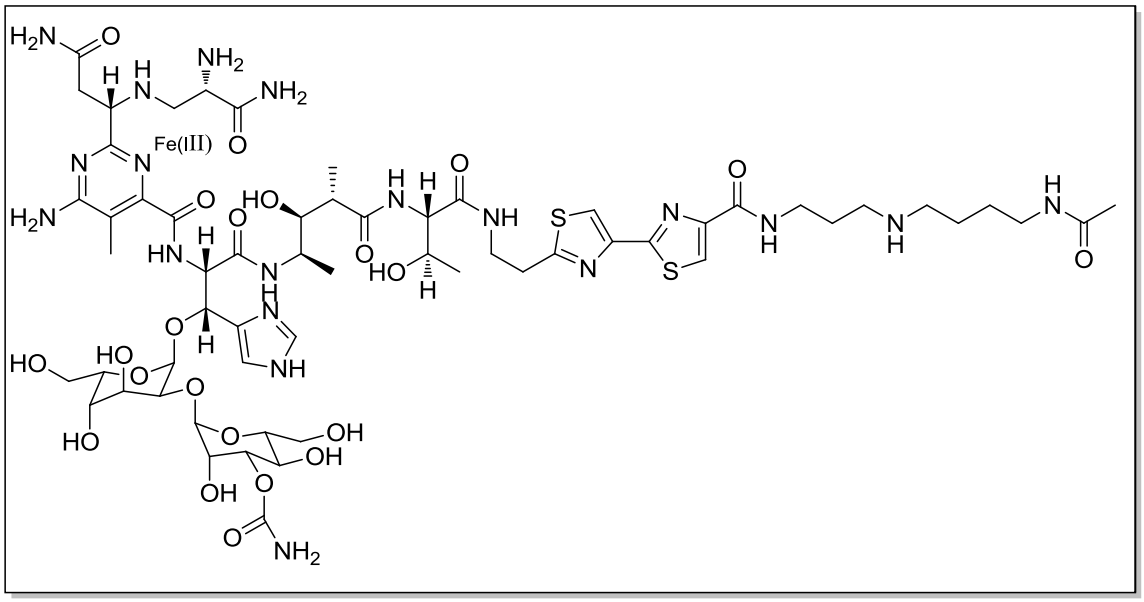


**Fe(III)•N-acetyl bleomycin $A_5$ (3.13).** N-acetyl bleomycin $A_5$ **(3.12)**, **(**1.72 mg, 1.16 μmol) of was treated with 413 μL (1.21 μmol) of a 2.944 mM aq $FeCl_3 \cdot 6H_2O$ solution at 25 $^oC$ for 12 h. The reaction mixture was frozen and then lyophilized to give a yellow solid: yield 1.79 mg (quant); mass spectrum (TOF $ES^+$), *m/z* 1481.6018 $(M\text{-}Fe)^+$ ($C_{59}H_{91}N_{19}O_{22}S_2$ requires 1481.6027).

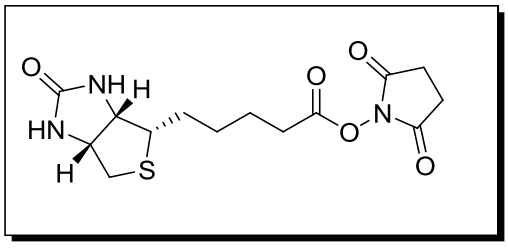

***N*-biotinyloxysuccinimide (3.14).**[66] To a stirred solution of 250 mg (1.02 mmol) of (+)-biotin and 130 mg (1.13 mmol) of *N*-hydroxysuccinimide in 15 mL of DMF was added 232 mg (1.13 mmol) of DCC at 0 $^oC$. The solution was allowed to warm to room temperature and stirred at 25 $^oC$ for 24 h. The solution was filtered and the filtrate was

concentrated under diminished pressure. The crude product was suspended in hot (~70 $^{o}$C) isopropyl alcohol for 20 min and then filtered. The filtrate cooled to room temperature and was then filtered. The precipitate was collected and crystallized from DMF–$Et_2O$ to give a colorless solid: yield 171 mg (49%); mp 204-206 $^{o}$C, lit.[66] mp 212 $^{o}$C; $^{1}$H NMR (DMSO) δ 1.42 (m, 3H), 1.65 (m, 3H), 2.58 (d, 1H, *J* = 12.4 Hz*)*, 2.67 (t, 3H, *J* = 7.4 Hz*)*, 2.81 (m, 4H), 3.11 (m, 1H), 4.15 (m, 1H), 4.30 (m, 1H), 6.37 (s, 1H) and 6.43 (s, 1H). $^{13}$C (DMSO) δ 24.2, 25.4, 27.5, 27.8, 29.9, 55.2, 59.1, 60.9, 162.6, 168.9 and 170.2; mass spectrum (MALDI-TOF), *m/z* 342.0138 $(M+H)^{+}$ ($C_{14}H_{20}N_3O_5S$ requires 342.0125).

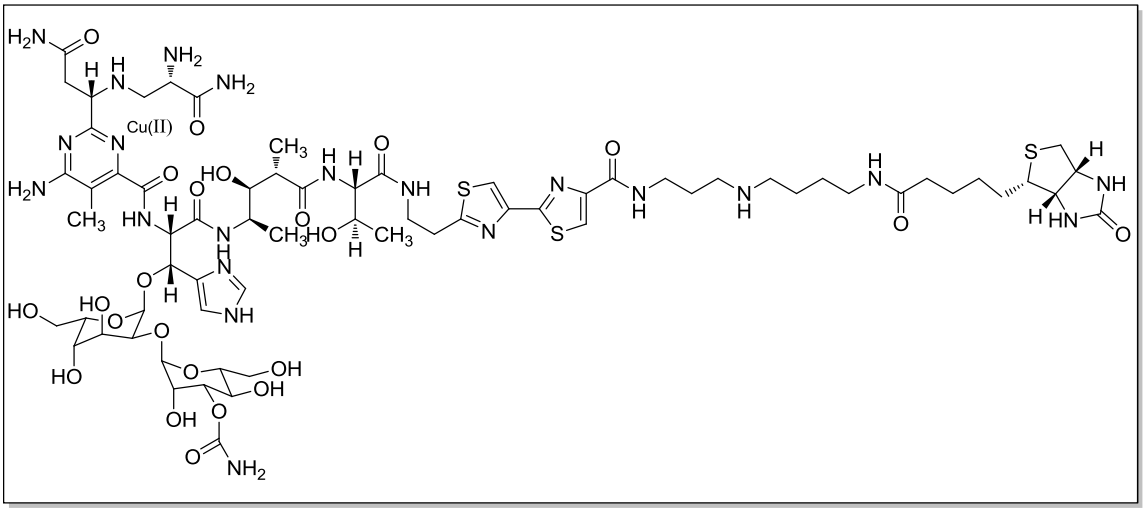

**Biotinylated Cu(II)•Bleomycin $A_5$ (3.15).** To a stirred solution of 6.0 mg (4.0 μmol) of Cu(II)·Bleomycin $A_5$ **(3.02)** in 1.0 mL of 1 M phosphate buffer pH = 8.2 was added 1.63 mg (4.80 μmol) of *N*-biotinyloxysuccinimide **(3.14)** at 25 $^{o}$C. The solution was stirred at 25 $^{o}$C for 12 h. The reaction mixture was purified on an Alltech $C_{18}$ reversed phase semi-preparative (250 x 10 mm, 5 μm) HPLC column using 0.1% aq TFA and $CH_3CN$ mobile phases. A linear gradient was employed (99:1 0.1% aq TFA–$CH_3CN$ →

63:37 0.1% aq TFA–$CH_3CN$) over a period of 20 min at a flow rate of 3 mL/min. Fractions containing the desired product eluted at 17.0 min and were collected, frozen and lyophilized to afford a blue solid: yield 2.59 mg (52%); mass spectrum (MALDI-TOF $ES^+$), *m/z* 1666.6788 $((M+H)\text{-}Cu)^+$ ($C_{67}H_{104}N_{21}O_{23}S_3$ requires 1666.6778).

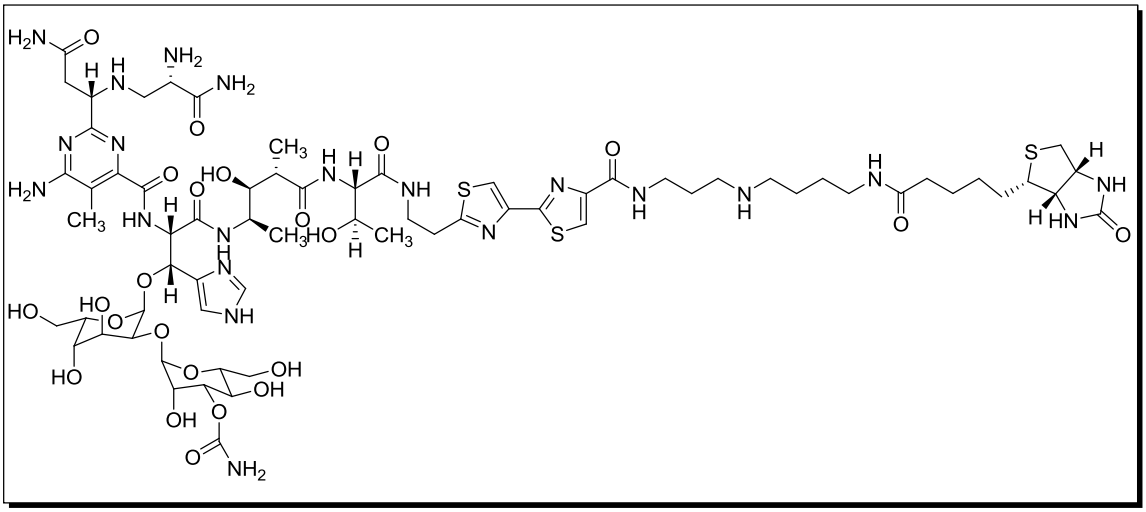

**Biotinylated bleomycin $A_5$ (3.16).** Biotinylated Cu(II)•bleomycin $A_5$ **(3.15)**, (4.86 mg, 2.80 μmol) was treated with 1.5 mL of 15% aq EDTA and stirred at 25 $^oC$ for 24 h. The reaction mixture was purified on an Alltech $C_{18}$ reversed phase semi-preparative (250 x 10 mm, 5 μm) HPLC column using 0.1% aq TFA and $CH_3CN$ mobile phases. A linear gradient was employed (99:1 0.1% aq TFA–$CH_3CN$ → 63:37 0.1% aq TFA–$CH_3CN$) over a period of 20 min with a flow rate of 3 mL/min. Fractions containing the desired product eluted at 16.7 min and were collected, frozen and lyophilized to afford a colorless solid: yield 2.25 mg (46%); mass spectrum (MALDI-TOF $ES^+$), *m/z* 1666.6799 $(M+H)^+$ ($C_{67}H_{104}N_{21}O_{23}S_3$ requires 1666.6778).

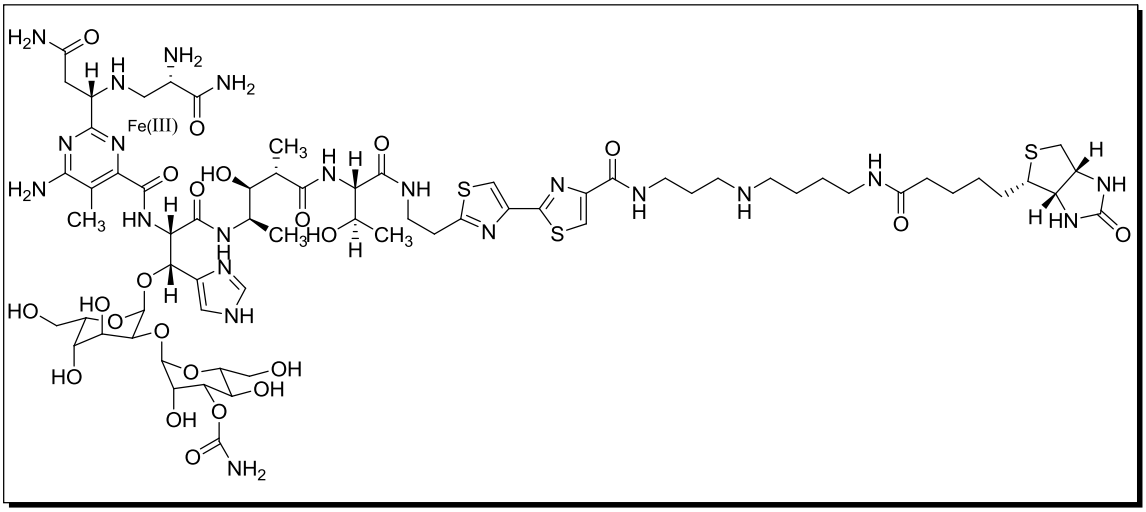

**Biotinylated Fe(III)•Bleomycin $A_5$ (3.17).** Biotinylated BLM $A_5$ **(3.16)**, (2.25 mg, 1.40 μmol) was treated with 481 μL (1.45 mmol) of a 2.944 mM aq solution of $FeCl_3 \cdot 6H_2O$ at 25 $^oC$ and stirred for 12 h. The solution was frozen and then lyophilized to afford a yellow solid: yield 2.33 mg (quant.); mass spectrum (MALDI-TOF $ES^+$), *m/z* 1666.6789 $((M+H)\text{-}Fe)^+$ ($C_{67}H_{103}N_{21}O_{23}S_3$ requires 1666.6778).

# Chapter 4

## 4.01 Introduction

Fluorescence microscopy provides an alternative method for studying small molecule interaction with nucleic acids and/or proteins by measuring light emitted from a fluorophore. Fluorophores traditionally consist of complex, conjugated ring systems that become excited when exposed to specific wavelengths of light. Typically in fluorescence microscopy systems, light is transmitted from a mercury or xenon arc lamp and is passed through an optical filter which only allows a very select range of wavelengths (corresponding to the excitation wavelength of the fluorophore) to penetrate the sample being examined (Figure 4.01). Once the fluorophore becomes excited, it then relaxes back to its ground state energy by emitting a photon of lower energy (longer wavelength) than the original excitation energy. The emitted photons are passed through a second filter to a detector that then renders an image to display.

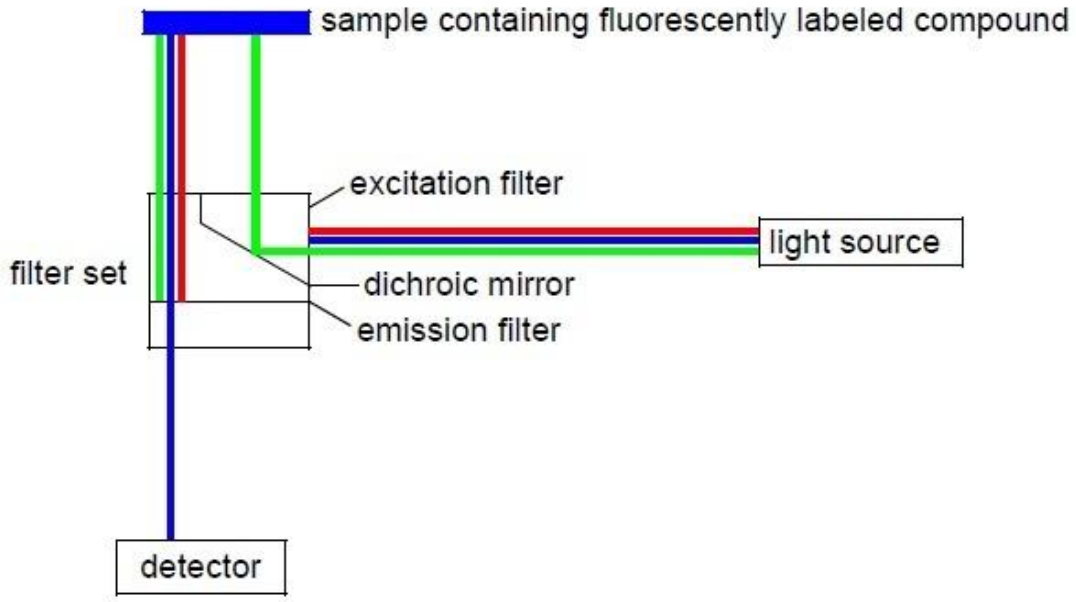


**Figure 4.01** Schematic representation of fluorescence microscopy

Fluorescence microscopy offers many advantages over other traditional methods,

not only for the study of molecular interactions but also for general imaging and diagnostics. This technique uses non-ionizing radiation and, if measured properly, can be used quantitatively.[91,92] In addition to its antitumor activity, BLM has shown the ability to specifically target tumors and has the potential for being a tumor-imaging agent.[93-98] Previous studies in the Hecht lab and others have provided evidence that the disaccharide moiety (L-gulose-D-mannose) is critical in cancer cell recognition and is possibly critical for cellular uptake as well (Figure 4.02). Identification of the specific structural elements of BLM responsible for tumor targeting would allow for the synthesis of analogues with improved properties, as well as the possibility for selective delivery of otherwise non-selective drugs to tumor (or otherwise pathogenic) cells.

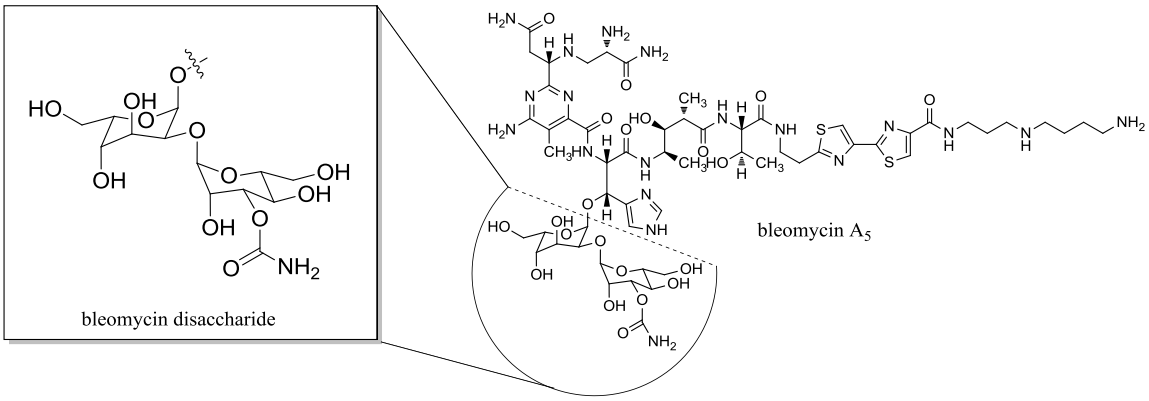


**Figure 4.02** Highlighted inset of the disaccharide moiety within BLM $A_5$

Previously in the Hecht laboratory it was shown that BLM $A_5$ conjugated to microbubbles binds selectively to tumor cells.[67] Traditionally, microbubbles have been used as ultrasonography contrast agents and more recently have been modified with specific (cancer and other) cell surface ligands in order to probe ligand–cell surface interactions.[99,100] In a previous study, similar to the SPR studies presented in Chapter 3, BLM was biotinylated on the C-terminus and bound to commercially produced

streptavidin microbubbles. It was then observed that only the BLM-derivatized microbubbles (but not the streptavidin-derivatized control ones) bound to MCF-7 human breast carcinoma cells but not to the "normal" MCF-10A human breast cells. It was shown that BLM $A_5$–microbubble conjugates exhibited selective binding to specific tumor cell lines.[67] In the previous study, the C-terminal amine of BLM was biotinylated and bound to commercially available streptavidin-derivatized microbubbles. It was observed that BLM-derivatized microbubbles (and not the streptavidin-derivatized ones) bound to MCF-7 human breast carcinoma cells but not to the "normal" counterpart; MCF-10A breast cell line. To delineate the structural elements responsible for this selective recognition, the same experiment was done using deglycoBLM $A_5$ (a BLM $A_5$, which lacks the disaccharide moiety). Cellular recognition was not observed for either cell line (MCF-7 and MCF-10A) indicating the necessity of the disaccharide moiety. To further investigate the role of the disaccharide moiety in selective tumor cell binding, fluorescence microscopy was employed. BLM $A_5$ and deglycoBLM $A_5$ were conjugated to a cyanine dye; Cy5** (Scheme 4.02).

Fluorescence microscopy studies were carried out using similar and analogous methodology by using BLM $A_5$ and deglycoBLM $A_5$ conjugated to a cyanine dye; Cy5** (Figure 4.03). Again, the imaging of cancer cells required the presence of the BLM disaccharide moiety.

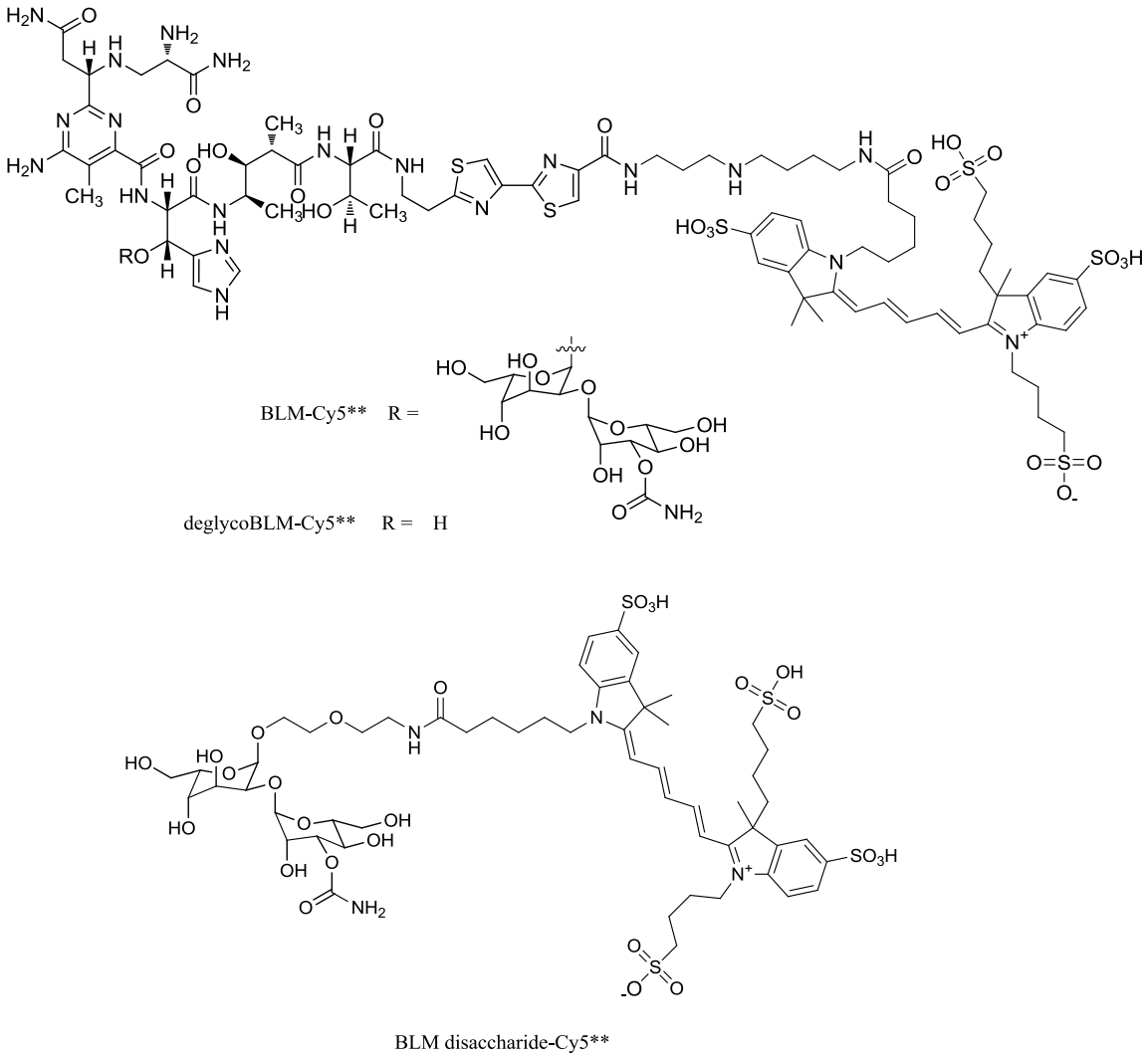


**Figure 4.03** Structures of BLM-Cy5**, deglycoBLM-Cy5**, and BLM disaccharide-Cy5**.[101.102]

Studies were also employed using simply the disaccharide conjugated through a linker to Cy5** and a wide variety of cell lines with matched "normal" counterparts were analyzed (prostate, colon, kidney, pancreas).

## 4.02 Results

Previous studies established the necessity of the disaccharide moiety for tumor cell recognition and binding but did not provide the advantage of direct visualization of the phenomenon as well as the possibility of subsequent quantification. The BLM disaccharide, comprised of L-gulose linked to 3-carbamoylmannose was synthesized using a procedure described previously.[78] The BLM disaccharide was tethered to the dye, Cy5** through a coupling reaction with a commercially available linker (protected as the CBz derivative) to give **4.01** in 66% yield (Scheme 4.01).

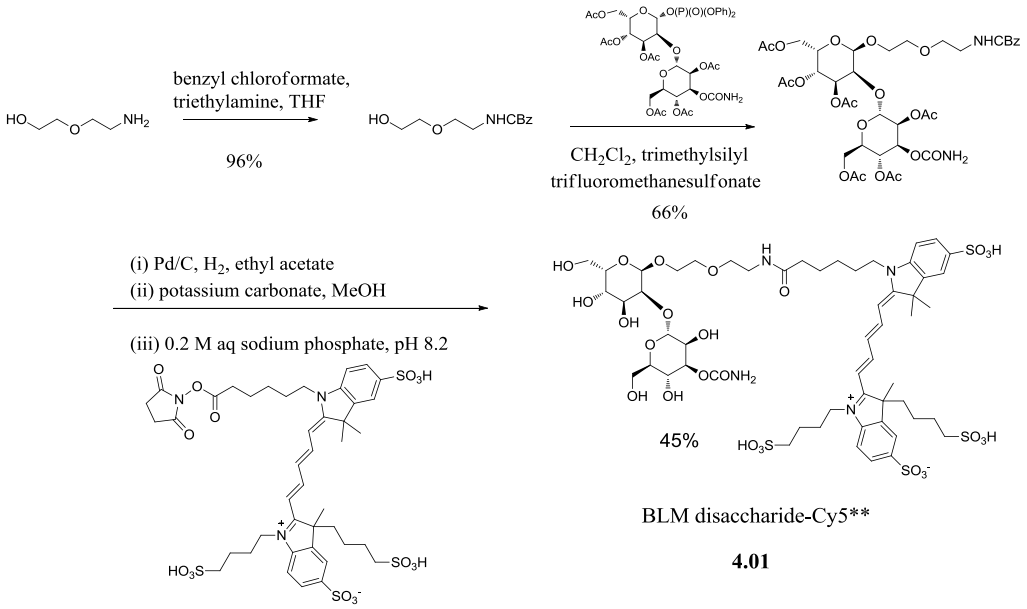


**Figure 4.04** Synthetic route employed for the preparation of BLM disaccharide-Cy5** (4.01) [102]

Deprotection to expose the primary amine followed by deacetylation and conjugation to Cy5** via treatment with the NHS ester of Cy5** (Cy5**–NHS) afforded the BLM disaccharide-Cy5** conjugate **4.01** in 45% yield over the last three steps. The Cy5** BLM $A_5$ and deglycoBLM $A_5$ dye conjugates were also prepared in an analogous

manner and gave the corresponding conjugates in 15% **(4.02)** and 11% **(4.03)** respective yields overall (Scheme 4.02).[67]

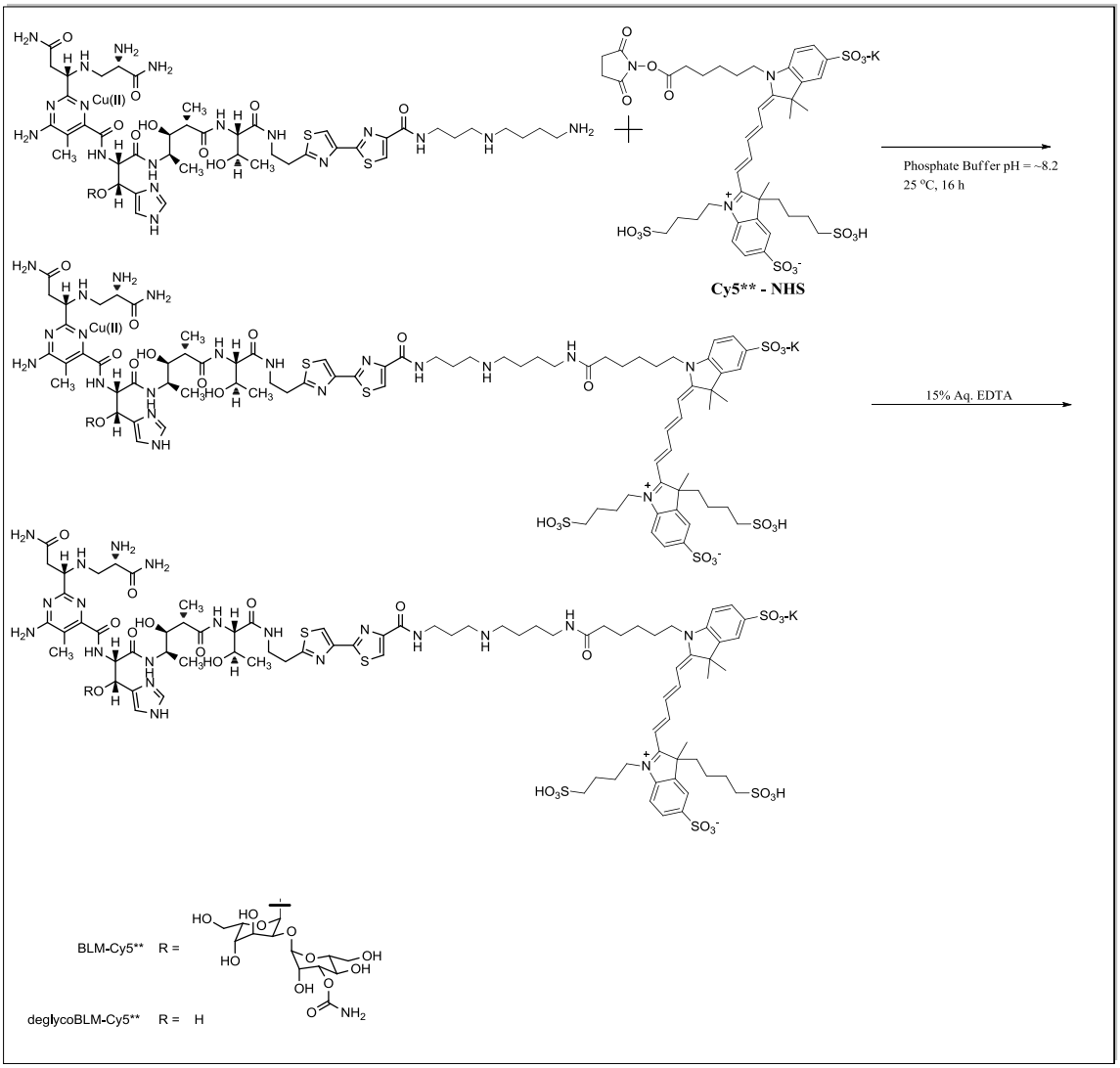


**Scheme 4.01** Synthetic route employed for the preparation of BLM $A_5$-Cy5** and deglycoBLM $A_5$

MCF-7 human breast carcinoma cells and MCF-10A "normal" breast cells were cultured in 16-well glass chamber slides for 48 h, and then treated with 50 μM of either BLM-Cy5**, deglycoBLM-Cy5** or the BLM disaccharide-Cy5** at 37 $^{o}$C for 1 h to allow adequate interaction with the cell surface. The cells were washed twice with PBS and fixed with a 4% paraformaldehyde solution. Fluorescence imaging was done using a

Zeiss Aviovert 200M inverted microscope with 40x oil objective and the appropriate Cy5(/Cy5**) optical filter set (excitation 651 nm, emission 666 nm). All images were recorded and target cells counted using a 40× oil objective. For comparative studies, the exposure time and laser intensity were kept identical for accurate intensity measurements. Pixel intensity was quantified using AxioVision Release 4.7 version software, and the mean pixel intensity was generated as gray level.

Treatment of MCF-7 cells with BLM-Cy5** resulted in significant cellular interaction and uptake, while no interaction or uptake was observed for the "normal" MCF-10A cells. The cells were also treated with DAPI in order to image the cell nuclei (Figure 4.05).

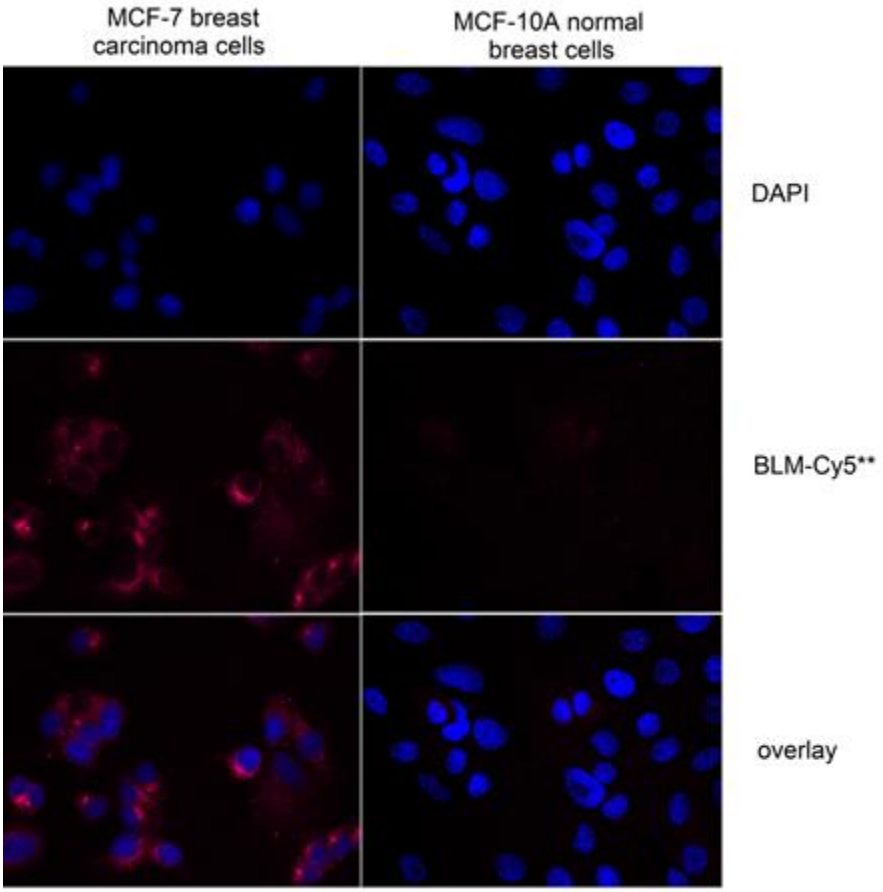


**Figure 4.05** Uptake of BLM-Cy5** in MCF-7 and MCF-10A breast cells[a]
[a] Images obtained by Dr. Zhiqiang Yu.

After the initial analysis using BLM $A_5$-Cy5** and MCF-7/MCF-10A cell lines, as were used in previous studies involving microbubbles, investigation of other fluorescence conjugates, a variety of cell lines and the presence of a metal co-factor (data not shown) were also studied. A similar experiment was carried out using all three conjugates with MCF-7/MCF-10A cell lines in addition to incubation with the Cy5** free dye itself. This served as a negative control to ensure that the cyanine dye itself was not responsible for facilitating binding or entry into the cell. The results of this study are summarized in Figure 4.09.

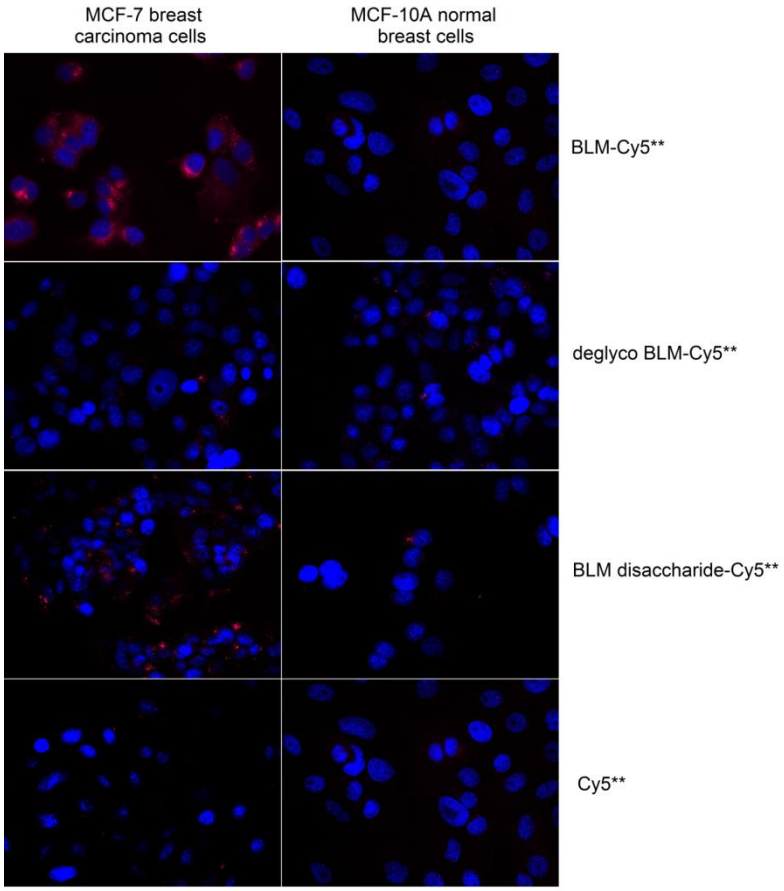


**Figure 4.06** Uptake of Cy5** conjugates in MCF-7 breast carcinoma cells and MCF-10A normal breast cells[a]; [a] Images obtained by Dr. Zhiqiang Yu.

As is clear from Figure 4.06, BLM-Cy5** and BLM disaccharide-Cy5** did not

associate with either cell line, as was the case for the negative control (Cy5** free dye). Additionally, a prostate cancer cell line DU-145 was also compared with its matched "normal" prostate cell line counterpart PZ-HPV-7. The results from these two cell lines (Figure 4.08) are qualitatively identical (possibly even showing stronger cellular interaction) to the results seen above in Figure 4.06.

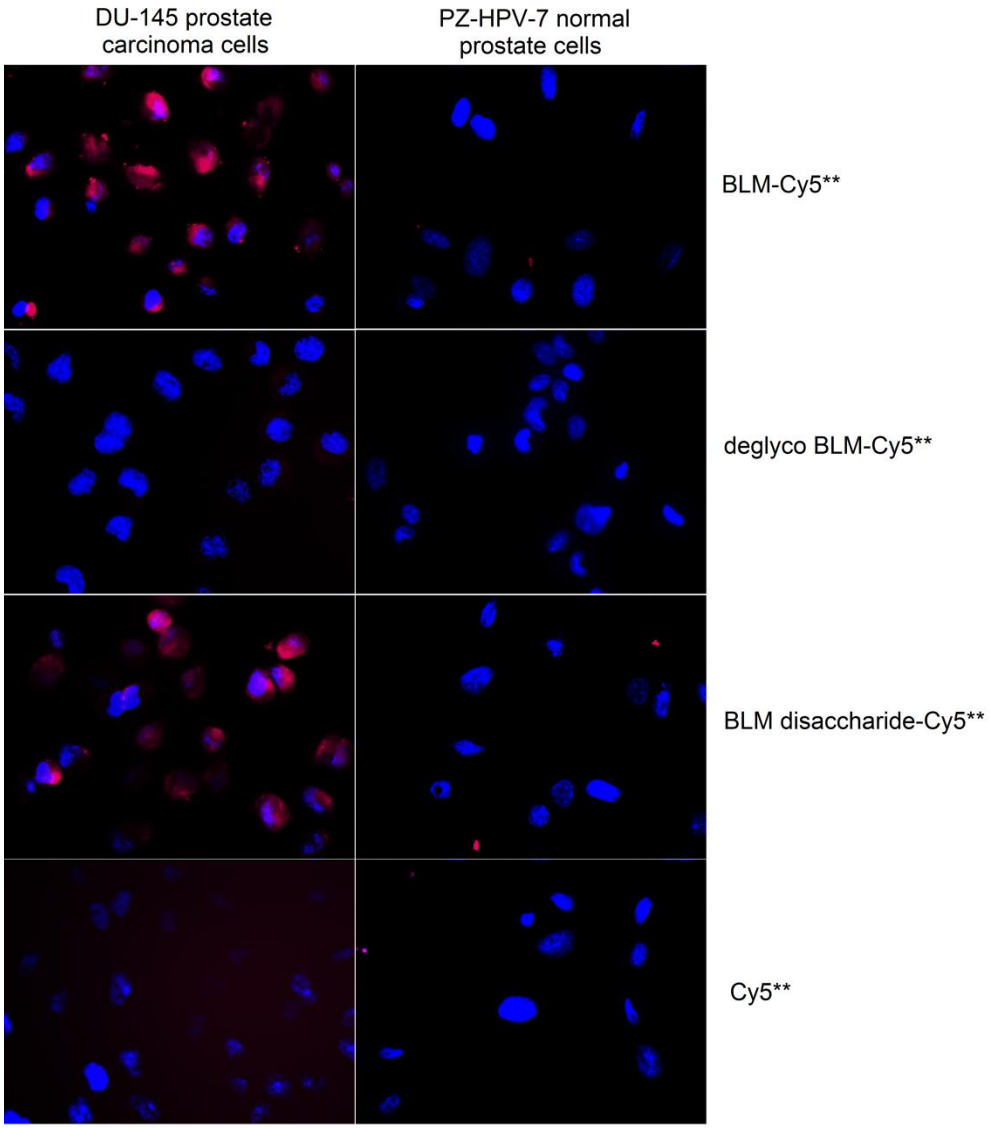


**Figure 4.07** Uptake of Cy5** conjugates in DU-145 prostate carcinoma cells and PZ-HPV-7 normal prostate cells[a]; [a] Images obtained by Dr. Zhiqiang Yu.

Again, the BLM-$A_5$-Cy5** and BLM disaccharide-Cy5** showed selectivity for the cancer cell line DU-145 (and not the "normal" prostate cells PZ-HPV-7). The deglycoBLM $A_5$-Cy5** conjugate showed no interaction with either cell line, as nor did the negative control (Cy5** free dye). The results in Figures 4.06 and 4.07 are quantified and summarized in Figure 4.08.

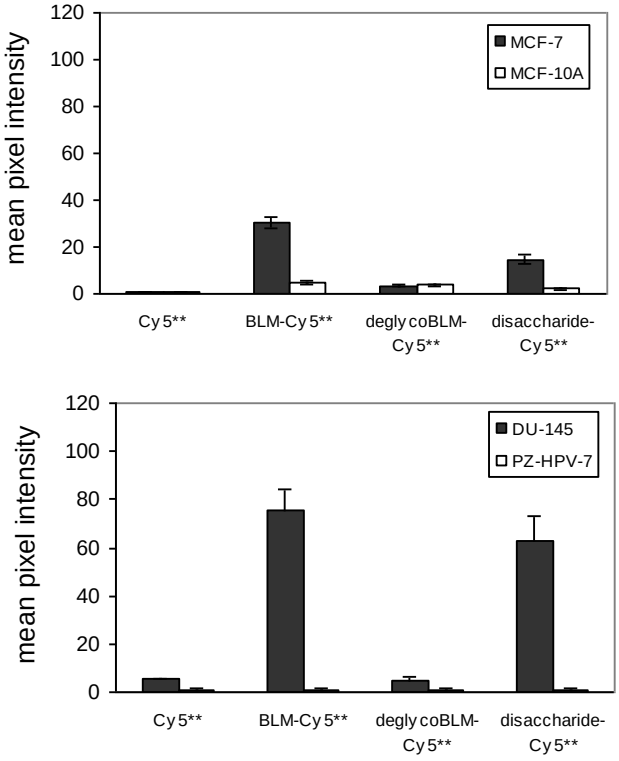


**Figure 4.08** Quantification of the binding/uptake of BLM-Cy5**, deglycoBLM-Cy5**, BLM disaccharide-Cy5** and Cy5** by MCF-7 and MCF-10A cells (upper panel) or by DU-145 and PZ-HPV-7 cells (lower panel)

The data presented above clearly demonstrate the need for the disaccharide moiety of BLM for cellular recognition/internalization. The fact that the experiments presented here showed similar qualitative results for two different matched cell lines is promising for further studies using other cancerous cell lines. These results also hold promise for the BLM disaccharide or BLM itself to be used as a diagnostic imaging tool.

### 4.03 Discussion

Almost all current chemotherapies are limited by side effects resulting from a lack of tumor cell selectivity. Shown in this study is an uncomplicated disaccharide, which has the ability to differentiate between tumor cells and normal cells. In addition to studying the Cy5** conjugates, several other commercially available (cyanine and otherwise) dyes were tried. The scope of the dyes available was defined by the need for easy functionalization and attachment, fluorescence range, quantum yield and the need to avoid auto-fluorescence when imaging fixed cells). Cy5** gave the most reproducible results and was used to synthesize the conjugates needed. Cy5** has a maximum absorbance of 651 nm and, therefore, did not contribute to auto-fluorescence during fixed cell imaging experiments.

Initial experiments were also done using the Cu(II) chelates of both the BLM $A_5$-Cy5** and deglycoBLM $A_5$-Cy5** conjugates and preliminary observations suggested markedly increased cellular interaction and uptake (of only the disaccharide containing BLM $A_5$ conjugate and not the deglycoBLM $A_5$ conjugate nascent the disaccharide moiety, results not shown). This strongly suggests that the binding of a metal cofactor and, either the subsequent change in secondary structure of BLM or the increase in overall positive character (or both) further facilitates cellular recognition and increased uptake into cells. Additionally these studies also displayed a similar trend in cancer cell line selectivity. This could possibly be a result of a particular secondary structure, that results in the disaccharide moiety being more readily accessible to cell surface receptors.

Given the uncomplicated nature of the disaccharide and its ability to selectively bind to cancer cells, its potential for use in cancer diagnosis, imaging and treatment is an

intriguing possibility. A cobalt derivative of BLM has been shown previously to successfully image brain tumor.[103] The use of the disaccharide modified by a radiolabel or a contrast agent could prove a more efficient approach to imaging tumors.[104] Attachment of the disaccharide to otherwise non-selective chemotherapeutic agents may allow a "magic-bullet" approach to future chemotherapy treatments.

## 4.04 Experimental

**General Methods:** All solvents used were of analytical grade. Anhydrous solvents were of DriSolv® quality and purchased from VWR. All experiments were run under a dry nitrogen atmosphere in flame-dried glassware. All other chemicals were purchased from Aldrich and used without further purification. Flash chromatography was carried out using Silicycle 200-400 mesh silica gel. Analytical TLC was carried out using 0.25 mm EM silica gel 60 $F_{250}$ plates that were visualized by UV irradiation (254 nm). HPLC separations were performed on an Agilent 1100 series HPLC system using a diode array detector. The crude products were purified on an Alltech Alltima $C_{18}$ reversed phase semi-preparative (250 x 10 mm, 5 μm) HPLC column using aq 0.1% TFA and $CH_3CN$ mobile phases. UV-Vis spectrophotometric analysis and quantifications were done using a Beckman DU Series 500 UV/Vis spectrophotometer equipped with a single cell module. $^1H$ and $^{13}C$ NMR spectra were recorded on a 400 MHz Varian Liquid-State NMR in chloroform-*d* (unless otherwise noted). Chemical shifts were reported in parts per million (ppm, δ) referenced to the residual $^1H$ resonance of the solvent ($CDCl_3$, 7.26 ppm). $^{13}C$ spectra were referenced to the residual $^{13}C$ resonance of the solvent ($CDCl_3$, 77.0 ppm). Splitting patterns were designated as follows: s, singlet; br, broad; d, doublet; dd, doublet of doublets; t, triplet; q, quartet; m, multiplet. High resolution mass spectra were obtained in the Arizona State University CLAS High Resolution Mass Spectrometry Laboratory or in the Michigan State University Mass Spectrometry Facility.

**Cell Growth Conditions**. MCF-7 cells (ATCC HBT-22) were grown in RPMI 1640 (Gibco, Grand Island, NY) supplemented with 10% fetal bovine serum (HyClone, South Logan, UT) and 1% penicillin–streptomycin mix antibiotic supplement (Cellgro,

Manassas,VA). MCF-10A cells (ATCC CRL-10317) were grown in MEGM (Invitrogen, Grand Island, NY) supplemented with 100 ng/mL cholera toxin (Sigma-Aldrich) and 1% penicillin–streptomycin mix antibiotic supplement. DU-145 (ATCC HTB-81) and PZ-HPV-7 (ATCC CRL-2221) prostate cells were grown in MEM (Gibco, Grand Island, NY) supplemented with 10% fetal bovine serum (HyClone) and 1% penicillin-streptomycin mix antibiotic supplement. Cell lines were maintained at 37 °C under a humidified atmosphere of 5% $CO_2$ and 95% air.

**Fluorescence microscopy.** Fluorescence images were obtained using a Zeiss Axiovert 200M inverted microscope fitted with an AxioCam MRm camera equipped with a 300-w xenon lamp (Sutter, Novato, CA), Cy5 cyanine filter (Chroma, Bellows Falls, VT). Adherent cancer cells were grown on 16-well Lab-Tek glass chamber slides at a cell density of 5000 cells/well (Thermo Scientific, Waltham, MA) at 37 °C for 48 h. Cells were rinsed twice with phosphate buffered saline (PBS) when the cell confluence was about 70%, then the medium was replaced with RPMI 1640 (no phenol red). The dye-labeled conjugates were subsequently added to the final desired concentrations. The cells were incubated at 37 °C for 1 h, washed with PBS, then fixed with 4% paraformaldehyde at 37 °C for 5 min. Finally the slide was mounted with Prolong Antifade Gold reagent with DAPI (Invitrogen), then covered with a glass coverslip and dried for 24 h before fluorescence microscope imaging analysis. All images were recorded and target cells counted using a 40× oil objective. For comparative studies, the exposure time and laser intensity were kept identical for accurate intensity measurements. Pixel intensity was quantified using AxioVision Release 4.7 version software, and the mean pixel intensity was generated as gray level.

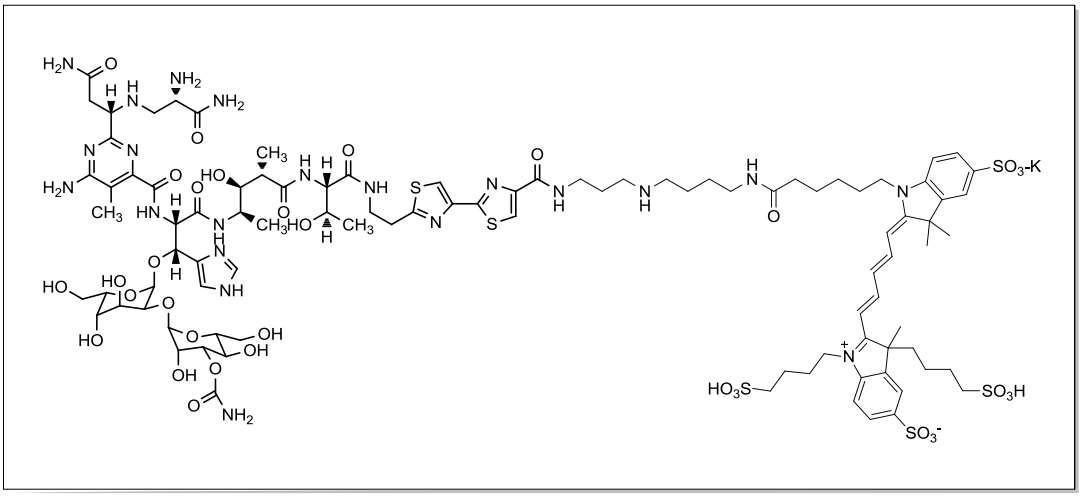

**Bleomycin-Cy5** (4.01).** To a solution containing 0.8 mg (0.5 μmol) of Cu(II)•BLM $A_5$ **(3.01)** in 500 μL of 0.2 M sodium phosphate, pH 8.2, at room temperature was added 0.3 mg (0.3 μmol) of Cy5** carboxylic acid succinimidyl ester. The reaction mixture was swirled overnight at room temperature in the dark and the crude reaction mixture was purified on an Econosil $C_{18}$ reversed phase semi-preparative (250 x 10 mm, 10 μm) HPLC column using 0.1% aq TFA and $CH_3CN$ mobile phases. A linear gradient was employed (99:1 0.1% aq TFA–$CH_3CN$ → 35:65 0.1% aq TFA–$CH_3CN$) over a period of 45 min at a flow rate of 3 mL/min. Fractions containing the desired product eluted at 20.8 min and were collected, frozen and lyophilized to afford a blue powder. The crude product was dissolved in 15% aq EDTA and stirred overnight at room temperature. The reaction mixture was purified on an Econosil $C_{18}$ reversed phase semi-preparative (250 × 10 mm,10 μm) HPLC column using 0.1% aq TFA and $CH_3CN$ mobile phases. A linear gradient was employed (99:1 0.1% aq TFA–$CH_3CN$ → 35:65 0.1% aq TFA–$CH_3CN$) over a period of 45 min at a flow rate of 3 mL/min. Fractions containing the desired product eluted at 20.9 min and were collected, frozen, and lyophilized to give bleomycin $A_5$-Cy5** **(4.01)** as a light colored solid: yield 120 μg (15% over two steps); mass

spectrum (TOF ESI), *m/z* 2308.8036 (M+) ($C_{95}H_{138}N_{21}O_{34}S_6$ requires 2308.8049).

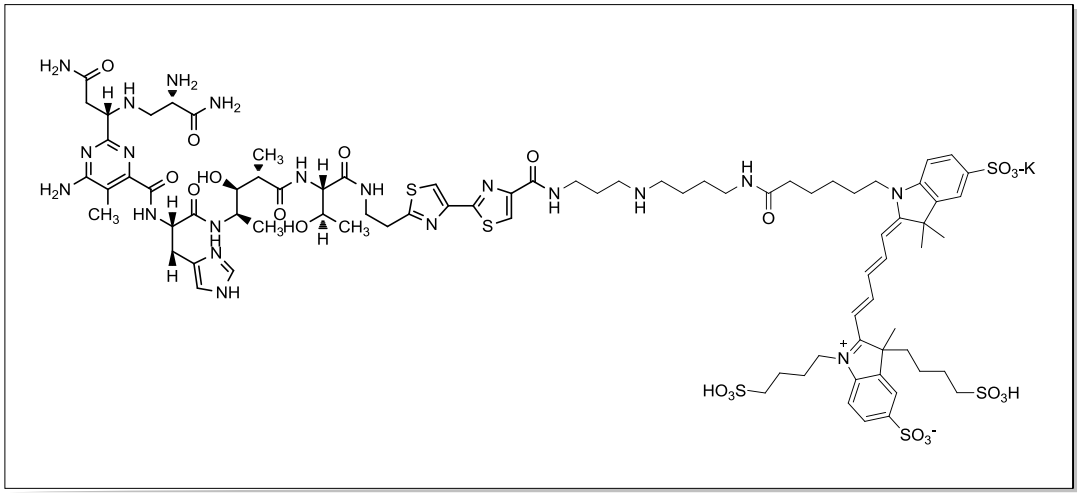

**Deglycobleomycin $A_5$-Cy5** (4.02).** To a solution containing 0.9 mg (0.8 μmol) of Cu(II)•deglycoBLM $A_5$ **(3.06)** in 1.0 mL of 0.2 M sodium phosphate, pH 8.0, at room temperature was added 0.3 mg (0.3 μmol) of Cy5** carboxylic acid succinimidyl ester. The reaction mixture was swirled overnight at room temperature and the crude reaction mixture was purified on an Econosil $C_{18}$ reversed phase semi-preparative (250 × 10 mm, 10 μm) HPLC column using 0.1% aq TFA and $CH_3CN$ mobile phases. A linear gradient was employed (99:1 0.1% aq TFA–$CH_3CN$ → 35:65 0.1% aq TFA–$CH_3CN$) over a period of 45 min at a flow rate of 3 mL/min. Fractions containing the desired product eluted at 21.5 min and were collected, frozen and lyophilized to afford a blue powder. The crude product was dissolved in 15% aq EDTA and stirred overnight at room temperature. The reaction mixture was purified on an Econosil $C_{18}$ reversed phase semipreparative (250 x 10 mm, 10 μm) HPLC column using 0.1% aq TFA and $CH_3CN$ mobile phases. A linear gradient was employed (99:1 0.1% aq TFA–$CH_3CN$ → 35:65 0.1% aq TFA–$CH_3CN$) over a period of 45 min at a flow rate of 3 mL/min. Fractions

containing the desired product eluted at 21.3 min and were collected, frozen, and lyophilized to give deglycoBLM-Cy5** **(4.02)** as a light colored solid: yield 75 μg (11% over two steps); mass spectrum (TOF ESI), *m/z* 1941.6907 (M+) ($C_{82}H_{117}N_{20}O_{23}S_6$ requires 1941.6925).

REFERENCES

1. Jemal, A.; Siegel, R.; Xu, J.; Ward, E. *CA Cancer J. Clin.* **2010**.

2. Nishimura, S.; Matsunaga, S.; Yoshida, M.; Hirota, H.; Yokoyama, S.; Fusetani, N. *Bioorg. Med. Chem.* **2005**, *13*, 449.

3. Balakin, K. V.; Ivanenkov, Y. A.; Kiselyov, A. S.; Tkachenko, S. E. *Anticancer Agents Med. Chem.* **2007**, *7*, 576.

4. Long, E. C. In *Bioorganic Chemistry: Nucleic Acids*; Hecht, S. M., Ed.; Oxford University Press: New York, NY, 1996, p 3-36.

5. Haq, I. *Arch. Biochem. Biophys.* **2002**, *403*, 1.

6. Galm, U.; Hager, M. H.; Van Lanen, S. G.; Ju, J. Thorson, J. S.; Shen, B. *Chem. Rev.* **2005,** *105,* 739.

7. Umezawa, H.; Suhara, Y.; Takita, T.; Maeda, K. *J. Antibiot.* **1966,** *19A,* 210.

8. Hoet, P. H. M.; Nemery, B. *Am. J. Physiol. Lung. Cell. Mol. Physiol.* **2000,** *278,* L417-L433.

9. Galm, U.; Wednt-Pienkowski, E.; Wang, L.; George, N. P.; Oh, T.; Yi, F.; Tao, M.; Coughlin, J. M.; Shen, B. *Mol. Biosyst.* **2009,** *5,* 77.

10. Claussen, C. A.; Long, E. C. *Chem. Rev.* **1999,** *99,* 2797.

11. Aoyagi, Y.; Katano, K.; Suguna, H.; Primeau, J.; Chang, L. H.; Hecht, S. M. *J. Am. Chem. Soc.* **1982,** *104,* 5537.

12. Takita, T.; Umezawa, Y.; Saito, S.; Morishima, H.; Naganawa, H.; Umezawa, H. Tsuchiya, T.; Miyake, T.; Kageyama, S.; Umezawa, S.; Muraoka, Y.; Suzuki, M.; Otsuka, M., Narita, M.; Kobayashi, S.; Ohno, M. *Tetrahedron Lett.* **1982,** *23,* 521.

13. Boger, D. L.; Honda, T.; Dang, Q. *J. Am. Chem. Soc.* **1994,** *116,* 5619.

14. Leitheiser, C. J.; Smith, K. L.; Rishel, M. J.; Hashimoto, S.; Konishi, K.; Thomas, C. J.; Li, C.; McCormick, M. M.; Hecht, S. M. *J. Am. Chem. Soc.* **2003,** *125,* 8218.

15. Buda, F.; Karawajczyk, A. *Mol. Sim.* **2006,** *32,* 1233.

16. Hecht, S. M. *Acc. Chem. Res.* ***1986,*** *19,* 383.

17. Burger, R. M. *Chem. Rev.* **1998,** *98,* 1153.

18. Aoyagi, Y.; Chorghade, M. S.; Padmapriya, A. A.; Suguna, H.; Hecht, S. M. *J. Org. Chem.* **1990.** *55,* 6291.

19. Kittaka, A.; Sugano, Y.; Otsuka, M.; Ohno, M. *Tetrahedron* **1988,** *44,* 2821.

20. Hamamichi, N.; Natrajan, A.; Hecht. S. M. *J. Am. Chem. Soc.* **1992**, *114*, 6278.

21. Thesis of Dr. Xiaquing Cai, Arizona State University Online 2013.

22. Thomas, C. J.; McCormick, M. M.; Vialas, C.; Tao, Z.-F.; Leitheiser, C. J.; Rishel, M. J.; Xu, X.; Hecht, S. M. *J. Am. Chem. Soc.* **2002**, *124*, 3875.

23. *Bleomycin Chemotherapy*; Sikic, B. I., Rozencweig, M., Carter, S. K., Eds.; Academic: Orlando, FL, 1985.

24. Muraoka, Y.; Saito, S.; Nogami, T.; Umezawa, K.; Takita, T.; Takeuchi, T.; Umezawa, H.; Sakata, N.; Hori, M.; Takahashi, K.; Ekimoto, H.; Minamide, S.; Nishikawa, K.; Kuramochi, H.; Motegi, A.; Fukuoka, T.; Fukuoka, T.; Nakatani, T.; Fujii, A.; Matsuda, A. In *Horizons on Antibiotic Research*; Davis, B. D., Ichikawa, T., Maeda, K., Mitscher, L. A., Eds.; Japan Antibiotic Research Association: Tokyo, 1988.

25. Boger, D. L.; Menezes, R. F.; Dang, Q.; Yang, W. *Bioorg. Med. Chem. Lett.* **1992**, *2*, 162.

26. Carter, B. J.; Reddy, K. S.; Hecht, S. M. *Tetrahedron* **1991**, *47*, 2463.

27. Rishel, M. J.; Thomas, C. J.; Tao, Z.-F.; Vialas, C.; Leitheiser, C. J.; Hecht, S. M. *J. Am. Chem. Soc*. **2003**, *125*, 10194.

28. Sugiuayama, H.; Ehrenfeld, G. M.; Shipley, J. B.; Kilkuski, R. E.; Chang, L.-H.; Hecht, S. M. *J. Nat. Prod.* **1985,** *48,* 869.

29. Burger, R. M.; Peisach, J.; Horwitz, S. B. *J. Biol. Chem.***1980,** *256*, 11636.

30. Giloni, L.; Takeshita, M.; Johnson, F.; Iden, C.; Grollman, A. P. *J. Biol. Chem.* **1981**, *256*, 8608.

31. Muller, W. E. G.; Yamazaki, Z.; Breter, H.-J.; Zahn, R. K. *Eur. J. Bichem.* **1972,** *31,* 518.

32. Haidle, C. W.; Bearden, J., Jr. *Biochem. Biophys. Res. Commun.* **1975,** *65,* 815.

33. Krishnamoorthy, C. R.; Vanderwall, D. E.; Kozarich, J. W.; Stubbe, J. *J. Am. Chem. Soc.* **1988,** *110,* 2008.

34. Magliozzo, R. S.; Peisach, J.; Ciriolo, M. R. *Mol. Pharmacol.* **1989,** *35,* 428.

35. Carter, B. J.; de Vroom, E.; Long, E. C.; van der Marel, G. A.; van Boom, J. H.; Hecht, S. M. *Proc. Natl. Acad. Sci. U.S.A.* **1990,** *87,* 9373.

36. Lim, S. T.; Jue, C. K.; Moore, C. W.; Lipke, P. N. *J. Bacteriol.* **1995,** *177,* 3534.

37. Padbury, G.; Sligar, S. G. *J. Biol. Chem.* **1985,** *260,* 7820.

38. Murugesan, N.; Hecht, S. M.; *J. Am. Chem. Soc.* **1985,** *107,* 493.

39. Sausville, E. A.; Peisach, J.; Horwitz, S. B.; *Biochem. Biophys. Res. Commun.* **1976,** *73,* 814.

40. Burger, R. M.; Horwitz, S. B.; Peisach, J.; Wittenberg, J. B. *J. Biol. Chem.* **1979**, *254,* 12299.

41. Decker, A.; Chow, M. S.; Kemsley, J. N.; Lehnert, N.; Solomon, E. I. *J. Am. Chem. Soc.* **2006,** *128,* 4719.

42. Thesis of Dr. Ryan Schmaltz, University of Virginia Library Online 2013.

43. Hecht, S. M. *J. Nat. Prod.* **2000,** *63,* 158.

44. Ma, Q.; Xu, Z.; Schroeder, B. R.; Sun, W.; Wei, F.; Hashimoto, S.; Konishi, K.; Leitheiser, C. J.; Hecht, S. M. *J. Am. Chem. Soc.* **2007,** *129,* 12439.

45. Akiyama, Y.; Ma, Q.; Edgar, E.; Laikhter, A.; Hecht, S. M. *Org. Lett.* **2008,** *10,* 2127.

46. Takita, T.; Umezawa, Y.; Saito, S.; Morishima, H.; Naganawa, H.; Umezawa, H. Tsuchiya, T.; Miyake, T.; Kageyama, S.; Umezawa, S.; Muraoka, Y.; Suzuki, M.; Otsuka, M., Narita, M.; Kobayashi, S.; Ohno, M. *Tetrahedron Lett.* **1982,** *23,* 521.

47. Boger, D.; Honda, T.; Menezes, R. F.; Colletti, S. L.; Dang, Q.; Yang, W. *J. Am. Chem. Soc.* **1994,** *116,* 82.

48. Mattingly, P. G.; Miller, M. J. *J. Org. Chem.* **1980,** *45,* 410.

49. Barker, P. L.; Gendler, P. L.; Rapoport, H. *J. Org. Chem.* **1981,** *46,* 2455.

50. Markees, D. G.; Kidder, G. W. *J. Am. Chem. Soc.* **1956,** *78,* 4130.

51. Morin, F. G.; Grant, D. M. *J. Org. Chem.* **1985,** *50,* 4865.

52. Bhattacharya, S.; Snehalatha, K.; Kumar, V. P. *J. Org. Chem.* **2003,** *68,* 2741.

53. Horvath, G.; Rusa, C.; Kontos, Z.; Gerencser, J.; Huszthy, P. *Synth. Comm.* **1999,** *29,* 3719.

54. Suga, A.; Sugiyama, T.; Otsuka, M.; Ohno, M.; Sagiura, Y.; Maeda, K. *Tetrahedron* **1991,** *47,* 1191.

55. The pyrimidoblamic analogues (**2.11, 2.13a-2.13c and 2.19**) were incorporated into solid phase synthesis and prepared for use in the DNA pSP64 supercoiled DNA relaxation assay by Mr. Parvez Alam.

56. Nguyen, B.; Tanious, F. A.; Wilson, D. *Methods* **2007,** *8,* 150.

57. Liu, Y.; Wilson, D. W. *Methods Mol. Biol.* **2010,** *613,* 1.

58. Biocore *Manual for Streptavidin Functionalized Sensor Chips; Biotin Capture Chips,* Accessed online; www.biocore.com, 2013.

59. Kampranis, S. C.; Gormley, N. A.; Tranter, R.; Orphanides, G.; Maxwell, A; *Biochem.***1999,** *38,* 1967.

60. Boger, D. L.; Saionz, K. W. *Bioorg. Med. Chem.***1999,** *7,* 315.

61. Stubbe, J.; Kozarich, J. W. *Chem. Rev.* **1987,** *87,* 1107.

62. Holmes, C. E.; Carter, B. J.; Hecht, S. M. *Biochemistry* **1993,** *32,* 9373.

63. Holmes, C. E.; Duff, R. J.; van der Marel, G. A.; van Boom, J.; Hecht, S. M. *Bioorg. Med. Chem.* **1997,** *5,* 1235.

64. Abraham, A. T.; Lin, J.-J.; Newton, D. L.; Rybak, S.; Hecht, S. M. *Chem. Biol.* **2003,** *10,* 45.

65. Tao, Z.-F.; Konishi, K.; Keith, G.; Hecht, S. M. *J. Am. Chem. Soc.* **2006,** *128,* 14806.

66. Wei, Y.; Wesson, P. J.; Kourkine, I. Grzybowski, B. A. *Anal. Chem.* **2010,** *82,* 8780.

67. Chapuis, J.-C.; Schmaltz, R. M.; Tsosie, K. S.; Behovlavek, M.; Hecht, S. M. *J. Am. Chem. Soc.* **2009,** *131,* 2438.

68. Chien, M.; Grollman, A. P.; Horwitz, S. B. *Biochemistry* **1977,** *16,* 3641.

69. Huang, C.-H.; Galvan, L.; Crooke, S. T. *Biochemistry* **1980,** *19,* 1761.

70. Holmes, C. E.; Hecht, S. M. *J. Biol. Chem.* **1993,** *268,* 25909.

71. Guenther, R.; Forrest, B.; Newman, W.; Malkiewicz, A. Agris, P. F. *Acta Biochem. Pol.* **1998,** *45,* 13.

72. Akiyama, Y.; Ma, Q.; Edgar, E.; Laikhter, A.; Hecht, S. M. *J. Am. Chem. Soc.* **2008,** *130,* 9650.

73. Ma, Q.; Akiyama, Y.; Xu, Z.; Konishi, K.; Hecht, S. M. *J. Am.Chem. Soc.* **2009,** *131,* 2013.

74. Giroux, R. A.; Hecht, S. M. *J. Am. Chem. Soc.* **2010,** *132,* 16987.

75. Myszka, D. G. *J. Mol. Recognit.* **1999,** *12,* 279.

76. Nanjunda, R.; Munde, M.; Liu, Y.; Wilson, W. D. *Methods for Studying Nucleic Acid/Drug Interactions*; CRC Press: Boca Raton, FL, 2011; Chap 4, pp 91.

77. Liu, Y.; Chai, Y.; Kumar, A.; Tidwell, R. R.; Boykin, D. W.; Wilson, W. D. *J. Am. Chem. Soc.* **2012,** *134,* 5290.

78. Bozeman, T.C.; Nanjunda, R.; Tang, C.; Liu, Y.; Segerman, Z. J.; Zaleski, P. A.; Wilson, D.; Hecht, S. M. *J. Am. Chem. Soc.* **2012,** *134,* 17842.

79. Wang, S.; Munde, M.; Wang, S.; Wilson, W. D. *J. Am. Chem. Soc.* **2011,** *35,* 7674.

80. Berry, D. E.; Kilkuskie, R. E.; Hecht, S. M. *Biochemistry* **1985,** *24,* 3214.

81. Umezawa, H.; Takita, T.; Sugiura, Y.; Otsuka, M.; Kobayashi, S.; Ohno, M. *Tetrahedron* **1984,** *40,* 501.

82. Aso, M.; Kondo, M.; Suemune, H.; Hecht, S. M. *J. Am. Chem. Soc.* **1999,** *121,* 9023.

84. Sugiura, Y. *J. Am. Chem Soc.* **1980,** *102,* 5208.

85. Goodwin, K. D.; Lewis, M. A.; Long, E. C.; Georgiadis, M. M. *Proc. Natl. Acad. Sci. U.S.A.* **2008,** *105,* 5052.

86. Boger, D. L.; Colletti, S. L.; Honda, T.; Menezes, R. F. *J. Am. Chem. Soc.* **1994,** *116,* 5607.

87. Manderville, R. A.; Ellena, J. F.; Hecht, S. M. *J. Am. Chem. Soc.* **1995,** *117,* 7891.

88. Wu, W.; Vanderwall, D. E.; Lui, S. M.; Tang, X. J.; Turner, C. J.; Kozarich, J. W. *J. Am. Chem. Soc.* **1996,** *118,* 1281.

89. Cortes, J. C.; Sugiyama, H.; Ikudome, K.; Saito, I.; Wang, A. H. *Biochemisrty* **1997,** *36,* 9995.

90. Lui, S. M.; Vanderwall, D. E.; Wu, W.; Tang, X.-J.; Turner, C. J.; Kozarich, J. W.; Stubbe, J. *J. Am. Chem. Soc.* **1997,** *119,* 9603.

91. Joshi, B. P.; Wang, T. D. *Cancers* **2010**, *2*, 1251.

92. Asai, D. J. In *Current Protocols Essential Laboratory Techniques*; Wiley Online Library: 2008.

93. Jones, S. E.; Lilien, D. L. ; O'Mara, R. E.; Durie, B. G.; Salmon, S. E. *Med. Pediatr. Oncol.* **1975**, *1*, 11.

94. Silverstein, M. J.; Verma, R. C.; Greenfield, L.; Morton, D. L. *Cancer* **1976**, *37*, 36.

95. Bekerman, C.; Moran, E. M.; Hoffer, P. B.; Hendrix, R. W.; Gottschalk, A. *Radiology* **1977**, *123,* 687.

96. Burton, I. E.; Todd, J. H.; Turner, R. L. *Br. J. Radiol.* **1977**, *50*, 508.

97. Goodwin, D. A.; Meares, C. F.; DeRiemer, L. H.; Diamanti, C. I.; Goode, R. L.; Baumert Jr., J. E.; Sartoris, D. J.; Lantieri, R. L.; Fawcett, H. D. *J. Nucl. Med.* **1981**, *22*, 787.

98. Stern, P. H.; Helpern, S. E.; Hagan, P. L.; Howell, S. B.; Dabbs, J. E.; Gordon, R. M. *J. Natl. Cancer Inst.* **1981**, *66*, 807.

99. Klibanov, A. L. *Invest. Radiol.* **2006**, *41*, 354.

100. Willmann, J. K.; Paulmurugan, R.; Chen, K.; Gheysens, O.; Rodriguez-Porcel, M.; Lutz, A. M.; Chen, I. Y.; Chen, X.; Gambhir, S. S. *Radiology* **2008**, *246*, 508.

101. Yu, Z.; Schmaltz, R. M.; Bozeman, T. C.; Paul, R.; Rishel, M. J.; Tsosie, K. S. Hecht, S. M. *J. Am. Chem. Soc.* **2013,** *135,* 2883.

102. The Disaccharide-Cy5** conjugate was prepared for use in the study by Dr. Rakesh Paul.

103. Grove, R.B.; Reba, R. C.; Eckelman, W. C.; Goodyear, M. J. *Nucl. Med.* **1974,** 15, 386.

104. DeRiemer, L. H.; Meares, C. F.; Goodwin, D. A.; Diamanti, C.I. *J. Med. Chem.* ***1979,*** *22,* 1019.